Development of biomarker assays to dissect subtype-specific heterogeneity and anti-EGFR treatment response in colorectal cancer

Elisa Fontana

Laboratory of Systems and Precision Cancer Medicine

The Institute of Cancer Research

University of London

Submitted for the degree of PhD

September 2019

Declaration of originality

I declare that the work presented in this thesis is my own.

Any work that is not mine has been referenced and any data originated from collaborative work has clearly been identified.

Elisa Fontana

Abstract

Colorectal cancer (CRC) is the third most frequently diagnosed type of cancer and the second leading cause of cancer death worldwide. Although extensive biological heterogeneity at multiple “-omics” levels has been demonstrated, a very limited number of biomarkers are currently taken into account to guide treatment decisions in the clinic. The reason for this is partially due to the lack of validated assays suitable for routine clinical application. Building on gene expression CRC subtypes previously identified (CRCAssigner: enterocyte, goblet-like, transit-amplifying, stem-like, inflammatory; Consensus Molecular Subtypes (CMS): CMS1, CMS2, CMS3, CMS4) as potential biomarkers of clinical interest, the aims of the work presented in this thesis were:

- Develop and validate assays able to stratify CRC patients into clinically meanigful subgroups based on the subtypes;
- Demonstrate the potential value of the assays as companion diagnostic tools for predicition of benefit from epidermal growth factor receptor (EGFR) targeted drugs cetuximab and panitumumab.

A total of 825 clinically annotated CRC samples were analysed. A gene expression assay for nCounter platform (NanoString Technologies) was developed to classify CRC samples into CMS. A second assay was developed to integrate the first CMS assay into a previously validated assay for CRCAssigner classification. The integrated assays enabled the simultaneous classification of samples into CRCAssigner and CMS subtypes. The accuracy of the assays was assessed in both fresh-frozen and formalin-fixed paraffin embedded samples. Orthogonal validation of the results was performed using matched RNAseq data and by confirming known subtype-specific associations with clinico-pathological features. Assay detection of similar biological features in multiple Caucasian and Asian populations was demonstrated. Finally, the potential of the assays as companion diagnostic for anti-EGFR benefit prediction was demonstrated in a retrospective cohort; the results were validated in samples prospectively collected from patients who received anti-EGFR monotherapy within an international phase III clinical trial.

Table of content

Publications

Original articles

As first author:

Ragulan C[*], Eason K[*], **Fontana E**[*], Nyamundanda G, Tarazona N, Patil Y, Poudel P, Lawlor RT, Del Rio M, Koo SL, Tan WS. Analytical Validation of Multiplex Biomarker Assay to Stratify Colorectal Cancer into Molecular Subtypes. Scientific reports. 2019 May 21;9(1):7665.

[*]Equal contribution

As collaborator:

Cremolini C, Benelli M, **Fontana E**, Pagani F, Rossini D, Fucà G, Busico A, Conca E, Di Donato S, Loupakis F, Schirripa M. Benefit from anti-EGFRs in RAS and BRAF wild-type metastatic transverse colon cancer: a clinical and molecular proof of concept study. ESMO open. 2019 Mar 1;4(2):e000489.

Smyth EC, Nyamundanda G, Cunningham D, **Fontana E**, Ragulan C, Tan IB, Lin SJ, Wotherspoon A, Nankivell M, Fassan M, Lampis A. A seven-Gene Signature assay improves prognostic risk stratification of perioperative chemotherapy treated gastroesophageal cancer patients from the MAGIC trial. Annals of Oncology. 2018 Nov 27;29(12):2356-62.

Dillon MT, Bergerhoff KF, Pedersen M, Whittock H, Crespo-Rodriguez E, Patin EC, Pearson A, Smith HG, Paget JT, Patel RR, Foo S (and 9 other authors including **Fontana E**). ATR Inhibition Potentiates the Radiation-induced

Inflammatory Tumor Microenvironment. Clinical Cancer Research. 2019 Jun 1;25(11):3392-403.

Reviews

Fontana E, Eason K, Cervantes A, Salazar R, Sadanandam A. Context matters—consensus molecular subtypes of colorectal cancer as biomarkers for clinical trials. Annals of Oncology. 2019 Feb 23;30(4):520-7.

Fontana E, Homicsko K, Eason K, Sadanandam A. Molecular Classification of Colon Cancer: Perspectives for Personalized Adjuvant Therapy. Current Colorectal Cancer Reports. 2016 Dec 1;12(6):296-302.

Editorials

Fontana E, Valeri N. Class(y) dissection of BRAF heterogeneity: beyond non-V600. Clinical Cancer Research 2019 [In press]

Nyamundanda G, **Fontana E**, Sadanandam A. Is the tumour microenvironment a critical prognostic factor in early-stage colorectal cancer?. Annals of Oncology. 2019 Aug 29.

In preparation:

Fontana E, Nyamundanda G, Cunningham D, Tu D, Cheang MCU, Jonker DJ, Siu LL, Sclafani F, Eason K, Ragulan C, Bali MA. Expression of transit-amplifying genes and benefit from anti-epidermal growth factor receptor therapy in colorectal cancer: the TA-ness signature.

Fontana E, Eason K, Nyamundanda G, Cunningham D, Tu D, Tarazona N, Jonker DJ, Siu LL, Sclafani F, Ragulan C, Hullki-Wilson S. A validated NanoString assay demonstrates the association between the Consensus Molecular Subtype-2 and benefit from the anti-epidermal growth factor receptor therapy.

Acknowledgements

Anguraj Sadanandam – Team Leader – Laboratory of Systems and Precision Cancer Medicine – The Institute of Cancer Research

Anguraj was the overall supervisor of the project. He provided guidance and critique of analyses. Prior to this project he led the development of multiple assays for NanoString Technologies and established collaborations with the Royal Marsden and a team in Singapore, which put the foundations for much of the work built here. He provided me with ad-hoc codes for R studio to classify samples into CRCAssigner and CMS subtypes.

Chanthirika Ragulan – High Scientific Officer – Laboratory of Systems and Precision Cancer Medicine – The Institute of Cancer Research

Chanthrika established and optimised protocols for nucleic acid extraction and for nCounter platform (NanoString Technologies). She taught me how to perform every single step related to the wet-lab part of this project, from dual DNA/RNA extraction to NanoString assay development. She also generated part of the RETRO-C data and led the development of the CRCA-38 assay.

Gift Nyamundanda – Bioinformatics Postdoctoral Fellow – Laboratory of Systems and Precision Cancer Medicine – The Institute of Cancer Research

Gift supervised me during multiple data analyses. He performed multivariate analyses of the Discovery cohort included in chapter 3 and ROC curves in the same chapter. He also performed batch correction of the Validation cohort and Figure 25 (chapter 3). He provided me with multiple codes to perform univariate analyses and to plot figures using R studio.

Katherine Eason – PhD student – Laboratory of Systems and Precision Cancer Medicine – The Institute of Cancer Research

Kate selected the genes for the CMS assay (Chapter 2) and developed the rankCMS-38 algorithm. She also produced Figures 3, 5, 7, 16 and 18 under my guidance.

Patrick Lawrence – Scientific Officer – Laboratory of Systems and Precision Cancer Medicine – The Institute of Cancer Research

Patrick helped with RNA extraction of part of the Validation cohort (chapter 3).

Chris O'Callaghan – Senior Investigator – Canadian Cancer Trial Group – Ontario, Canada

Chris was instrumental in gaining access to the CO.20 trial tissue collection. He chaired the CCTG steering committee in Canada and presented the translational proposal developed by myself.

Dongsheng Tu - Senior Statistician – Canadian Cancer Trial Group – Canada

Dongsheng performed the statistical analysis of the Validation cohort (Chapter 3) using three different biomarkers. He developed multiple Cox and Logistic regression models and produced the ROC curve in Figure 39. He provided me with the estimated to re-draw Kaplan Meier figures.

Francesco Sclafani – Clinical Research Fellow – Royal Marsden Hospital

Francesco led the data collection and coordinated the DNA sequencing of the RETRO-C cohort (Chapter 3).

Sanna Hulkki-Wilson – High Scientific Officer – Molecular Pathology – The Institute of Cancer Research

Sanna performed the targeted panel sequencing of RETRO-C and FOrMAT samples (Chapter 3).

Filippo Pietrantonio – Medical Oncologist – University of Milan and National Institute of Cancer (Milan, Italy)

Filippo was principal investigator of the PRESSING study. He coordinated the sample and data collection of the Milan cohort (Chapter 3).

Livio Trusolino – Medical Oncologist – University of Turin, Italy

Livio and his team developed the xenograft models and performed experiments using cetuximab. He shared the RNA extracted from liver metastases and matched xenografts and growth inhibition data.

Iain Bee Huat Tan – Medical Oncologist – National Cancer Centre – Singapore

Iain was principal investigator of a translational project in Singapore. He coordinated the sample and data collection and RNA extraction of the Singapore cohorts (Chapters 2, 3 and 4).

Noelia Tarazona – Medical Oncologist – INCLIVA Institute – Valencia, Spain

Noelia coordinated the prospective collection of fresh frozen and FFPE samples and performed the RNA extraction of the INCLIVA-Valencia cohort (Chapter 2 and 4).

Elizabeth C Smyth - Cambridge University Hospital

Elizabeth provided style and content feedbacks.

Udai Banerji – Drug and Development Unit – The Royal Marsden Hospital

Professor Banerji was back-up supervisor of this project. As internal assessor he provided me with directions and feedback at the beginning of the project and after my transfer viva.

Other contributions

Andres Cervantes (INCLIVA Institute, Valencia), David Cunningham (Royal Marsden Hospital) and Naureen Starling (Royal Marsden Hospital) were Principal Investigators of sample collections included in this thesis.

Funding

This work was funded by Cancer Research UK through The Institute of Cancer Research. Other funding included The MedTech SuperConnector accelerator program.

I acknowledge National Institute for Health Research funding to The Royal Marsden and The Institute of Cancer Research Biomedical Research Centre.

Abbreviations

AUC – Area Under the Curve

BRAF – Raf murine sarcoma viral oncogene homolog B

CAPOX – Capecitabine and oxaliplatin

CEA – Carcinoembryonic Antigen

CMS – Consensus Molecular Subtype

CRC – colorectal cancer

CRCA-38 – Colorectal Cancer Assigner (38 gene signature)

CRCSC – Colorectal Cancer Subtyping Consortium

DA – Digital Analyzer

DCR – Disease Control Rate

dMMR – deficient Mismatch Repair

EGFR – Epidermal growth factor receptor

EMT –Epithelial to mesenchymal transition

FF – Fresh frozen

FFPE – Formalin Fixed Paraffin Embedded

FOLFOX – fluorouracil and oxaliplatin

FOLFOXIRI – fluorouracil, oxaliplatin and irinotecan

FOLFIRI – fluorouracil and irinotecan

5-FU – fluorouracil

IHC – Immuno-histochemistry

KRAS – Kirsten Rat Sarcoma virus

MLH 1 – MutL homolog 1

MSH 2 and 6 – MutS protein homolog 2 and 6

MSI – Microsatellite instability

ORR – Overall Response Rate

OS – Overall Survival

PCA – Principal Component Analysis

PMS 2 – Postmeiotic Segregation homolog 2

PFS – Progression-free Survival

rankCMS-38 – Consensus Molecular Subtype (38 gene signature and rank algorithm)

qRT-PCR – quantitative Reverse Transcription Polymerase Chain Reaction

RCC – Reporter Code Count

RF – Random Forest

RLF – Reporter Library File

RNAseq – RNA sequencing

ROC – Receiver Operating Characteristic

SCNA – Somatic Copy Number Alterations

SSP – Single-Sample Prediction

TCGA – The Cancer Genome Atlas

TGF beta – Transforming Growth Factor beta 1

TME – Total Mesorectal Excision

List of Figures

List of Tables

Chapter 1 Introduction

1.1 Colorectal cancer

1.1.1 Historical notes

The beginning of the 20th century expanded the understanding of the aetiology and molecular events associated with hereditary colorectal cancer (CRC). The study of the “Family G” (suspected CRC family) started with Dr Aldred Warthin in 1895 followed by Lynch and Krush in 1971, when they reported what became known as the Lynch syndrome (1-3).

In parallel with these studies, mutations in the *adenomatous polyposis coli* (*APC*) gene were initially associated with the familial adenomatous polyposis (FAP) hereditary syndrome (1930) and subsequently with the initial step of tumorigenesis by Fearon and Vogelstein (1,4).

The vast majority (~75%) of CRC cases are sporadic; of the remaining 25%, approximately 20% of cases are considered familial in view of a positive family history of CRC whereas only about 5% are hereditary and linked to highly penetrant gene mutations (**Table 1**) (1).

	Germline mutation associated gene(s)	Molecular alteration(s)	Hereditary	Associated phenotype	CRC risk
Lynch Syndrome	*MLH1/ MSH2/ PMS2/ MSH6*	Deficit in mismatch repair process	Autosomal dominant	Increased risk of colorectal, endometrial, gastric, ovarian, ureteral and renal pelvis cancer	52-82% lifetime
Familial Adenomatous Polyposis (FAP)	*APC*	Deregulation in WNT-signalling, intercellular adhesion, microtubules assembly and stabilization	Autosomal dominant	>100 adenomatous polyps in young age, increased risk of CRC and duodenal cancer	100% risk by age of 50
Attenuated FAP (aFAP)			Autosomal dominant	10-100 adenomatous polyps, CRC (later onset than FAP), upper gastrointestinal and duodenal cancer risk similar to FAP	70% risk by age of 80
MUTYH-associated polyposis (MAP)	*MUTYH*	Dysfunctional adenine glycosylate excision repair	Autosomal recessive	Increased risk of CRC and duodenal cancer	63% risk by age of 60

Table 1. Main hereditary syndromes associated with CRC risk (1).

1.1.2 Incidence, prevalence, mortality worldwide and in the UK

Cancer is the first leading cause of death before the age of 70 years in developed countries. For combined male and female data, CRC is the third most commonly diagnosed cancer after lung and breast with more than 1.8 million new cases per year estimated to occur in 2018 and the second most common cause of death for cancer after lung cancer with over 881,000 deaths per year (5). Incidence and mortality rates differ significantly across world regions. Colorectal cancer is typically associated with high or very high Human Development Index (HDI) countries and considered a marker of socioeconomic development (5). In the United Kingdom (UK), CRC was the fourth most common cancer in 2015 with more than 41,000 new cases and more than 16,000 deaths (6).

Three different patterns in changes in trends have been recently identified: 1) increasing incidence and mortality (Russia, China and Brazil); 2) increasing incidence and decreasing mortality (UK, Canada and Singapore); 3) decreasing incidence and mortality (US, Japan, France) (7). While the decreased mortality could be associated with effective screening programs leading to early detection and overall improvement in global management, the increasing incidence especially in younger age groups is not completely understood. More convincing evidence of the negative impact of processed meat, alcohol intake and obesity in increased colon cancer risk are available; however these factors are not so clearly associated with the increased risk of developing a rectal cancer (5).

With respect to age groups, a recent analysis of incidence patterns in the United States demonstrated increasing incidence of colon cancer in young adults (up to 2.4% per year in the very young adults age 20-29) and even steeper for rectal cancer (3.2%) in the same age group. Opposite trends were shown for patients older than 55 years of age (8).

1.1.3 Diagnosis and staging

In screening programmes, the detection of faecal occult blood (FOB) before the occurrence of clinical symptoms demonstrated a reduction in mortality from CRC by 15% to 30% within randomised control trials (9) and annual/biannual FOB test for individuals aged 50-74 is a recommended screening method in adjunction with a colonoscopy at the age of 50 (10). A positive test justifies endoscopic procedures (sigmoidoscopy or preferably total colonoscopy), which allow localization and biopsy of any lesions. After the diagnosis of cancer, clinical assessment, blood tests including the carcinoembryonic antigen (CEA) and a computed tomography (CT) scan are recommended to rule out metastatic disease. A pelvic magnetic resonance imaging (MRI) is recommended during the clinical staging of rectal cancer. Surgical staging includes the assessment of nodal and liver spreading and the extension of the primary tumour through the bowel wall and adjacent organs. A minimum of 12 lymph nodes yield is

recommended in particular to accurately distinguish between stages II and III (10). A thorough risk assessment is necessary to define patients' prognosis and treatment approach. The TNM staging system takes into account the level of tumour penetration into the bowel wall (T), the presence of node metastases and the numbers of lymph nodes involved (N) and the presence of distant metastases (M). In rectal cancer, the evaluation of the circumferential resection margin (CRM) involvement, total mesorectal excision (TME) quality and extranodal extension, extramural vascular invasion, peritoneal invasion and tumour budding should also be evaluated (11). After surgical resection the 5-year survival is in the order of 85%-95% in stage I disease (T1-2, N0, M0), 60%-80% in stage II (T3-4, N0, M0), 30%-60% in stage III (any T, N1-2, M0) and less than 10% in stage IV (any T, any N, M1) (6,10).

1.1.4 Recommended treatment strategies by stage

1.1.4.1 Early stage

Surgical resection is the standard treatment approach in the absence of metastatic disease (stages I-III). Following radical resection, adjuvant chemotherapy is recommended in case of stage III disease while the benefit in stage II patients is very limited. A meta-analysis demonstrated a non-significant decrement in 5-year disease-free survival of about 2% (from 81.4% to 79.3%) in stage II patients who received adjuvant therapy (12). International guidelines do not recommend adjuvant therapy in unselected patients with stage II disease (10,13). However, adjuvant therapy should be considered in high-risk stage II disease. Common criteria to define the high-risk stage II disease include the presence of one or more of the following factors: poor differentiation; vascular, lymphatic or perineural invasion; obstructive tumour or colonic perforation; pathological T4 with tumour penetration into the surface of the visceral peritoneum or invasion of adjacent organs; lymph nodes yield less than 12 (10). Careful considerations need to be taken in the presence of tumours harbouring mismatch-repair-deficiency (dMMR) or high microsatellite instability (MSI-H), as discussed in the biomarker section.

The thymidylate synthase inhibitor fluorouracil (5-FU) was initially patented in 1956 and came into clinical use in 1962 (14). Initially established in the metastatic setting, it entered the first adjuvant studies in CRC in the early 1970s. In the 1980s a series of studies in the Mayo Clinic tested the activity and toxicity profiles of different types of schedules in combination with folinic acid. About 30% reduction in the risk of death was confirmed by multiple studies at the beginning of the 1990s (15). Its orally available pro-drug capecitabine was patented in 1992 and was approved for medical use six years later (14). Its equivalence to 5-FU in the adjuvant treatment of stage III CRC was demonstrated in 2005 (16).

Oxaliplatin is the only agent that has demonstrated survival benefit when added to a fluoropyrimidine-based regimen in adjuvant setting. Three randomised phase III trials (Multicentre International Study of Oxaliplatin/5-fluorouracil/leucovorin in the Adjuvant Treatment of Colon Cancer [MOSAIC], the NO16968 and The National Surgical Adjuvant Breast and Bowel project [NSABP-C07]) demonstrated an overall reduction in the relative risk of relapse between 16% and 20% with an increase in disease free survival (DFS) rates in the order of 5% (17-19). Two of these trials also demonstrated about 20% relative risk reduction in the risk of death (17,18). Subgroup analyses of the MOSAIC and NSABP-C07 trials demonstrated that the significant benefit of oxaliplatin is observed in stage III patients but not in stage II patient (17,18), with only a trend towards improvement in the high-risk stage II patients (17). Age is another factor to be considered when offering adjuvant therapy. A pooled analysis of seven randomised trials of fluorouracil (with folinic acid or levamisole) or surgery alone demonstrated a significant effect of adjuvant therapy in improving overall survival (OS) and time-to-recurrence (TTR) in patients older than 70 years of age; this benefit was not different from what seen in other age groups (20). Furthermore, no significant increase of toxic effect compared to younger patients was observed (20). These data justify the consideration of adjuvant fluoropyrimidine in stage III patients independently of their age group. However, the use of oxaliplatin is less justifiable based on the fact that no significant benefit in DFS, OS and TTR was demonstrated when the

three oxaliplatin-based trials were pooled together in the Adjuvant Colon Cancer End Point (ACCENT) meta-analysis (21).

In view of the significant neurotoxicity related to oxaliplatin (grade 3 in 12.5% of patients during treatment and still present at least as a grade 1 in about 15% of patients in the MOSAIC trial) its optimal duration according to different stages of risk was evaluated in the International Duration Evaluation of Adjuvant therapy (IDEA) pooled analysis (22). Six randomised phase 3 trials evaluating 3 versus 6 months of oxaliplatin-based therapy in stage III patients were included. Although less toxic, non-inferiority of the shorter regimen was not demonstrated overall. However, pre-specified subgroup analyses demonstrated the non-inferiority of 3 versus 6 months of capecitabine and oxaliplatin (CAPOX) in particular in stage III lower-risk patients (T1-3, N1).

While extensively used in metastatic setting, neither irinotecan nor biological agents, including the anti-vascular endothelial growth factor (VEGF) and anti-epidermal growth factor receptor (EGFR) agents, demonstrated improved outcomes in adjuvant setting (23-27).

Neoadjuvant therapy (chemoradiation or radiotherapy alone) is recommended in case of locally advanced rectal cancer or of intermediate cases when a good quality mesorectal excision cannot be assured (11). The role of adjuvant chemotherapy after neoadjuvant treatment and surgery is less clear than in colon cancer in view of the fact that patients with rectal tumours were generally excluded from adjuvant studies. The quality of clinical staging and suboptimal surgery in different studies may also impact in understanding the benefit from adjuvant chemotherapy, which in general seemed smaller than in colon cancer in terms of DFS and possibly minimal in OS (11).

Neoadjuvant chemotherapy is not recommended in operable colon cancer. A UK national study already demonstrated the feasibility, acceptable toxicity and perioperative morbidity of three cycles of preoperative oxaliplatin, fluorouracil and folinic acid (28). Full publication of long-term oncological outcomes is awaited.

1.1.4.2 Metastatic setting

In presence of metastatic disease a multidisciplinary team management is recommended in first instance to determine whether the disease is initially clearly resectable or initially unresectable (29). In the presence of oligometastatic disease (typically confined to the liver or a few organs e.g. liver and lungs), a chance of cure or long-term survival exists and can be up to 20-50% in patients who obtained a complete resection (R0) (29). Both surgical criteria (feasibility and chance to achieve an R0 resection maintaining an adequate liver function) and oncological criteria (number of lesions, suspicion of extrahepatic disease and in general aggressive tumour biology) need to be taken into account (29).

In case of technically up-front resectable disease, surgery either with or without peri-operative treatment (3 months of oxaliplatin and fluoropyrimidine-based therapy pre-operatively and 3 months post-operatively) is a standard approach without a definitive consensus for one or the other strategy (29). The milestone EPOC trial demonstrated a significant 3-year progression-free survival (PFS) rate improvement using peri-operative therapy in the order of 9% in patients undergoing resection (30). However there was only a trend towards an overall survival benefit in the randomised population. Peri-operative chemotherapy should be considered in presence of unclear prognostic features suggestive of a more aggressive disease. The addition of cetuximab is not recommended in view of the detrimental results demonstrated in the New EPOC trial, while the role of bevacizumab has not yet been fully established (31).

In presence of “not clearly resectable” disease, systemic therapy is recommended. The treatment strategy varies depending on the overall goal and patient’s fitness. More aggressive regimens with two (a fluoropyrimidine and irinotecan, FOLFIRI/CAPIRI, or oxaliplatin FOLFOX/CAPOX) or three chemotherapy agents (FOLFOXIRI) with or without a biological agent (cetuximab/panitumumab or bevacizumab) may be considered when the overall goal is to reduce the disease burden. In a pooled analysis of 11 studies, the four-drug regimen FOLFOXIRI-bevacizumab demonstrated a 69% objective response rate (ORR) with surgical conversion rate of distant metastases of

39.1% (32). Multiple phase II studies demonstrated the feasibility and safety of a doublet chemotherapy regimen and bevacizumab or cetuximab with variable liver resection rates ranging from 30-90% (29). Recently, FOLFOXIRI and anti-EGFR agents demonstrated very high ORR when used as first-line approach reaching 90.6% using panitumumab in the phase II VOLFI study and 71.6% using cetuximab in the phase II MACBETH study (33,34). However, these studies were not intended to define the conversion rate of not upfront resectable disease. Furthermore, in view of the high rate of grade 3/5 toxicities related to these regimens (over 30%) careful consideration is required when deployed not within the context of a clinical trial.

When surgery with radical intent is not feasible due to the unfavourable location of the disease or patients' fitness, local ablation techniques are usually considered in centres with adequate expertise and after multidisciplinary team discussion. These techniques include thermal or radiofrequency ablation, high conformal radiation techniques, chemoembolization or radioembolization with yttrium-90 microspheres in case of parenchymal lesions (35). Cytoreductive surgery and hyperthermic intraperitoneal chemotherapy (HIPEC) may be considered in case of metastatic disease limited to the peritoneum and in centres with expertise with this approach (35). Although some degree of benefit in terms of local disease and symptoms control may be achieved, the evidence of long-term benefit remains to be established.

Finally, in presence of clearly unresectable disease with a low likelihood of achieving a radical resection and cure, systemic treatment or best supportive care are the recommended approaches. The aims are symptoms control, maintenance of the best possible quality of life and life prolongation. A fluoropyrimidine monotherapy is indicated for patients not able to tolerate a more aggressive treatment. A doublet with oxaliplatin or irinotecan is the most commonly used approach. The choice between the two agents is usually based on whether the patient previously received oxaliplatin in adjuvant setting, the time to progression from oxaliplatin and the presence of residual peripheral neuropathy. In chemo-naïve patients, the choice is based on patients' comorbidities and preferences (the alopecia related to irinotecan is the most common discriminatory factor). The sequential use of oxaliplatin-based followed

by irinotecan-based chemotherapy at progression or the opposite sequence demonstrated to be equally effective (36). When used in first-line, oxaliplatin has the advantage of being potentially re-challenged in more advanced settings especially when previously interrupted in a non-refractory setting (37,38). Biological agents are appropriate in first-line setting unless contraindicated based on patients' comorbidities and subject to countries' specific restrictions. While in patients with tumours carrying a mutant Rat Sarcoma Virus (*RAS*) gene the only biological agent indicated is bevacizumab (or ramucirumab/aflibercept in second-line setting), in *RAS* wild-type patients either anti-angiogenic or anti-EGFR agents are possible options (35). Subgroups analyses of the FIRE-3 phase III clinical trial (FOLFIRI plus cetuximab versus FOLFIRI plus bevacizumab) demonstrated a significant survival benefit using the anti-EGFR agent in the *RAS* wild-type population (39). Similar results were demonstrated in the phase II PEAK study using panitumumab instead of cetuximab and FOLFOX as chemotherapy backbone (40). Conversely, no difference were demonstrated in The Cancer and Leukemia B and Southwest Oncology Group (CALGB/SWOG) 80405 trial, where the difference in chemotherapy backbones (both FOLFOX and FOLFIRI were used) and the longer OS in the overall population better than expected (29 months observed compared to 22 months expected) possibly had an impact on the final results (41). In patients that do not progress during treatment, discontinuation with a chemotherapy-free interval or maintenance therapy should be discussed. While oxaliplatin is more frequently interrupted after 16-24 weeks due to cumulative peripheral neuropathy, irinotecan may be continued until progression or until no longer tolerated (35).

The choice of regimen in the second-line setting is commonly dictated by what received in first-line. More commonly both the chemotherapy backbone and biological agent (if indicated) are switched. However, different strategies are justified by several clinical trials. As examples, after first-line regimen including the anti-angiogenic agent bevacizumab, the switch to a different chemotherapy backbone plus bevacizumab or another anti-angiogenic agent like ramucirumab or aflibercept is justified by randomised phase III trial (42-44). Less evidence is available for the continuation of anti-EGFR therapy beyond progression.

Although the phase II CAPRI-GOIM study demonstrated a marginal benefit in PFS in RAS wild-type population, emerging evidence may support an intermittent rather than continuous use of anti-EGFR agents (45,46). The available biomarkers currently used to inform treatment decisions and evidence related to anti-EGFR therapy will be extensively discussed in the next paragraphs.

Two further agents are available in the treatment of previously treated metastatic CRC based on randomised phase III trials. The small molecule multikinase inhibitor regorafenib demonstrated a small (in the order of 2 months) but significant benefit in OS prolongation when compared to placebo in both Caucasian and Asian population (47,48). More recently, the oral cytotoxic agent trifluridine-tipiracil also demonstrated a significant 2-months improvement in OS when compared to placebo (49). The study included also patients that previously received regorafenib in about 20% of the cases. Therefore, both the drugs represent evidence-based treatment options after second-line therapies. The choice of one agent over the other is usually based on residual toxicities and organ function, in particular limited bone-marrow reserve (regorafenib preferred) and limited hepatic reserve (trifluridine-tipiracil preferred).

Although recommended by international guidelines, the access to and reimbursement of biological agents differ from country to country. In the UK, none of the anti-angiogenic agents including regorafenib is available outside the context of a clinical trial and anti-EGFR therapies are recommended only as first-line therapy in conjunction with doublet chemotherapy (50).

1.1.5 Molecular mechanisms of action of approved drugs for CRC

Table 2 summarises the drug agents commonly used in metastatic CRC and their mechanisms of actions.

Drug	Class	Mechanism of action	Reference
Chemotherapy agents			
5-Fluorouracile	Fluorinated analogue of the uracil base	Inhibition of thymidilate synthase (and consequent pyrimidine biosynthesis); false base incorporation into RNA and DNA.	51
Capecitabine	Antimetabolite	Pro-drug activated into fluorouracil by thymidine phosphorylase	52
Oxaliplatin	Organoplatinum complex	Intra-strands DNA adducts with block of replication and transcription	53
Irinotecan	Semisynthetic derivative of camptothecin	Stabilization of topoisomerase I/DNA complexes causing replication arrest and replication fork disassenbly	54
Trifluridine/tipiracil	Flurorinated antimetabolite agent (trifluridine) and thymidine phosphorylase inhibitor (tipiracil)	DNA incorporation and thymidilate synthase inhibition	55
Mitomycin C	Antitumour antibiotic	DNA alkylation with inter-strands DNA-DNA formation	56
Temozolamide	Imidazotetrazine	DNA alkylation with replication fork collapse	57
Raltitrexed	Folate antimetabolites	Thymidilate synthase inhibitor	58
Anti-angiogenic agents			
Bevacizumab	Humanized monoclonal IgG1 antibody	Selective binding of circulating VEGF	59
Ziv-Aflibercept	Recombinant fusion protein fused to humanized IgG1 antibody	Selective binding of VEGF-A, -B and PlGF	60
Ramucirumab	Fully humanized monoclonal IgG1 antibody	Selective binding of VEGFR-2	61
Regorafenib	Small molecule	Multiple-kinase inhibitor including VEGFR-1,-2,-3, TIE2, FGFR-1, PDGFR, KIT, RET, RAF-1, BRAF	62
Anti-EGFR agents			
Cetuximab	Human-mouse chimeric monoclonal antibody	Competitive binding of the extracellular domains of EGFR to inhibit dimerization	63
Panitumumab	Fully humanized monoclonal IgG2 antibody	Competitive and selective binding of EGFR	64
Immunotherapy agents			
Pembrolizumab	Humanized monoclonal IgG4 antibody	Selective binding of PD-1 with dysruption of interaction with its ligands (inhibitors of cellular immune response)	65
Nivolumab	Humanized monoclonal IgG4 antibody	Selective binding of PD-1	66
Ipilimumab	Fully humanized monoclonal IgG1 antibody	Selective binding and inhibition of CTLA-4, enhancing T-cell response to cancer cells	67

Table 2. Chemotherapy, targeted agents and monoclonal antibodies frequently used as systemic treatment of CRC.

1.1.5.1 Chemotherapy agents

Multiple fluorinated antimetabolites demonstrated anticancer activity by interfering with DNA synthesis in proliferating cells. The inhibition of the activity of the thymidilate synthase enzyme results in reduced availability of deoxythymidine triphosphate and 5,10-methylentetrahydrofolate, both essential for thymidine synthesis (51). Fluorouracil and deoxyfluorouracil triphosphate could also be directly incorporated into RNA and DNA, respectively, because of their analogy with the naturally occurring uracil base. Different schedules of administration of fluoropyrimidines were developed in order to modulate their different mechanisms of action in different phases of the cell cycle to ultimately increase their cytotoxic effect (51). The most commonly adopted regimens for 5-FU is as a bolus followed by continuous infusion (instead of pulse administration

over 5 days) after intravenous load of folinic acid (5-FU modulator by increasing the intracellular pool of folates which stabilises the inhibition of thymidilate synthase) (51).

Oxaliplatin, a third generation platinum compound, is the only platinum salt that demonstrated activity in CRC (53). Although differences in the type of DNA adducts platinum-induced have been clearly documented, the reason behind this selective sensitivity to oxaliplatin in CRC but not to carboplatin or cisplatin (both also active in other cancers including gastric cancer) are not completely understood (53). Different DNA-repair mechanisms are involved in the interaction with cisplatin or oxaliplatin-induced adducts which partially justify this differential tissue-sensitivity (68).

Irinotecan is a semisynthetic derivative of camptothecin, a natural alkaloid produced by the Camptotheca acuminate Chinese tree (54). After enzymatic conversion, the active metabolite SN-38 stabilises the DNA-Topoisomerase I complex during cell replication, leading to cell death (54).

Both oxaliplatin and irinotecan demonstrated modest single agent activity (in the order of 20% in terms of response rate) and well-tolerated toxicity profiles, making both these agents suitable for combination regimens with fluoropyrimidines (69).

DNA alkylating agents including temozolamide and mitomycin C demonstrated very modest activity in CRC and they are currently not considered in clinical practice, especially after more effective regimens with oxaliplatin and irinotecan were developed (56,57,70).

1.1.5.2 Anti-angiogenic agents

The high metabolic rate of cancer cells with consequent high demand of oxygen frequently exposes the tumoural bed to hypoxic conditions. Hypoxia is one of the drivers of neo-angiogenesis (71). The overexpression of elements of the VEGF gene family induced by the hypoxia-inducible factor-1alpha made these elements attractive targets for anti-cancer therapies (59). Four anti-cancer agents are approved in CRC (**Table 2**). The three monoclonal antibodies

selectively bind the ligands (bevacizumab and ziv-aflibercept) or the receptor (ramucirumab) of the VEGF gene products. None of them demonstrated significant single agent activity but synergistic effect when added to chemotherapy regimens (72-74). Multiple mechanisms of action of these agents have been described and include the inhibition of new vessels formation and the regression of newly formed vessels, vasoconstriction via the activation of endothelial cell-derived nitric oxide with consequent reduced blood supply to cancer cells; normalization of vasculature with increased delivery and uptake of chemotherapy agents (synergistic effect); potential direct effect on cancer cells with inhibition of invasion and migration induced by VEGFR-1 (75). While these functions are mediated by the antigen-binding fragment (Fab) of these antibodies, the fragment crystallisable (Fc), or tail region, mediates the antibody-dependent cell-mediated cytotoxicity (ADCC) activity of these antibodies. Via ADCC, innate and adoptive immune responses are triggered and have been frequently reported as further effect of monoclonal antibodies (76).

1.1.5.3 Anti-EGFR agents

Currently two monoclonal antibodies, cetuximab and panitumumab, are approved for the treatment of CRC (**Table 2**). For both agents the mechanisms of actions are initiated by the selective binding of the extracellular portion of the EGFR. An in-depth description of the molecular events following EGFR blockade, mechanisms of resistance and different activity based on cancer molecular characteristics are discussed in Chapter 4.

1.1.5.4 Immunotherapy agents

Historically, CRC has been considered not immunogenic based on numerous observations including no reported cases of spontaneous tumour regression (opposite to melanomas or renal cell cancers), controversial reports on the presence and prognostic meaning of tumour-infiltrated lymphocytes and no response demonstrated in first generation immunotherapy studies (77).

However, the subgroup of patients with tumours harbouring genetic (microsatellite) instability due to defective mismatch repair mechanisms showed presence of intraepithelial T-cytotoxic lymphocytes and, clinically, a better prognosis (77). Mismatch repair deficient (MMRd) CRCs have up to 100 times more somatic mutations than proficient tumours (78). Using whole-exome sequencing, Le et al. found a mean of 1782 somatic mutations per tumour versus only 73 in patients with proficient tumours (78). More than 30% of these mutations were potentially immunogenic, as associated with peptides with high affinity for Major Histocompatibility Complex (MHC) class I (neoantigens), able to activate a T-cell response (78-79). These findings explain why MMRd CRC have a better prognosis, possibly due to their enhanced host immune response (80). When treated with an immunotherapy checkpoint inhibitor (pembrolizumab), MMRd tumours responded, while no responses where observed in MMR proficient tumours (78). Conversely, the presence of MMRd is associated with resistance to fluoropyrimidines (80). In line with pre-clinical studies in cell lines showing resistance to 5FU in MMRd lineages, the use of adjuvant 5-FU did not demonstrate significant benefit in early stage disease (81). The immune suppressive effect of chemotherapy may potentially justify the detrimental effect observed in 5-FU treated MMRd CRC (80).

1.1.6 Mechanisms of therapy response and resistance in CRC

The majority of chemotherapy agents active in CRC interfere with DNA synthesis or replication (**Table 2**). Their preferential effect on cancer rather than normal cells is explained by the higher proliferation rate of cancer cells, requiring higher DNA synthesis/replication activities. However, not all CRCs respond to chemotherapy at the same way. **Table 3** describes the most commonly used regimens and their expected response rates.

Regimens	3rd drug	4th drug	Response rate	Line	Subtype	Reference
Two-drugs regimens						
Fluoropyrimidine + oxaliplatin			54%	1 line	All comers	82
Fluoropyrimidine + irinotecan			56%	1 line	All comers	82
Fluoropyrimidine + anti-angiogenic			19%	1 line (elderly)	All comers	83
Irinotecan + anti-EGFR			16%	>1 line	All comers	84
Capecitabine + temozolamide			16%	2 line	MGMT methylated	85
Capecitabine + Mitomycine			15%	>2 lines	All comers	70
Ipilimumab + Nivolumab			55%	>2 lines	MSI High	86
Three-drugs regimens						
Fluoropyrimidine + oxaliplatin	Anti-angiogenic		49%	1 line	All comers	87
Fluoropyrimidine + oxaliplatin	Anti-EGFR		46%	1 line	60% in RAS7BRAF wt	88
Fluoropyrimidine + irinotecan	Anti-angiogenic		58%	1 line	All comers	89
Fluoropyrimidine + irinotecan	Anti-EGFR		62%	1 line	72% in RAS wt	90,91
Fluoropyrimidine + oxaliplatin	Irinotecan		60%	1 line	All comers	91
Four-drugs regimens						
Fluoropyrimidine + oxaliplatin	Irinotecan	Anti-angiogenic	65%	1 line	All comers	92
Fluoropyrimidine + oxaliplatin	Irinotecan	Anti-EGFR	87%	1 line	All comers	93

Table 3. Regimens commonly used for the treatment of metastatic CRC and their expected response rates.

One of the most intuitive answers justifying these different behaviours is the potential diversity in proliferation rates. However, controversial results related to the role of the expression of the antigen KI-67 (proliferation marker) have been published (94). Some studies identified increased benefit from adjuvant treatment in highly proliferating tumours compared to low proliferating one, and a recent meta-analysis demonstrated the overall poor prognostic value of high KI67 expression (95). However, no convincing evidence is currently available to justify the routine assessment of this marker.

Multiple enzymatic reactions are involved in the activation of chemotherapy agents and in their metabolism. Hence, diverse levels of activity and expression of these enzymes may affect the anti-tumour effect and the toxicities caused by drugs. As example, fluoropyrimidines are metabolised by the dihydropyrimidine dehydrogenase (DPD) enzyme, which demonstrated a variable level of activity based on inherited polymorphisms of the gene (96). Heterozygosis for mutant DPD alleles is estimated in about 5% of the population, with increased risk to suffer from severe toxicities during fluoropyrimidine treatment, therefore testing for DPD deficiency is now recommended to guide treatment dose adjustments (29). When measured in the tumour, low levels of DPD expression were

significantly associated with increased response to 5-FU (96). Conversely, altered activities of enzymes related to pro-drug activation as in the case of irinotecan (activated by the carboxylesterase or the uridine diphosphate-glucuronyl transferase) may lead to reduced drug response (54). Synergistic effect between fluoropyrimidines and irinotecan is also related to a more prolonged enzymatic inhibition, of the thymidilate synthase in this case, leading to enhanced cytotoxic effect (54).

Overall, both tumour intrinsic characteristics and enzymatic activity in normal tissues play a role in modulating the drug exposure and ultimately efficacy. However, the definition of normal, enhanced or reduced activity of enzymes in their more common variants or in mutant forms is challenging, extremely variable according to physiological statuses and external factors. The activity of the cytochrome p450 is an example: this cytochrome is involved in the metabolism of multiple chemotherapy drugs; its activity is modulated by age, intake of certain foods and polypharmacy (especially in the elderly) and environmental factors like exposure to smoking (97). Similarly, the presence of germ line polymorphisms in genes related to the chemotherapy drugs pharmacodynamics, as example the methylentetrahydrofolate reductase (MTHFR) or the Excision Repair Cross-Complementing group 1 (ERCC1) genes, has been associated with different response to treatments (98, 99).

1.1.7 Recent successes and failures in the treatment of colorectal cancer

Following the success in melanoma and lung cancer, treatment with immune checkpoint inhibitors also reached a subset of CRC patients. Pembrolizumab and nivolumab, both inhibiting the programmed cell death 1 (PD1) receptor predominantly expressed on cytotoxic T lymphocytes, received Food and Drug Administration (FDA) approval in 2017 for previously treated CRC patients with tumours harbouring mismatch-repair-deficiency (dMMR) or high microsatellite instability (MSI-H). The approval was based upon phase II studies demonstrating response rates up to 50% in dMMR/MSI-H patients with more than 70% of them still alive after one year (100,101). Multiple promising studies

testing immunotherapy agents in non-chemorefractory setting are on-going (102). Recently, the combination of nivolumab and ipilimumab (targeting the cytotoxic T lymphocyte antigen 4 or CTLA4) demonstrated an ORR of 60% and a disease control rate (DCR) of 84% in 45 previously untreated dMMR/MSI-H CRC patients enrolled in the phase II study Checkmate 142 (103). The same combination demonstrated promising results in a small cohort of stage III dMMR/MSI-H CRC patients with 4 out of 7 patients reaching complete tumour response (104). Although very encouraging, none of these drugs is currently available as standard treatment option in Europe. The results of phase III trials are largely awaited for potential European Medicines Agency (EMA) approval. Other encouraging signals are coming from studies targeting the human epidermal growth factor receptor 2 (HER2) in chemorefractory CRC patients. The Italian HERACLES phase II trial demonstrated the activity of the combination of transtuzumab and lapatinib in HER2-positive tumours with 30% of ORR (105). Similarly, the combination of pertuzumab and transtuzumab in HER2-amplified CRC patients demonstrated the same level of activity (32% ORR) (106). Although exciting, both dMMR/MSI-H and HER2 positive tumours represent 5% of the metastatic CRC population.

Sadly, the number of recent failures seems overwhelmingly higher than successes. Firstly, no response to immunotherapy has been seen in MMR proficient patients who represent the vast majority of metastatic CRC. Multiple trials are evaluating potential strategies to overcome this immune resistance (102).

Secondly, a number of phase III trials unfortunately missed the primary end-point in both early (as previously discussed in the adjuvant setting paragraph) and metastatic setting, leading to a very limited OS improvement in CRC over the last decade in comparison with other tumour types. Examples are the stem-cell inhibitor napabucasin and the multikinase inhibitor nintedanib, both tested in the chemorefractory setting (107,108). Other disappointing results were presented at The European Society of Medical Oncology (ESMO) World GI Conference 2018 by Bendell *et* al. The combination of the anti-PD-L1 agent atezolizumab with the MEK1/MEK2 inhibitor cobimetinib did not improve OS when compared to regorafenib in a phase III study in previously treated CRC

patients with microsatellite stable (MSS) tumours or low MSI tumours (109). This disappointment came after preclinical studies and the phase Ib study demonstrated a synergistic effect in increasing the T cytotoxic activity (110,111). Atezolizumab added to 5FU and bevacizumab also failed to improve PFS as switch-maintenance strategy after induction chemotherapy compared to 5-FU plus bevacizumab alone (112).

1.1.8 Potential reasons for treatments failure

Multiple reasons are frequently considered as potential justification for these failures, including tumour heterogeneity, tumour evolution and lack of reproducible biomarkers able to identify different tumour biology more or less likely to respond to different treatment (CRC biomarkers will be discussed in the next sub-chapter).

1.1.8.1 Tumour heterogeneity

Tumour heterogeneity is defined by the existence of cancer cells genotypically and phenotypically different that may consequently have distinctive biological behaviours within the same tumoural mass (intra-tumoural heterogeneity), between tumours with same histological type (inter-tumoural heterogeneity) or between the primary tumour and metastatic sites (113).

Colorectal cancer is a very heterogeneous disease at multiple “omics” levels (114). Inter-tumoural heterogeneity was demonstrated in The Cancer Genome Atlas where 276 primary tumour samples were analysed at multi-dimensional levels. Although all histologically classified as adenocarcinomas, different subgroups of cancers could be identified using unsupervised analyses (114). These groups represent inter-tumoural heterogeneity. Other authors demonstrated how multiple biopsies from the same bulky tumoural mass expressed different types of genes with different phenotypes expressed by the central region of the tumour and the invasive front (115). This study represented

an example of intra-tumoural heterogeneity in CRC. Higher heterogeneity estimated as number of subclones using whole-exome sequencing data has been associated with poorer survival and higher tendency to metastasize to the liver (116).

Conversely, remarkably high concordance between the type of mutations found in the primary tumour and in matched metastatic sites has been demonstrated in multiple studies (117). This suggests a less degree of heterogeneity in space (different sites of disease) and time (in case of metachronous metastases) within the same patient. However, from a gene expression point of view a lesser degree of concordance between primary and metastases has been demonstrated, with up to 5 different clusters of tumours in the primary tumours but only 2 clusters in liver metastases (118). These differences may be potentially justified by the pattern of tumour evolution in CRC.

1.1.8.2 Tumour evolution

Tumour evolution is a field that studies the changes of tumour cell populations under selective pressures (119). Selection and persistency of certain clones over others can be secondary to the fitness of each clone and ability to survive in different conditions, as for example in presence of hypoxia in the tissue (119). The natural evolution of CRC has been demonstrated to be punctuated, where a high number of genomic aberrations occur in a short time-period at a very early stage with only few dominant clones expanding (119, 120). This evolutionary model is characterised by high intratumoural heterogeneity at baseline with expansion of stable clones that minimally modify during tumour progression (119).

Similarly, chemotherapy selective pressure or the ability of the immune system to recognise and destroy specific clones may also affect tumour composition and evolution (121, 122).

While heterogeneity may be responsible for primary treatment resistance (the up-front lack of response to therapy), tumour evolution may justify secondary resistance to therapies (the lack of response in tumours that previously

responded to the therapy). The emergence of *RAS* mutant clones during treatment with anti-EGFR therapy is an example of clonal selection under therapy pressure and will be discussed further in Chapter 4 (46).

Furthermore, the vast majority of new agents are tested in a chemorefractory setting, when the level of heterogeneity has possibly exponentially increased and the only notions of tumour molecular biology available are from archival tissue samples collected before the deployment of multiple lines of therapy. Robust biomarkers to guide personalised medicine and a more successful development and implementation of new drugs in CRC are eagerly awaited.

1.2 Biomarkers in colorectal cancer

1.2.1 Genomic biomarkers

According to the National Cancer Institute Dictionary of Cancer Terms, a biomarker is "a biological molecule found in blood, other body fluids or tissue that is a sign of a normal or abnormal process or of a condition or disease". Based on the capacity to provide certain evidence, a biomarker is commonly classified as pharmacodynamic (evidence about a direct pharmacological drug effect), prognostic (evidence about patients' outcomes independent of any intervention), predictive (evidence about the probability of benefit/toxicity from a specific intervention) and surrogate (substitute for a clinically meaningful endpoint) (123).

A PubMed search for "biomarker" and "colorectal cancer" identified more than 3500 articles in May 2019. However, only three biomarkers [MMR/MSI status, *RAS* mutational status and B-Raf and v-Raf murin sarcoma viral oncogene homolog B (*BRAF)* mutational status] are recommended by international guidelines in routine clinical practice (13, 35).

The MMR/MSI status plays multiple roles in different settings. In stage II disease, dMMR is present in about 10-15% of the patients and has a positive

prognostic value (10). Therefore, even in the presence of high-risk features, adjuvant chemotherapy should be omitted. Moreover, multiple studies suggested the lack of benefit (negative predictive value) from adjuvant fluorouracil regimens (124). A possible explanation for the better prognosis of MSI-High tumours compared to MSS tumours is the presence of mutation-associated neoantigens (MANAs) due to defective mismatch-repair mechanisms in MSI-High cancers; the MANAs can be recognised by the immune system, which reacts against tumours, contributing to long-term control (121).

In stage III disease, the prognostic role is unclear and no definitive conclusions related to effect of oxaliplatin are available. Consequently, the MMR status should not be taken into account in the risk assessment and in the decision for adjuvant treatment of stage III cancers outside the context of a clinical trial (13). In metastatic setting, the presence of dMMR status (about 5% of metastatic population) has a dual biomarker role: it has a negative prognostic value (shorter PFS and OS compared to pMMR) and a positive predictive value for benefit from immunotherapy as discussed previously (100, 101, 125).

The negative predictive value of *RAS* and *BRAF* mutations for anti-EGFR agents will be discussed in chapter 4. From a prognostic perspective, the negative value of *BRAF* mutation is well established (126). The aggressive behaviour of *BRAF* mutant tumours led clinicians to approach these patients with intensified regimens associated with higher response rates (as example FOLFOXIRI with or without bevacizumab) (32). The *BRAF* mutation has a well established positive predictive role in melanoma where *BRAF* targeted agents are successfully deployed (127). The same success was not replicated in CRC, potentially in view of the feedback activation of the MAPK signalling pathway driven by EGFR in epithelial cells (but not in melanoma cells) (128,129). These evidence lead to triplet targeted therapy combinations, simultaneously targeting *BRAF* and possible feedback loops via *EGFR* and *MEK*. These combinations are feasible; the outcome of the randomised BEACON trial is largely awaited and may potentially benchmark a new standard of care for these aggressive tumours (130).

The prognostic value of *RAS* mutation is less clear and possibly confounded by the different clinical features associated with mutations in different exons of the three *RAS* human genes, *KRAS*, *NRAS* and *HRAS* (131). These mutations are still widely considered undruggable; however multiple trials of new agents targeting *RAS* downstream effectors are on-going (132).

Some other genomic markers including HER2 and MET amplification and kinase gene rearrangements involving ALK and NTRK1 recently raised interest because these are potentially actionable with exceptional responses reported; however their frequency is less than 5% in the overall CRC population (133).

1.2.2 Gene expression biomarkers

A multitude of single gene biomarkers have been investigated as prognostic or predictive markers in both early and metastatic settings of CRC with inconsistent results (134). The development of high-throughput technologies, e.g. microarray technology, allowed the simultaneous measurement of a large number of genes. Hence, new molecular classifications of cancer exclusively based on gene expression became more and more popular (135). Several multi-gene assays have been developed and validated in independent CRC clinical trial cohorts. The majority of these aimed to classify early stage CRC patients into different risk classes for disease relapse: of these, ColoPrint, Oncotype DX and ColDx are the most extensively studied (136-138). Their major characteristics are summarized in **Table 4**. Although all these tests were validated in independent cohorts and demonstrated to identify different risk groups, their use is not recommended (13). Reasons for this are mainly related to the limited value in predicting benefit from adjuvant therapy and therefore to the limited impact on any treatment decisions. Moreover, whether the different signatures are representative of existing biological entities is unclear.

	Patients in discovery cohort(s) (n, stage)	Number of genes	Patients in validation cohort (n, stage)	Prognostic value	Predictive of adjuvant therapy benefit
Oncotype DX (136)	1851, stage II/III	12	1436, stage II	Yes	No
ColoPrint (137)	188, stage I/II/III/IV	18	206, stage I/II/III	Yes	No
ColDx (138)	215, stage II	634	144, stage II	Yes	No

Table 4. Multi-gene assays previously developed as potential prognostic tools in CRC.

In an effort to identify potential differences in biology, prognosis and response to different treatments, Sadanandam *et al.* previously defined five gene expression subtypes of CRC using unsupervised clustering methods and a 786-gene signature (CRCAssigner-786) (139). The subtypes were named based on their similarities with different regions of the normal colonic crypt: (i) goblet-like, characterised by increased expression of *MUC2* and *TFF3* genes, typically associated with normal goblet cells; (ii) enterocyte, resembling the highly differentiated enterocyte cells of the upper crypt; (iii) transit-amplifying (TA), an heterogeneous group representing the highly proliferative TA compartment in differentiation from the stem niche to specialised epithelium; (iv) stem-like, with high expression of genes of the Wnt signalling pathway, stem-ness signatures and mesenchymal cells; and (v) inflammatory, associated with increased expression of chemokines and interferon-related genes and enriched for MSI tumours. The subtypes were associated with distinctive prognostic value in the early disease setting, with TA and goblet-like demonstrating very good prognosis after curative surgery, inflammatory and enterocyte associated with intermediate prognosis and the stem-like, expressing epithelial-to-mesenchymal (EMT) features, associated with the worse prognosis. In terms of treatment prediction, the stem-like subtype was associated with increased likelihood of response to FOLFIRI regimen, while the TA subtype demonstrated enrichment for tumours sensitive to anti-EGFR agents. Distinctive association between subtypes and genomic features were demonstrated. These included the association between *KRAS* mutations and the goblet-like, dMMR/MSI-H and

BRAF mutations and the inflammatory subtype (and with the goblet-like to a lesser extent). Cell lines of CRC were also classified according to the subtypes, demonstrating that the subtypes retain their identity even under culture conditions (139,140).

Five other independent groups identified gene expression subtypes with different algorithms. De Sousa E Melo *et al.* identified three CRC groups: CCS1, associated with *KRAS* mutations, CCS2 enriched for dMMR/MSI-H tumours and CCS3, characterised by poor prognosis (141). The three subtypes were subsequently reconciled with the CRCAssigner subtypes (142). At the same time, Marisa and colleagues identified six CRC subtypes; Roepman *et al.* identified three subtypes while both Schliker *et al.* and Budinska *et al.* identified five subtypes (143-146). In a review article we extensively described differences and similarities of the different subtypes identified by each group (147). Taken together these studies underlined the heterogeneity of CRC: a subtype associated with dMMR/MSI-H status and one associated with mesenchymal signatures were consistently identified as distinctive entities across all the different classification systems. The rest of the tumours were grouped all together in one classifier or further subdivided in two, three or four entities in others.

In 2015, the six independent groups formed the Colorectal Cancer Subtyping Consortium (CRCSC) lead by the SAGE Bionetworks, with the aim of reconciling the six classifiers and providing a joint classification system that could unify the communication across the entire research and clinical community (148). By analysing more than 3000 patient samples, four consensus molecular subtypes (CMS) were defined: CMS1 (MSI immune), characterized by microsatellite instability and strong immune activation; CMS2 (canonical), with an epithelial profile, chromosomally unstable, with marked WNT and MYC signalling activation; CMS3 (metabolic), epithelial with evident metabolic dysregulation; and CMS4 (mesenchymal) with transforming growth factor beta (TGF-β) activation, prominent angiogenesis, stromal invasion and poor prognosis. Up to 13% of the samples were unclassified, possibly due to the co-existence of more than one subtype within each sample (mixed subtype).

The CRCAssigner and CMS classifications were highly associated. The inflammatory subtype was represented by CMS1; TA and enterocyte were merged together in the CMS2; goblet-like and stem-like were represented by CMS3 and CMS4, respectively (**Figure 1**). Similarly to the CRCAssigner, the CMS classification demonstrated to be highly prognostic: the outcomes of CMS1 tumours were comparable to what previously described in dMMR/MSI-H tumours (excellent prognosis after surgery but worse survival after relapse); CMS2 and CMS3 demonstrated intermediate outcomes while CMS4 was associated with worse relapse-free survival.

The prognostic role of the CMS classification was subsequently validated in multiple correlative analyses of clinical trial samples in both early stage and metastatic setting (149-152). Conflicting results were shown when the CMS subtypes were assessed as predictive factors of benefit from standard treatment options. In a perspective article we recently analysed potential strengths and weaknesses of the CMS classification as clinically useful biomarker (153). Though using the classifier to prospectively stratify patients in biomarker-enriched clinical trials is very appealing, multiple contexts and possible equivocal factors need to be further clarified; these have been analysed in the review article (153). The type of sample analysed from each patient, the number of genes and the algorithm used to identify the subtypes are critical and may make the comparison across different studies difficult to interpret. Also, a robust assay with optimal characteristics for routine application is mandatory to successfully use a biomarker in the clinic. The lack of such an assay to implement gene expression subtypes from bench to bedside is the main driver of this project.

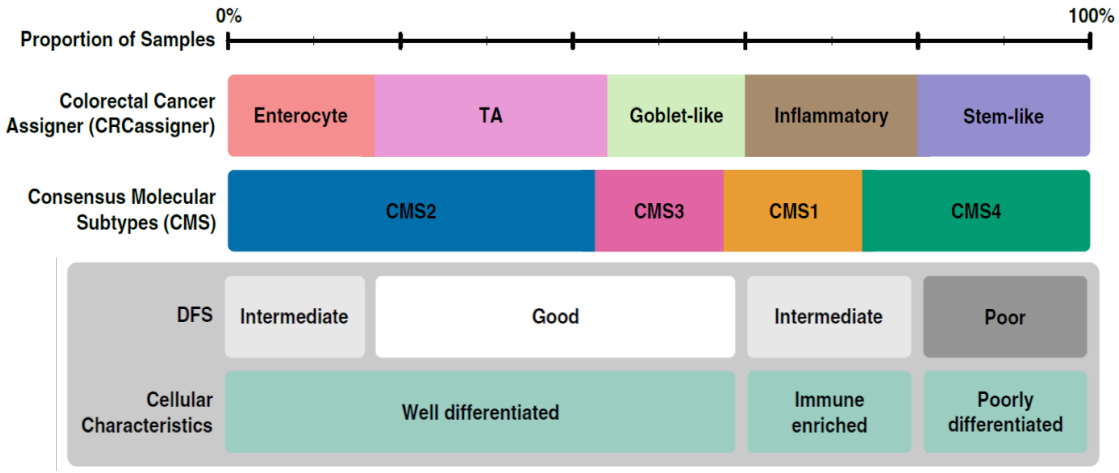

Figure 1. Associations between CRCAssigner and CMS subtypes and their prognostic and cellular characteristics (modified from Fontana *et al.* (147). Although highly associated, the two classifications are not completely overlapping, particularly in the case of CMS4 disease (including stem-like but also a non-negligible proportion of inflammatory subtypes).

1.3 Aims and significance of the thesis

The lack of low-cost, easy-to-use assays with a turn-around time suitable for clinical application is a major limiting factor to prospectively validate the potential prognostic and predictive value of the subtypes. Previous subtype data were generated using microarray, which is expensive, time-consuming and requires high bioinformatics input. This platform has been gradually replaced by RNAseq, which is in addition less suitable for formalin-fixed paraffin-embedded (FFPE) samples (outside research settings), limiting further its applicability.

Based on the original CRCAssigner-786, a small gene panel assay for nCounter platform (NanoString Technologies) has been recently developed in The Sadanandam lab and validated using fresh frozen samples (NanoCRCAssigner). A low-cost protocol was optimised (154).

In this project, I aimed to test the clinical utility of this assay using FFPE samples, to further develop it to concurrently identify CMS subtypes and to assess the potential prognostic and predictive values. Overall, confirming that these assays are able to identify clinically meaningful subgroups may facilitate patient stratification and the assessment of new drugs in biomarker-selected trials for precision medicine.

In doing that, I developed wet-lab and basic bioinformatics skills thank to the multidisciplinary nature of The Sadanandam lab. What described in this thesis was performed by myself, unless otherwise specified.

Aim 1: Assays development for CRC subtypes identification

Develop low-cost and robust gene expression subtype assays for nCounter platform (NanoString Technologies) to classify CRC samples (fresh frozen and FFPE) and validate the results using data generated with alternative platforms (microarrays, RNAseq).

Aim 2: Assays validation using clinico-pathological features in Caucasian population and comparison with Asian population

Assess whether the newly developed assays are able to capture the known subtype-related features in the Caucasian population as indirect validation; then assess for the first time whether similar clinical and molecular characteristics are present in the Asian population.

Aim 3: Assays as tools to predict treatment response

Assess the potential predictive value of the newly developed assays and the biomarkers therein in predicting anti-EGFR therapy response.

Chapter 2 Development of biomarker assays to define CRC subtypes

2.1 Introduction

As described in the chapter 1 and section 1.2.2, it is essential to develop biomarker assay(s) to predict prognosis and drug responses in early and/or metastatic CRC. While multiple assays failed to show its utility in the clinic as those in **Table 4**, here I have attempted to develop a biomarker assay using the published gene expression subtypes.

2.1.1 Steps for assay development: choice of the platform

With the view of developing a multiplexed assay suitable for routine clinical application, the nCounter platform (NanoString Technologies) was chosen. Customized assays for this platform have been previously developed for subtyping purposes in other cancer types. Specifically, the Prosigna® Breast Cancer Prognostic Gene Signature Assay for nCounter platform received United States and European approvals to predict the risk of relapse in patients with breast cancer, based on the intrinsic gene expression subtypes previously identified by Perou *et al.* (155,156). Other assays were developed to classify lymphoma and medulloblastoma subtypes (157,158). These studies demonstrated the feasibility of subtypes assessment using FFPE samples. In fact the lack of pre-amplification and complementary DNA conversion steps is particularly effective in avoiding potential biases in the presence of degraded RNA (as is typical of FFPE preparations). The user-friendly protocol with short hands-on (about 15 minutes in total) and quick turn-around times (2 days) makes the platform attractive for clinical application.

2.1.2 NanoString Technologies

The nCounter platform is a barcoding technology for multiplexed single molecule digital counting, which allows the detection and quantification of up to 800 different RNA, DNA or protein targets (159). The workflow is divided into three main steps: 1. Hybridization; 2. Purification and immobilization; 3. Count (detailed in Methods, section 2.3.7). Two different protocols for RNA are available: the standard protocol for pre-made gene panels curated and pre-formatted by the company as well as for customized gene panels; the Elements chemistry protocol, for customized panels only. For the Standard protocol, pre-built biotin-labelled capture probes (for pre-selected genes) and fluorescently colour coded reporter probes are pre-mixed in the so-called CodeSet formulation. For the Elements protocol, only capture and reporter tags are pre-mixed in the nCounter Elements TagSet formulation; custom-designed target-specific oligonucleotide probe pairs (reporter and capture probes can be obtained separately [from Integrated DNA Technologies, Inc., Leuven, Belgium in our case)]. **Figure 2** shows a schematic of the hybridization product using the Elements protocol.

The Elements protocol includes a few initial extra-steps compared to the standard protocol (described in Methods, section 2.3.4). With the exception of hybridization times and final volume, the workflows of Standard and Elements protocols are the same.

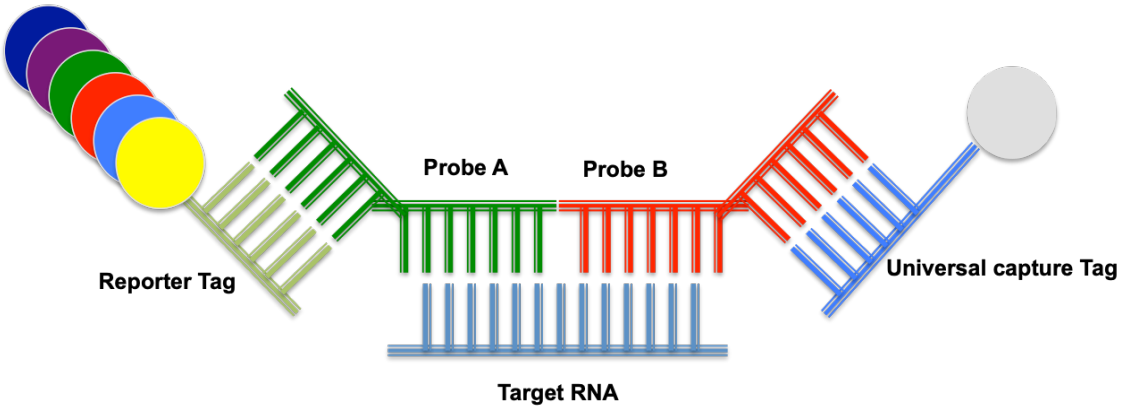

Figure 2. Schematic of the hybridization product (Elements protocol). Each target RNA hybridises with probes A and B. Probe B includes a sequence to hybridize with the universal capture Tag (the same for all genes). The Universal capture Tag will bind the product to the cartridge in the Prep Station, avoiding the product being washed away. Probe A binds the target RNA and the Reported Tag (unique colour code for each gene) that will be counted in the Digital Analyser.

2.1.3 On-going development of a customized assay for nCounter platform

When I joined the lab, the development of a customised panel for the detection of the CRCAssigner subtypes was on-going using the modified protocol for Elements chemistry. Briefly, a limited panel of 50 genes were initially selected based on the original CRCAssigner-786 publication (139). These included 7 genes originally proposed as subtype biomarkers for quantitative Reverse Transcription Polymerase chain Reaction (qRT-PCR) and immunohistochemistry (IHC); among the top 2 to 9 highest scoring genes for each subtype from predictive analysis of microarrays (PAM) centroids (160), three genes differentially expressed between the cetuximab-sensitive and cetuximab-resistant TA sub-subtypes and other genes representing subtype-specific pathways like epithelial-to-mesenchymal transition (EMT), MET tyrosine kinase signaling and NFkB signaling. Ten housekeeping genes were added to the customised panel to enable expression normalization. Hence, a 60-gene assay was developed as per Elements protocol (NanoCRCA) (154).

Six CRC cohorts of primary tumour samples were collected: three derived from fresh-frozen samples with microarrays or RNA-seq data available for comparison; two derived from FFPE samples and one with matched FFPE and fresh-frozen samples.

I contributed to this project with the identification of samples (match FFPE/fresh-frozen cohort), generating part of the data with the Elements protocol and with the manuscript writing, gaining a co-first authorship (154).

Using an in-house published machine-learning pipeline (*intPredict:* available at: https://rdrr.io/github/syspremed/intPredict/), the number of genes to robustly classify samples into subtypes was further reduced to 38 and new centroids (average expression of each gene in each subtype) were developed. Hence the CRCAssigner subtypes will be from now on called CRCA-38 subtypes. High correlations (>0.88) between Standard and Elements protocol and between technical replicates (>0.96) were demonstrated (154).

This study established the feasibility of customized assay development for CRC subtypes classification and the background for this thesis.

2.2 Specific aims

1. Develop a gene expression subtype assay for molecular classification of CRC samples into CMS subtypes (NanoCMS);
2. Implement the NanoCMS assay into the previously developed NanoCRC for simultaneous classification of CRC samples into CMS and CRCA-38 subtypes;
3. Evaluate the newly developed assays in FFPE and fresh-frozen samples.

2.3 Methods

2.3.1 Subtypes classification methods

In order to understand the performance of a new classification system, different classifiers were deployed in this chapter. A summary of the most commonly deployed methods is provided below:

a) Network-based method: the CMS subtypes were originally identified using a network-based method by the CRC Subtyping Consortium (CRCSC) (148). In the CRCSC, the newly built gene expression database of primary CRC (from public and private databases) was deployed to classify the samples into subtypes according to the six different pre-consensus classification systems available (for a total of 27 different subtypes labels). Markov Cluster (MCL) algorithm (unsupervised method based on finding natural grouping of items using graphs and weighted connector lines) was used to identify recurrent subtypes patterns and consolidate the 27 different labels into 4 consensus labels (and one undetermined category) (148,161). Each sample included in the CRCSC study has a “Network label”; hence, this classification is not reproducible outside the CRCSC database. The “Network label” of samples included in one of the CRCSC databases (E-MTAB-990) was downloaded and used in this chapter (as per following sections).
b) Random Forest classifier: unsupervised clustering method based on multiple decision-trees; each sample is classified multiple times according to the multiple decision–trees built within the algorithm; the final classification for each sample is the class that was assigned to that sample for the highest number of times (162).
c) Prediction of Microarray Method (PAM)-centroids correlation: this method was originally developed to identify gene expression subtypes using microarrays data. It uses subsets of genes that best characterise each subtypes (centroids) and compares each expression profile with the centroids. Each sample is assigned to the subtype of the centroid with higher correlation (160).

d) CMS single-sample prediction (SSP) classifier: this classifier was developed by the CRCSC and used a similar-to-centroids method (148). By definition, a SSP method requires that the output for each sample remains the same independently by the composition of series that the sample is analysed within. Twenty different centroids were built using 693 genes and five datasets included in the consortium paper; only datasets that were previously normalised without median-centering (where the expression level of each gene is not affected by the expression of that gene in the other samples of the series) were included to define the centroids. Using this method, the similarity between expression profiles of each sample and the 20 centroids is calculated.
e) Rank classifier: rank-based classifiers of highly dimensional data are based on the transformation of the real expression values with their rank (163). Here we adopted a rank-based method to compare the ranked value of genes in each CMS centroids with the rank value of the corresponding gene in each sample (further details are explained in the following sections).

2.3.2 Gene selection for a custom NanoCMS assay

In line with the NanoCRCA development, the initial step for the development of an assay for CMS subtypes prediction included the selection of subtype-specific genes from the previously developed CMS centroids (148). The original CMS classifier was developed based on a random-forest-based network algorithm and definition of multiple centroids using different datasets derived from distinct platforms (Agilent versus *Affymetrix* versus RNAseq) and tissue preservation methods (FFPE versus fresh-frozen). With the view to deploying the assay in a clinical setting where FFPE is the most commonly available type of tissue (and assuming to work in all the platforms), the centroids derived from the only available FFPE dataset within the consortium were chosen (E-MTAB-990 from the PETACC-3 trial (23), described in section 2.3.3).

The following steps were performed by Ms Katherine Eason (PhD student, The Sadanandam lab):

1. Data download:
    a. The CMS centroids were retrieved form the CMSclassifier R package (https://github.com/Sage-Bionetworks/CMSclassifier);
    b. Subtypes labels and expression data were downloaded from the CRCSC Synapse page (labels: https://www.synapse.org/#!Synapse:syn4978511; gene expression: https://www.synapse.org/#!Synapse:syn4983432);
2. Gene selection: The 10 highly expressed genes for each of the four CMS subtypes were selected. Two genes (*AGR3* and *REG4*) were in common between the CMS1 and CMS3, resulting in a 38-gene panel (**Figure 3**).

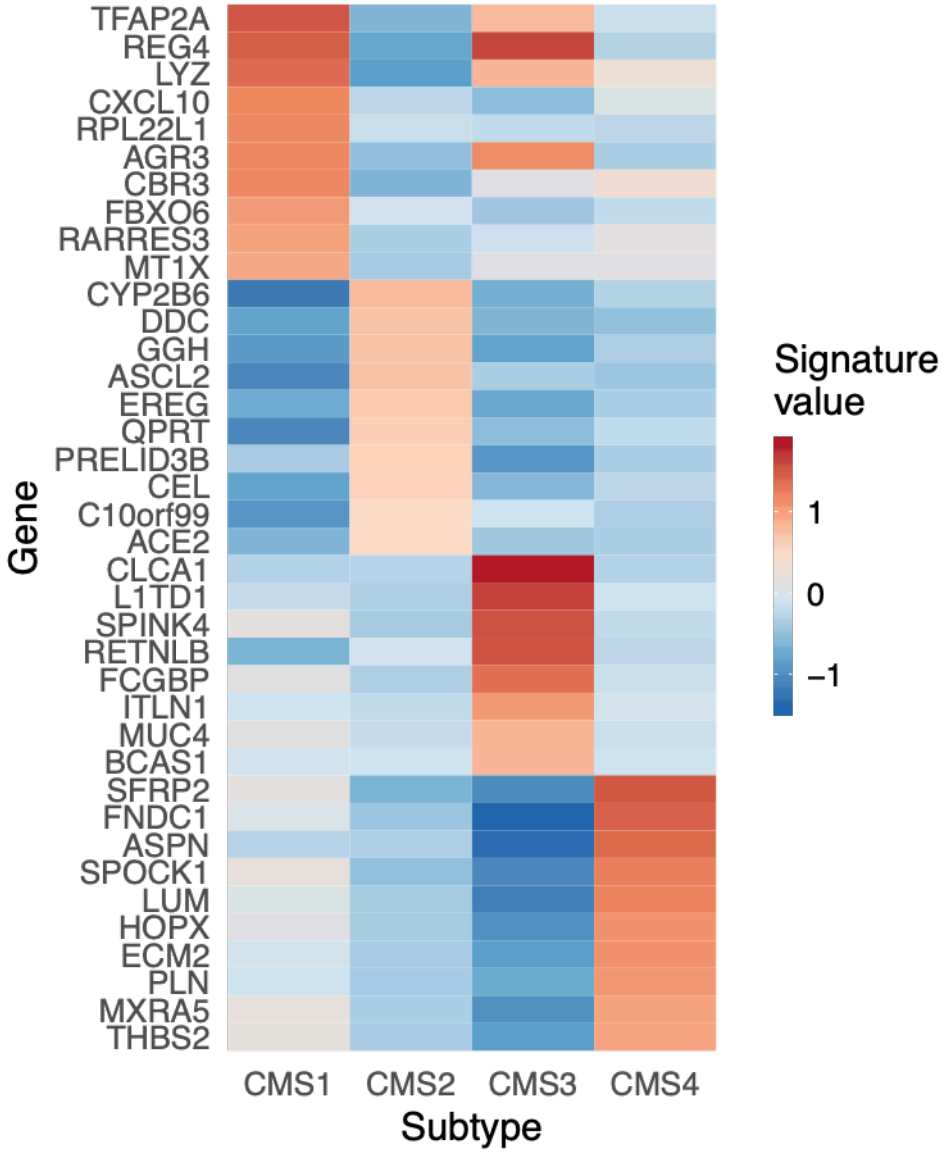

Figure 3. Heatmap including the top 10 highly expressed genes in each of the subtypes selected from the PETACC-3 dataset (23) included in the final custom 38-gene panel for the CMS assay.

2.3.3 Gene pair rank-based subtyping algorithm

A novel classifier was developed by Ms Katherine Eason (PhD Student, The Sadanandam Lab). This was based on ranking the expression of pairs of genes. The ranking was firstly performed in the PETACC-3 centroids; then in each samples' gene expression profile:

1. A list of all the pairs of genes included in the 38-gene panel is created;
2. For each pair (e.g. *gene A* and *gene B*), the gene which has the higher weight is recorded (e.g. *gene A* > *gene B*);
3. The number of times that every gene pair has the same ranking in both the PETACC-3 centroids and the sample (e.g. *gene A* > *gene B* in both the centroids and sample) is counted;
4. This count is normalised to the number of gene pairs;
5. A percentage of concordant gene pairs between the sample and each subtype centroid is obtained.
6. The subtype centroid which has the highest percentage of gene pairs concordance is assigned as the subtype of that sample.

2.3.4 Publicly available data

As described above, gene selection and classifier development were based on the E-MTAB-990 dataset from the PETACC-3 trial (23) because the gene expression was derived from FFPE material; the classifier was subsequently validated in the TCGA dataset. Major characteristics of these datasets are here described:

1. E-MTAB-990 datasets: microarrays gene expression data derived from 688 FFPE primary tumour samples from patients with stage III CRC enrolled in the adjuvant PETACC-3 clinical trial; in this trial patients were randomised to receive adjuvant 5-FU alone or in combination with irinotecan (23);
2. TCGA dataset: RNAseq gene expression data derived from prospective series of 603 fresh-frozen primary tumour samples from patients with stage I to IV CRC (114).

2.3.5 Biomarker assay development for CMS subtypes

The selected 38 subtype-specific genes for CMS subtypes and the 10 housekeeping genes previously included in the NanoCRCA assay were shared with the NanoString Bioinformatics Team. Specific oligonucleotide sequences in the region of 100 base pairs were designed to target each gene. Half of the sequence was extended at the terminal end with the complementary sequence of the universal capture probe. This sequence represented the Probe B. The other half was extended with a pre-codified sequence unique for each gene able to hybridize with a pre-defined reporter tag. This sequence represented the Probe A. Probe A and B sequences were assessed with The Basic Local Alignment Search Tool (BLAST, available at: https://blast.ncbi.nlm.nih.gov/) to confirm the identity and coverage of each gene variant (this step was performed by the NanoString Bioinformatics Team and crossed-checked by myself and other members in The Sadanandam Lab). With the view to integrating the 38 new gene-assays into the previously developed NanoCRCA, each sequence was also crossed-checked with the sequences of the pre-existing probes for the 50 genes included in the NanoCRCA assay; this to avoid possible dimerization and artefacts.

Each probe was built from Integrated DNA Technologies, Inc., based on the developed sequences produced by NanoString. Upon receipt, the oligos were pooled and diluted as per Elements protocol: firstly, all the target-specific reporter codes are pooled-together and diluted in TE buffer (Pool A, final dilution: 20 pM); similarly, all capture probes are pooled together and diluted in TE buffer (Pool B, final dilution: 100 pM). Then, an aliquot of each set of pools is emulsified in a TE-Tween 20 solution (working pools). Working pools and hybridization buffer are then added to the TagSet. The obtained solution is the equivalent of the pre-made CodeSet formulation for Standard protocol.

2.3.6 Samples collection

Four CRC cohorts of primary tumour samples collected prior to any treatment were investigated:

1. The RETRO-C cohort: FFPE samples were collected within a retrospective study at the Royal Marsden Hospital (ethic committee reference: 10/H0308/28): A retrospective translational study: characterisation of molecular predictors of response to cetuximab or panitumumab in patients with colorectal cancer (Principal Investigator, PI: Professor David Cunningham). Full details of this study and patients' characteristics are provided in Chapter 4;
2. The Singapore fresh frozen cohort (SG-FF): fresh-frozen samples of a consecutive series of CRC patients who consented to an approved research protocol at the Singapore General Hospital, Singapore (SingHealth Institutional Review Board: 2013/110/B; named collaborator: Dr Iain Beehuat Tan);
3. The Singapore FFPE (SG-FFPE): FFPE samples of consecutive CRC patients enrolled in the same study described above (SG-FF);
4. The INCLIVA-Valencia match cohort: prospectively collected samples of CRC patients who received surgery for stage I, II or III disease at the Research Institute INCLIVA, Valencia, Spain (Comité Etico de Investigacion Clinica del Clìnico Universitario de Valencia: F-CE-GEva-15; named collaborators: Prof. Andrés Cervantes and Dr. Noelia Tarazona).

2.3.7 Nucleic acid extraction and quality control steps

For the RETRO-C cohort, nucleic acids were extracted by myself; for the INCLIVA cohort, the extraction was performed by Dr Tarazona in Spain using the same protocol and kit suggested by us. For both the Singapore cohorts, the

extraction was performed in Singapore using the QIAGEN RNAeasy™ FFPE kit.

After initial training from Ms Chanthirika Ragulan (High Scientific Officer, The Sadanandam Lab), I proceeded with the extraction independently. Firstly, the blocks were evaluated by trained pathologists (from the different institutions, RMH, Singapore and Valencia) and only those with at least 30% of tumour content were selected; areas with high tumour cellularity were marked on haematoxylin and eosin slides and macrodissected in unstained slides (7-10 μm thickness, up to 10 slides for each block depending on the dimensions of the area available for macrodissection). Following deparaffinization with xylene, graded washes in ethanol and rehydration in pure water, total RNA and DNA were simultaneously isolated using the Ambion RecoverAll™ kit and quantified with NanoDrop™ 2000 Spectrophotometer (Thermo Fisher) according to manufactures' instructions.

During year one, before the optimization of the in-house protocol was completed, the level of RNA fragmentation (RNA Integrity Number, RIN) and smear analysis (percentage of fragments below 300 base pairs) of a few samples from the RETRO-C cohort were analyzed using the Bioanalyzer 6000 Nano assay™ from Thermo Fisher (subsequently dropped after technical replicates assessment, described below).

2.3.8 Gene expression analysis

The expression level of the 38 subtype-specific genes (or 86 genes after integration of the two assays) and the 10 housekeeping genes was measured using the nCounter Max Analysis System (nCounter Prep Station plus nCounter Digital Analyzer) from NanoString Technologies and the Element XT protocol following the three-step workflow:

1. In the hybridization step, the CodeSet (or the equivalent solution for the Elements protocol) are mixed with up to 100 ng of RNA. Hybridization reactions are prepared as per manufactures' instructions for 18 hours at

65°C. A modification of the Elements protocol was optimized in our lab, with hybridization time extended to 20 hours at a temperature of 67°C.

2. In the purification and immobilization step, the hybridized products are pipetted using the nCounter Prep Station (NanoString Technologies) and immobilized on a sample cartridge with streptavidin-coated imaging surface; then all oriented in the same direction using an electromagnetic field. This automated step takes about 3.5 hours.
3. In the final step, the cartridge is placed in the nCounter Digital Analyzer where each fluorescent barcode is counted in about 5 hours. The data are collected in a Reporter Code Count (RCC) file for quality control and downstream analyses.

Hybridization temperature and duration were modified to 67°C and 20 hours as per the previously optimised protocol (154). In the nCounter Max Analysis System samples are processed in batches of 12.

In order to understand whether increased RNA input was necessary when using degraded RNA extracted from FFPE samples, a small pilot study was designed. Technical replicates were generated using 50 ng, 100 ng, 150 ng and an adjusted input based on the smear analysis and calculated according to the following formula:

$$Adjusted\ Input = \frac{Target\ Input}{100 - [\%between\ 50 - 300nt]} * 100$$

In view of the high Pearson correlation demonstrated using 100 ng, 150 ng and the adjusted input of RNA (slightly dropping when using 50 ng), 100 ng was chosen as target input for all the subsequent analyses performed in this thesis (**Figure 4**).

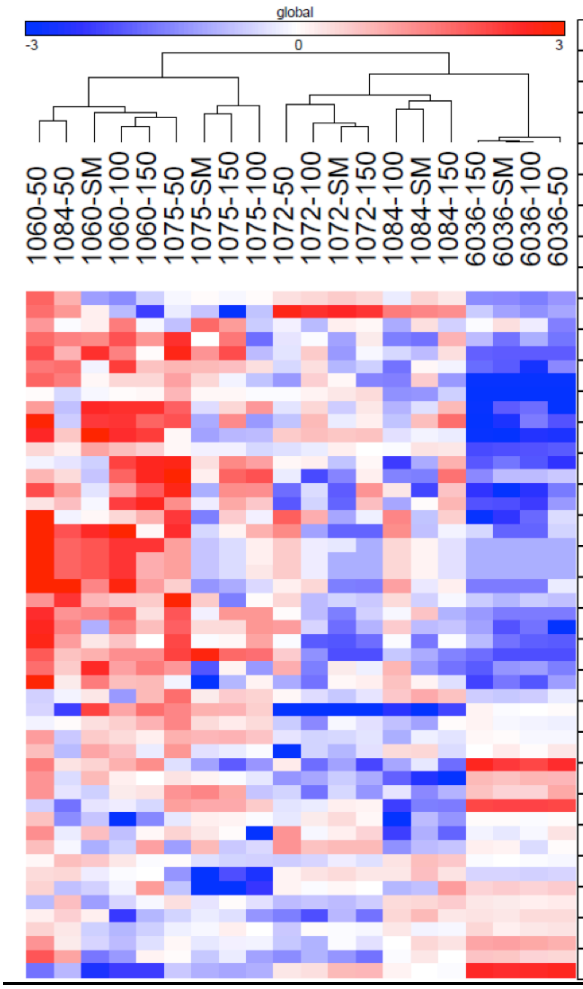

Sample ID	Adj input (ng)	Correlation	
1060	188	SM-150	0.81
		SM-100	0.84
		SM-50	0.80
		150-100	0.87
		150-50	0.70
		100-50	0.73
1072	169	SM-150	0.96
		SM-100	0.95
		SM-50	0.92
		150-100	0.95
		150-50	0.88
		100-50	0.90
1084	192	SM-150	0.90
		SM-100	0.90
		SM-50	0.86
		150-100	0.87
		150-50	0.84
		100-50	0.88
6036	192	SM-150	0.99
		SM-100	0.99
		SM-50	0.98
		150-100	0.98
		150-50	0.97
		100-50	0.98
1075	270	SM-150	0.91
		SM-100	0.87
		SM-50	0.83
		150-100	0.89
		150-50	0.91
		100-50	0.90

Figure 4. Sample input titration study. Heatmap showing the gene expression of five samples (in four replicates) clustered by expression similarities (left). Table with Pearson correlation coefficient for each pairs of RNA input (right). SM (smear) represents the input calculated based on the different degrees of RNA integrity.

2.3.9 Quality control steps using nSolver Analysis System

The RCC files generated by the nCounter Digital Analyser (DA) were uploaded into the nSolver analysis software version 3.0 from NanoString Technologies.

Here, four parameters with standardised cut-offs are systematically analysed:

1. Imaging quality control (QC): the percentage of field of views (FOVs) successfully counted by the DA;

2. Binding density QC: assessing whether too many of too few probes are present within the FOVs;
3. Positive control linearity: assessing the correlation of spikes-in probes targeting positive control molecules in pre-defined and escalating concentrations added by NanoString into any of the CodSets or TagSets;
4. Positive control limit of detection: assessing the metrics of positive and negative controls, with the positive control with lower concentration expected to produce a raw count higher than the mean of 8 negative controls (targeting non-human genes).

If any of the standard QC parameters is out of range, the sample is flagged with a red flag and should be excluded from any downstream analyses. Once all the RCC files are generated, those that have passed the first QC control step (no red flags) are selected in a new nSolver experiment and read with the appropriate Reporter Library File (RLF). The RLF file is produced by the NanoString Bioinformatics Team and contains information required to match each barcode with the assigned gene (either target or housekeeping). Both raw counts and normalised counts are automatically produced. In details, the normalised counts are generated after subtraction of the geometric mean of the 8 negative controls, followed by normalization based on the geometric mean of 6 positive controls (to account for difference in TagSet input due to pipetting errors) and geometric mean of the 10 housekeeping genes. Samples are flagged if the computed normalization factor is between 0.3 and 3 (for positive controls) and between 0.1 and 10 (for housekeeping genes).

In order to evaluate the performance of the 10 selected housekeeping genes in each sample cohort and consequently select only those suitable for the analysis, the nCounter Advanced Analysis version 2.0 plugin for nSolver Software was used.

To perform this analysis another file from NanoString is required: the Probe Annotation File specific for each assay. This file contains functional and cell profiling annotations for each gene of the panel. However, in the case of our

newly developed custom assays this file was required exclusively to be able to proceed in the analysis with built-in R libraries. The raw count data are assessed using the geNorm algorithm integrated in the analysis protocol; only housekeeping genes selected by the algorithm are used for data normalization. The program also provides Principal Component Analysis (PCA) plots to assess for the presence of batch effect and possible outlier samples.

Once the housekeeping genes to use are established a new experiment is generated: the normalised data can now be exported in a log2 scale for downstream analysis.

2.4 Results

2.4.1 Assessment of the need for a new algorithm for subtype prediction using the PETACC-3 on-line dataset

As discussed in Chapter 1 and in a recently published perspective manuscript (153), the number and type of genes and the type of algorithm used to predict gene expression subtypes may significantly affect the classification. In recent studies post-CRCSC publication, the CMS subtypes were determined using unselected sets of genes included in the CMS centroids and the publicly available CMS algorithms (Random Forest classifier, RF; single-sample prediction classifier, SSP).

Once the 38 genes were selected from the PETACC-3 centroids (methods) two main points required clarification:

1. Which classification (whether that one obtained with the RF or SSP algorithm) should be considered as the reference;
2. Whether either the RF or SSP algorithms could be maintained or whether a new algorithm was required when using the reduced set of genes in order to minimise the misclassification error.

With the help of Ms Eason, we aimed to demonstrate that a minimal discordance between network classification (available on-line for the PETACC-3 samples and derived from a network-based approached described in the original publication (148)), RF and SSP algorithms exists using the entire sets of genes available within the PETACC-3 datasets (**Figure 5**). Up to 4% (19/526) of samples were unclassified when switching from network to RF algorithm; similarly 21% (109/526) of samples were unclassified using the SSP algorithm and another 2% (8/526) switched subtype.

We then selected the 38-gene panel and applied the RF algorithm: compared to the RF classification obtained with the entire set of genes, 97% (491/507) of the previously classified samples were re-classified as CMS2. Similarly, when using the SSP algorithm and 38-gene panel and the standard SSP labels, 62%

(260/417) of samples switched to another subtype and 12% (52/417) were unclassified.

With this exercise we demonstrated that the algorithm used affects the classification; furthermore, using a reduced number of genes without modifying the algorithm leads to a high percentage of misclassified samples.

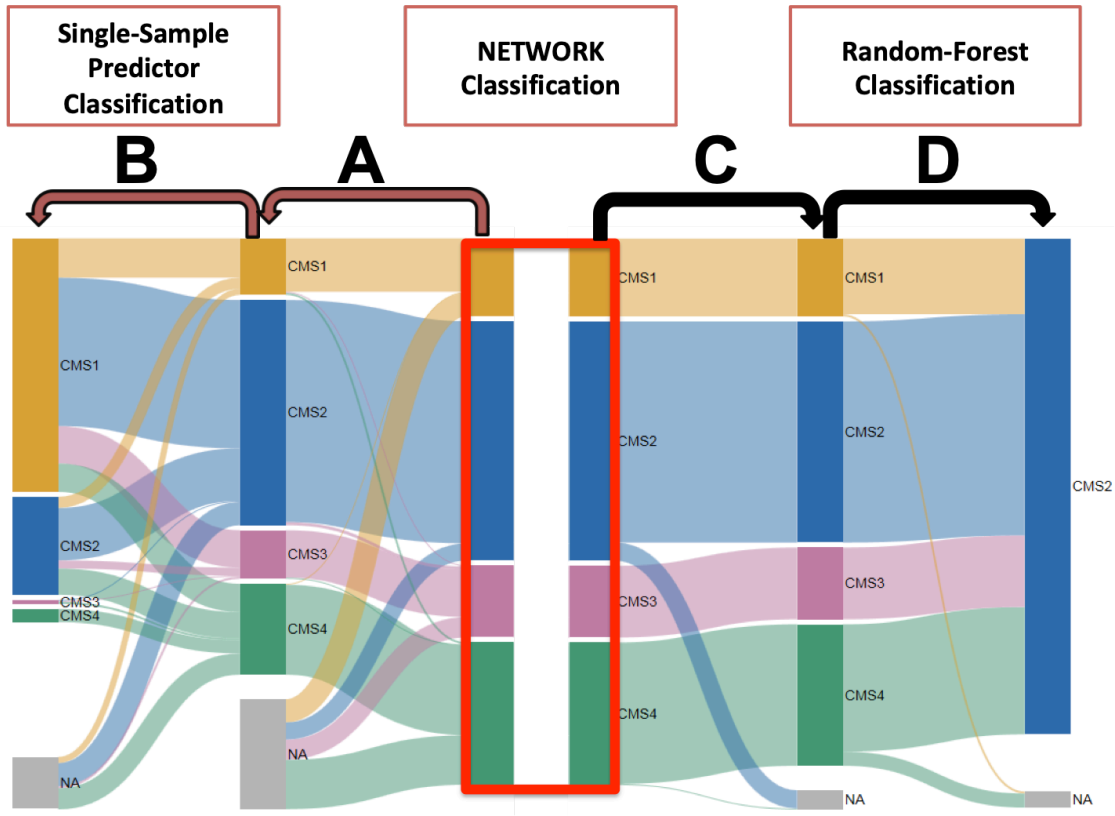

Figure 5. Sample misclassification due to different algorithms and sets of genes (PETACC-3 dataset) (Sankey plot). Classification derived from the network analysis, available on-line (central column).

From centre to the left:

- Comparison A shows the concordance between Network classification and SSP (extensive signature) classification: 21% of samples originally classified becomes unclassified using the SSP algorithm and further 2% of samples switch subtype;
- Comparison B shows the concordance between SSP algorithm (extensive signature) and SSP using only 38 genes: 12% of samples become unclassified while 62% of samples switch subtype;

From the centre to the right:

- Comparison C shows the concordance between Network classification and Random Forest (RF) algorithm (extensive signature): 4% of the samples become unclassified;
- Comparison D shows the concordance between RF extensive signature and RF using only 38 genes: 3.5% of samples become unclassified and 51% of samples switch subtype.

2.4.2 Performance of a newly developed algorithm for CMS subtypes prediction: rankCMS-38

After the rankCMS-38 classifier was developed (Ms K. Eason), its performance was assessed using the RF classification as a reference. The overall accuracy was 0.82 (95% Confidence Interval 0.78-0.86). The accuracy was considered satisfactory given this was similar to 0.86, which is the accuracy of a similar assay developed by Genentech Inc. using the NanoString platform and more than 300 genes (described in Chapter 5) (164).

In Figure 6 the confusion matrix and the overall performance of the classifier in the PETACC-3 dataset are presented.

Overall Accuracy (95% Confidence Interval): 0.8216 (0.7832-0.8557)

		Reference (Random-Forest method)				
		CMS1	CMS2	CMS3	CMS4	Total
RankCMS-38	CMS1	**64**	0	7	25	96
	CMS2	6	**177**	11	25	219
	CMS3	5	0	**54**	0	59
	CMS4	1	1	0	**78**	80
	Total	76	178	72	128	454

	CMS1	CMS2	CMS3	CMS4
Sensitivity	0.8421	0.9944	0.7500	0.6094
Specificity	0.9153	0.8478	0.9869	0.9939
Positive Predictive Value	0.6667	0.8082	0.9153	0.975
Negative Predictive Value	0.9665	0.9957	0.9544	0.8663
Prevalence	0.1674	0.3921	0.1586	0.2819
Detection Rate	0.1410	0.3899	0.1189	0.1718
Detection Prevalence	0.2115	0.4824	0.1300	0.1762
Balanced Accuracy	0.8787	0.9211	0.8685	0.8016

Figure 6. Overall performance of the newly developed rankCMS-38 algorithm when compared to RF classification (PETACC-3 dataset). The upper table represents a confusion matrix; the lower table summarises the results of the accuracy analysis for each subtype.

A Receiver Operating Characteristic (ROC) curve measuring the Area Under the Curve (AUC) for each subtype was built (**Figure 7**).

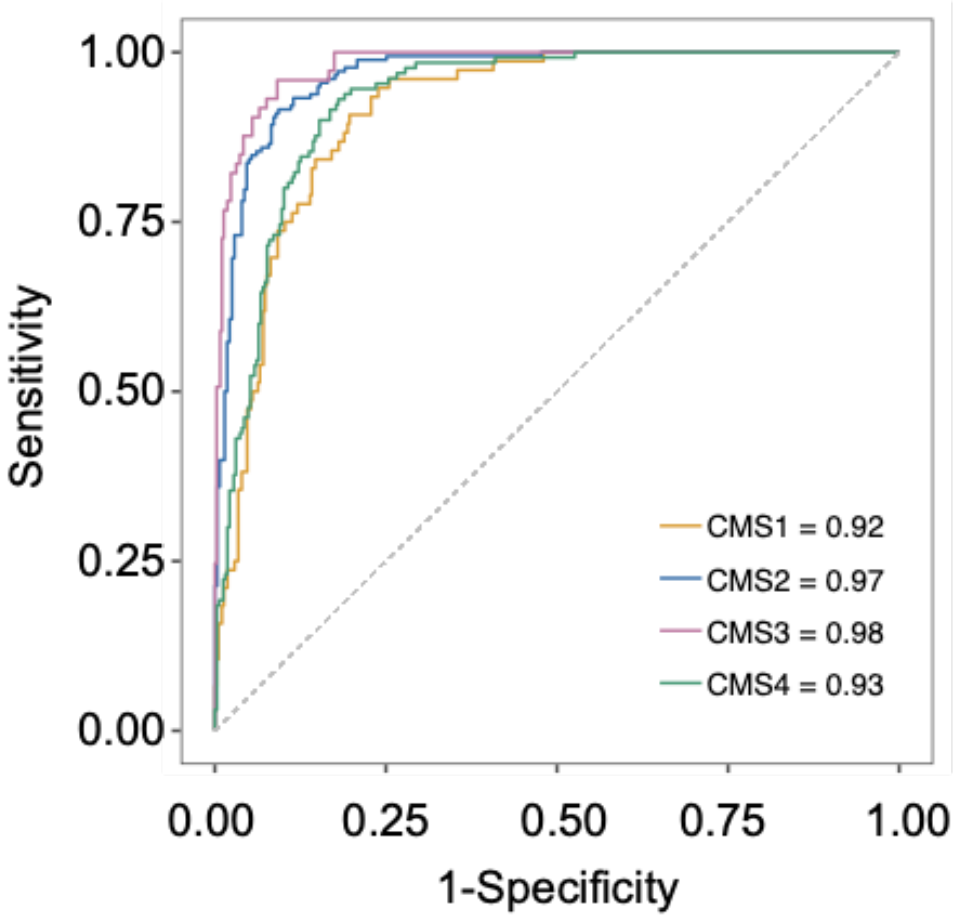

Figure 7. Receiver Operating Characteristic curve evaluating the Area Under the Curve for each subtype and overall accuracy of the rankCMS-38 in the PETACC-3 dataset

2.4.3 Performance of the newly developed NanoString assay for RankCMS-38 classification

Following the selection of the 38 genes and assay assembly (methods), the first cohort of 48 FFPE samples (RETRO-C cohort) was processed in batches of 12 samples. Data pre-processing pipeline is describes in **Figure 8**.

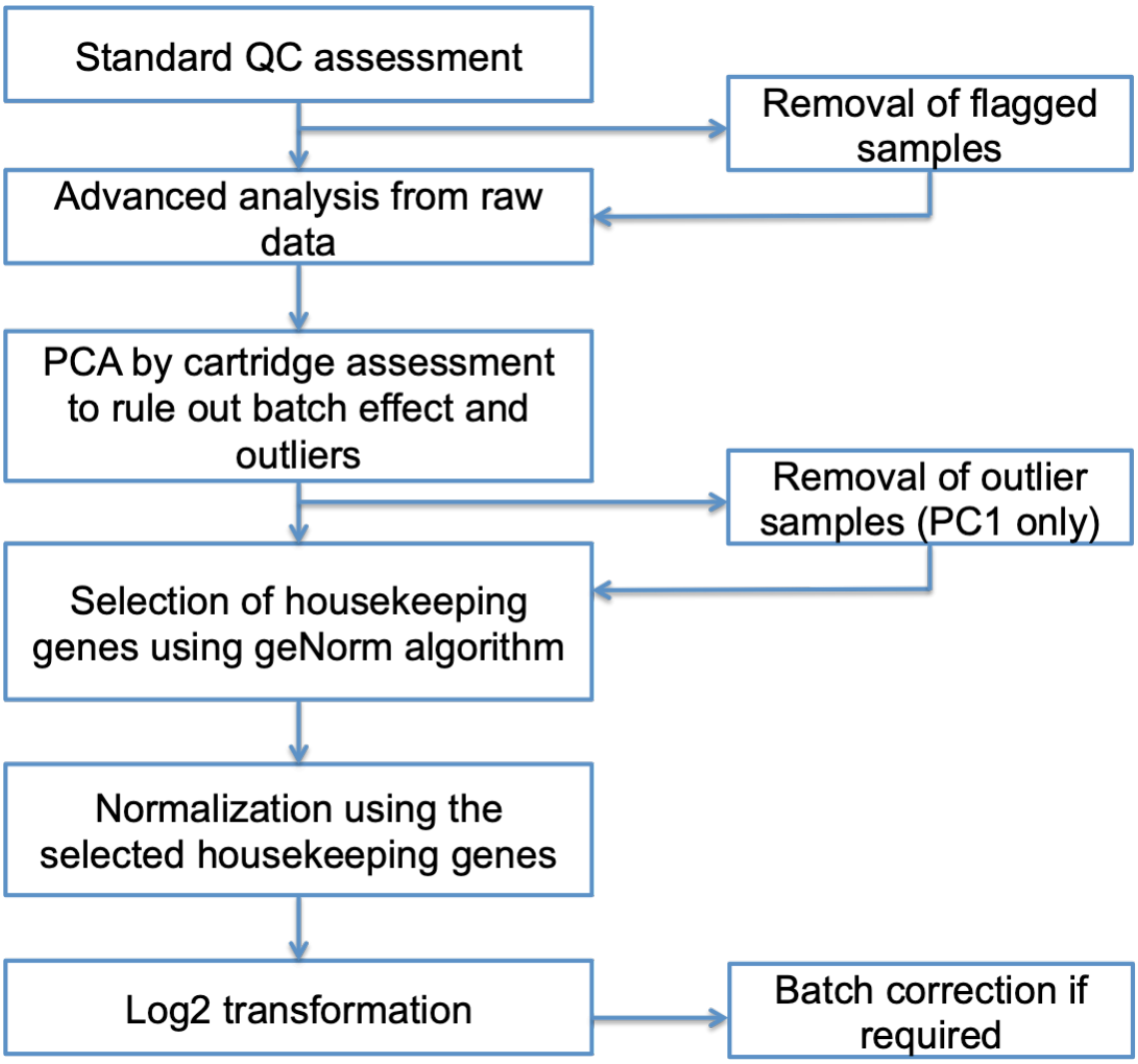

Figure 8. Pipeline for nSolver analysis. QC: quality control; PCA: principal component analysis.

The following results relative to the first RETRO-C cohort (n: 48 samples) are described according to the pipeline:

1. Standard QC assessment: there were no technical red flags, raising no concerns on the technical performance of the newly developed assay.
2. Advanced analysis of raw data: **Figure 9** represents the heatmap of the raw data including endogenous, housekeeping and both positive and negative controls. Positive and negative controls were easily visualised due to the homogeneous expression across all samples. Negative controls were all red, representing a level less than 25 barcodes counted for each of them. Only one endogenous gene (*RARRES3*) had less than 25 barcodes counted in all the samples. This may reflect a poor performance of the probe in hybridizing with its target RNA. However, due to the fact that the same probe was used in the previously developed NanoCRCA assay without significant impact on the overall assay performance, the probe was not replaced.
3. Principal Component Analysis (PCA) plot and outliers assessment (**Figure 10**): the samples appeared to be randomly distributed in the plot with none of the samples from the same cartridge clearly separated in distinct clusters from the others. This step is usually performed as a visualization procedure for early recognition of technical artefacts (fine batch effect assessment and correction may be performed in each study with different tools using normalised data). If present, outliers and their association with a certain component are automatically highlighted by the software at this point. In the pipeline, we established to discard only outliers associated with the first principal component.
4. Selection of housekeeping genes: only the most stably expressed (housekeeping) genes across all samples being tested are selected during normalization using the geNorm algorithm built-in the software as *R* package. In this case, all the 10 housekeeping genes were selected (**Table 5**).
5. Lastly, log2 transformed data normalised using the 10 housekeeping genes were exported from the nSolver™ Analysis Software as a ".txt" file.

Overall, no technical issues were raised from this first pilot study using the newly developed custom assay. **Figure 9-10** and **Table 5** were generated using the nSolver™ Analysis Software.

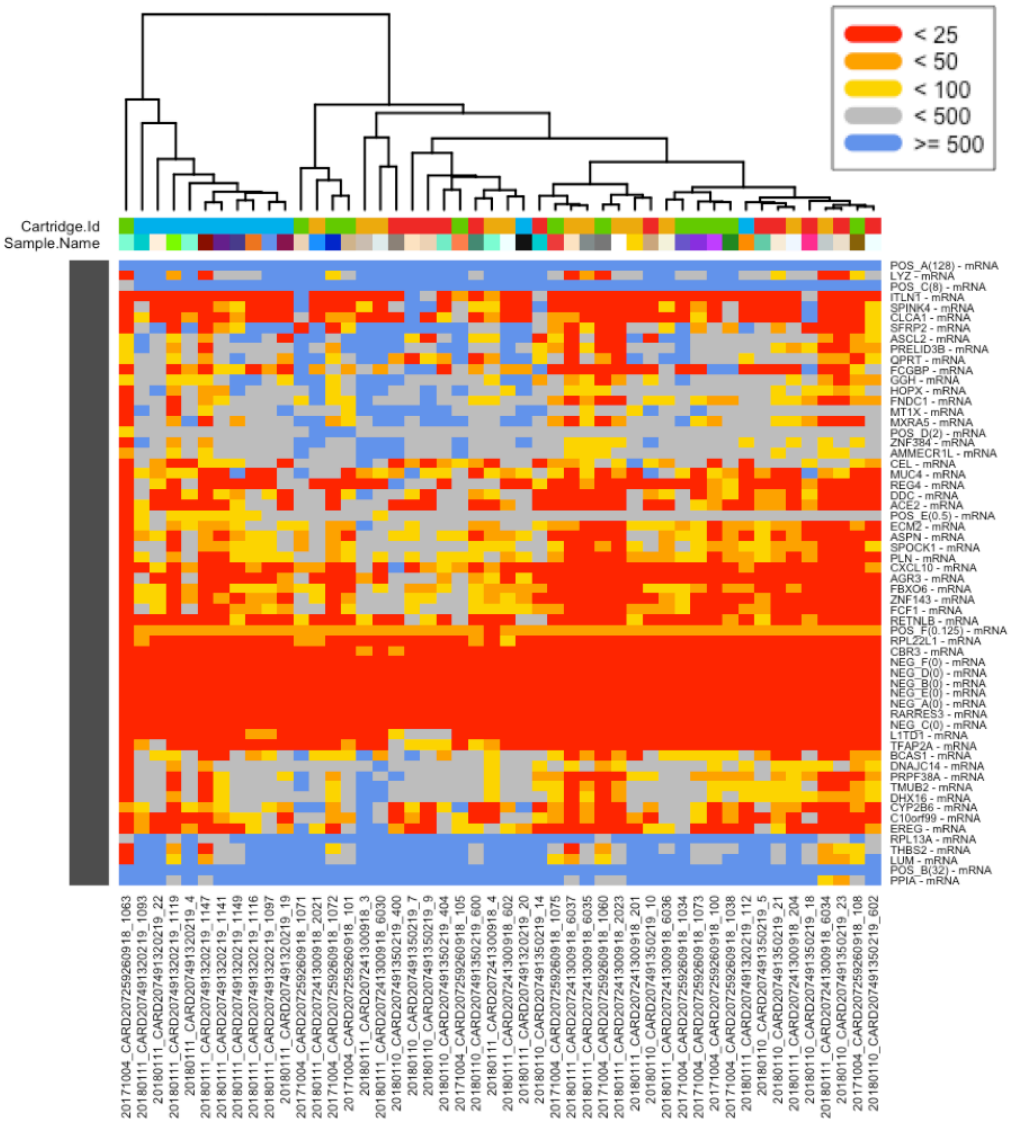

Figure 9. Heatmap of the first 48 RETRO-C samples assessed with the NanoCMS assay (raw data). The range of gene expression is shown in the legend.

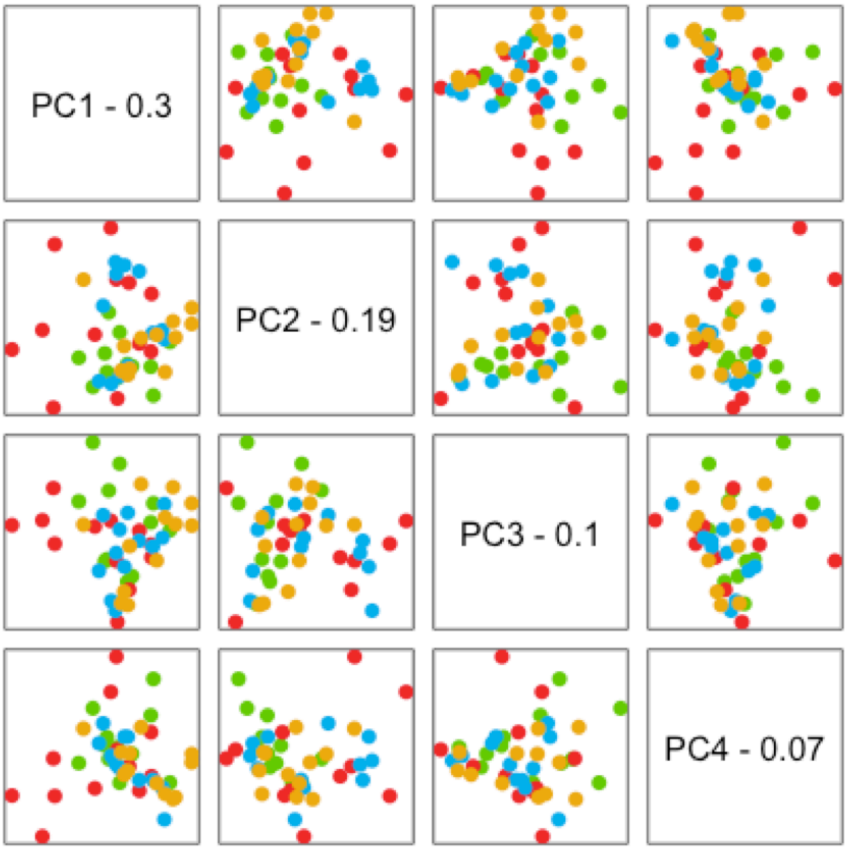

Figure 10. Principal Component Analysis plot generated with nSolver Analysis Software to assess batch or technical effect between experiments. Each dot represents a sample; each dozen processed in the same cartridge has the same colour.

Gene Name	Gene	Order selected by geNorm	SD after normalization
TMUB2-mRNA	NM_024107.2:1485	1	0.395
DHX16-mRNA	NM_001164239.1:2490	2	0.348
ZNF384-mRNA	NM_001039920.2:1720	3	0.548
AMMECR1L-mRNA	NM_031445.2:252	4	0.547
DNAJC14-mRNA	NM_032364.5:1166	5	0.815
RPL13A-mRNA	NM_012423.2:720	6	0.791
PRPF38A-mRNA	NM_032864.3:335	7	0.666
ZNF143-mRNA	NM_003442.5:925	8	0.741
PPIA-mRNA	NM_021130.3:200	9	0.836
FCF1-mRNA	NM_015962.4:228	10	0.93

Table 5. Housekeeping genes selected using the geNorm algorithm integrated in the nSolver Analysis software. The order of the genes and the standard deviation are shown.

2.4.4 RankCMS-38 classification

Once log2-transformed gene expression data were generated, they were used as input file for a fit-for-purpose *R* package. In the output .txt file each sample is assigned to the CMS class. The pie chart in **Figure 11A** represents the distribution of the CMS subtypes within the pilot study. All 4 subtypes were identified. The samples were collected within a retrospective tissue collection of patients who developed metastatic disease and received at least 3 lines of treatment. Hence, to understand whether the low percentages of CMS1 and CMS3 subtypes were due to biology or technical artefact, the distribution was compared with the only available cohort of samples in a similar setting (chemorefractory) from a correlative analysis of the phase III CORRECT trial (regorafenib or placebo after progression on standard chemotherapy) (47, 165). The subtype distribution of the RETRO-C cohort was similar to the subtype distribution in the CORRECT analysis (Fisher's Exact Test, p-value=0.06) (**Figure 11B**). The lower proportion of CMS3 in favour of CMS4 subtypes was expected due to the limited number of RAS mutant samples in the RETRO-C cohort (including patients who received anti-EGFR therapy; details in chapter 4).

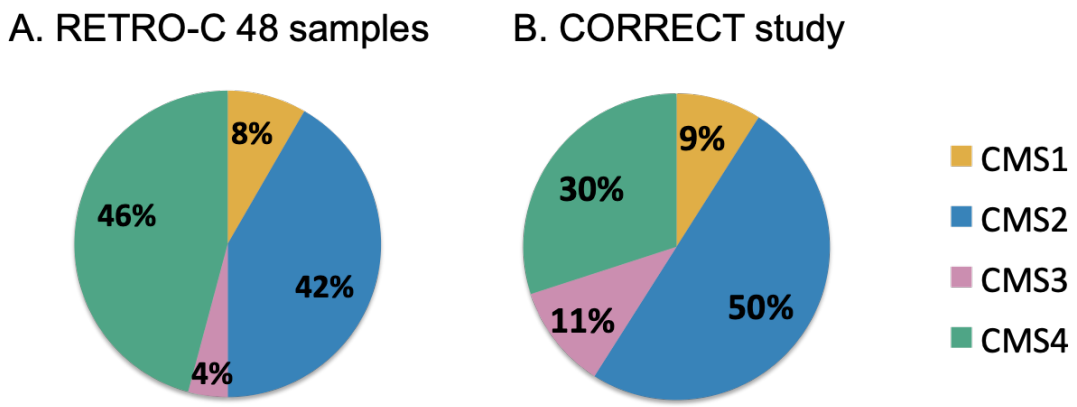

Figure 11. Subtype distribution in the RETRO-C cohort (48 samples) (A) and in the correlative analysis of the CORRECT phase III clinical trial (B); Fisher's Exact Test p-value= 0.06.

2.4.5 Development of a custom NanoString assay for simultaneous detection of CRCA-38 and CMS subtypes

Using the same protocol for Elements chemistry described in methods, a new biomarker assay was developed: this included the 50 endogenous genes and 10 housekeeping genes of the previously developed NanoCRCA assay (for CRCA-38 classification) plus the new set of genes for rankCMS-38 classification to form a 96-gene assay (including 7 genes in common between the two signatures). A summary of the final assay is presented in **Appendix 1**; 10 genes included in the assay were no longer used after refinement of CRCA-38 signature; 7 non subtype-specific genes were also included as genes of interest in CRC but not used for subtyping purposes (inclusion of these genes was due to the technical requirements of reaching multiple a of 12 for assay assemble).

A new cohort of FFPE samples of primary tumours was analysed in collaboration with Dr Iain Tan, Singapore (SG-FFPE cohort). The same pipeline described in **Figure 8** was deployed; no standard QC flags were observed. A total 108 samples were analysed; 2 samples were removed after normalization due to normalization flags. **Figure 12** demonstrates the subtype distribution according to both CRCA-38 and rankCMS-38 subtypes. Given the known association between CRCAssigner and CMS subtypes (described in Chapter 1), a hypergeometric test was used to understand whether this association was maintained using the new classifiers. As expected, strong association was demonstrated for the two more prevalent subtypes (CMS2-TA; CMS4-Stem-like). Only weak association was observed for the others possibly due to the low frequency of CMS1 and CMS3 in this cohort (**Figure 13**).

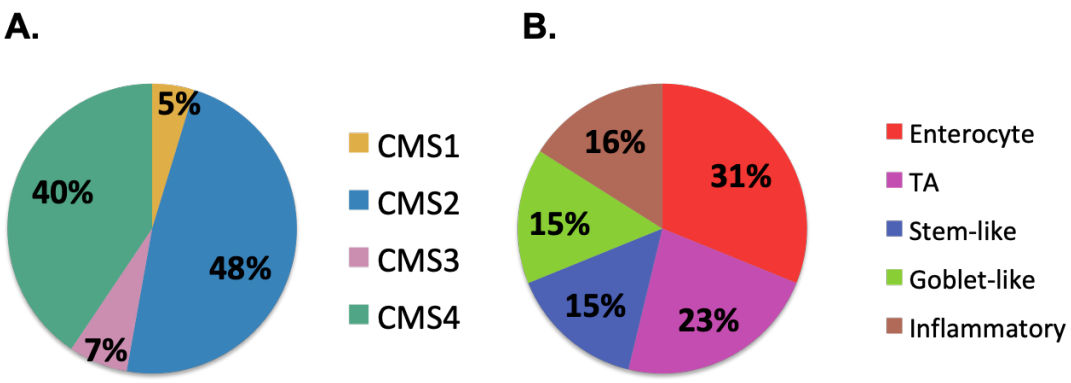

Figure 12. RankCMS-38 subtype distribution (A) and CRCA-38 subtype distribution (B) in the SG-FFPE cohort (n: 106)

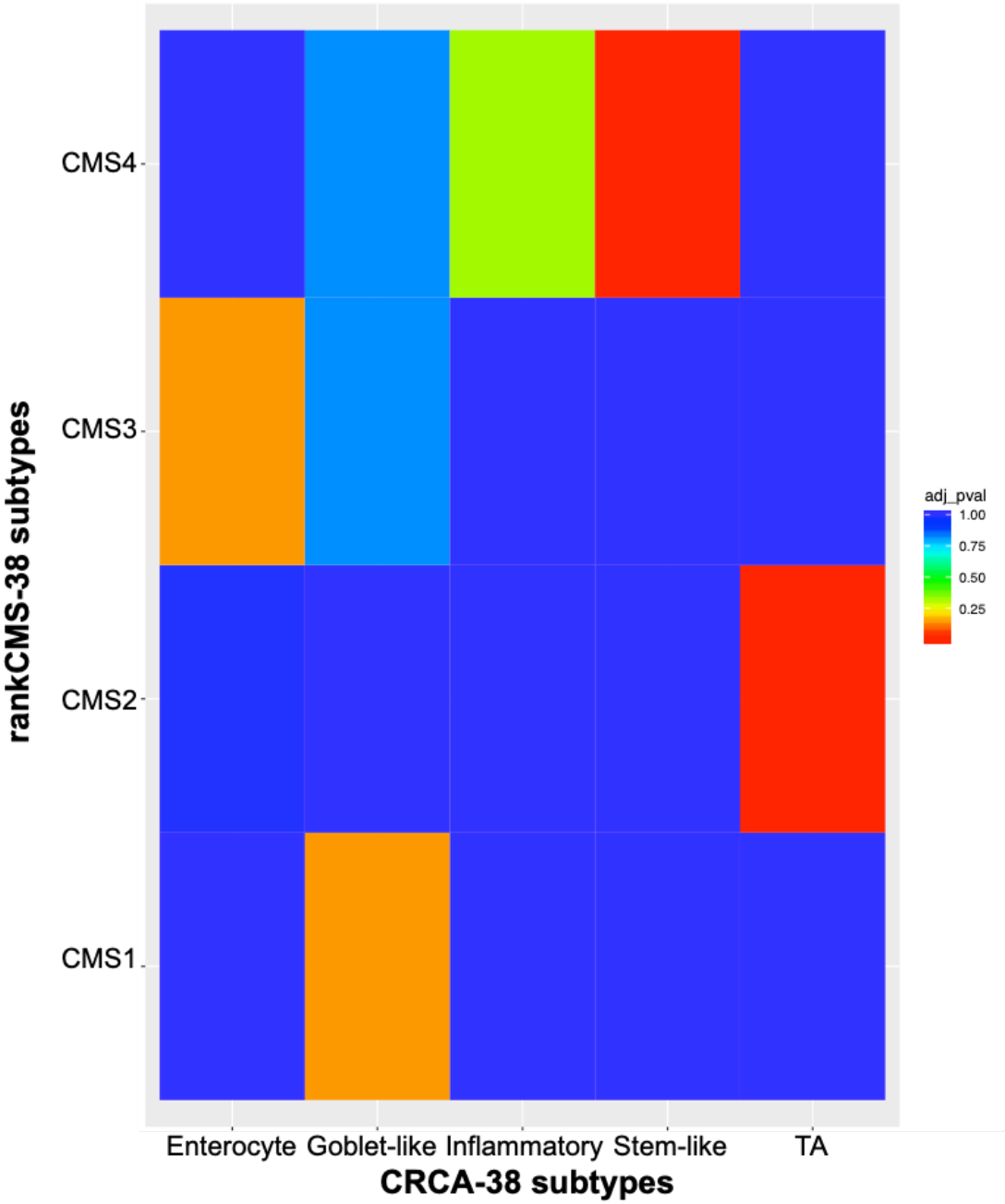

Figure 13. Hypergeometric test assessing the association between rankCMS-38 and CRCA-38 subtypes in the SG-FFPE cohort. Each square represents the degree of association (in terms of adjusted p-value) between a pair of subtypes: blue colour means no association; red colour means highly significant association. The legend shows the range of colours and their equivalent adjusted p-value.

Overall p-value = 2.659e-11

2.4.6 Assessment of the performance of the rankCMS-38 classifier in fresh-frozen samples

Although FFPE samples are the most commonly available samples for clinical use, fresh-frozen samples are increasingly used in research especially for high throughput analyses. Hence, the performance of the new rank algorithm was assessed using public data from the TCGA CRC cohort; then algorithm and NanoString assay results were validated in the SG-FF cohort.

Using TCGA gene expression data, the rankCMS-38 classification was compared to the RF classification. The performance of the classifier was comparable with that demonstrated in the PETACC-3 cohort. The confusion matrix and the overall performance are presented in **Figure 14**. Although the overall accuracy was lower than that one demonstrated in the PETACC-3 dataset, the four subtypes identified maintained their expected prognostic characteristics: the two Kaplan Meir (KM) survival curves in **Figure 15** demonstrate the overall survival by CMS groups with the CMS4 associated with the poorest prognosis. While the relapse-free survival (RFS) of the reference CMS subtypes (using RF algorithm) was not significantly different, statistical significance was demonstrated using the new rankCMS-38 classification.

Overall Accuracy (95% Confidence Interval): 0.7915 (0.7530 - 0.8265)

		Reference (Random-Forest method)				
RankCMS-38		CMS1	CMS2	CMS3	CMS4	Total
	CMS1	**53**	0	0	23	76
	CMS2	2	**190**	9	17	218
	CMS3	16	7	**61**	12	96
	CMS4	5	11	1	**87**	104
	Total	76	208	71	139	494

	CMS1	CMS2	CMS3	CMS4
Sensitivity	0.6974	0.9135	0.8592	0.6259
Specificity	0.9450	0.9021	0.9173	0.9521
Positive Predictive Value	0.6974	0.8716	0.6354	0.8365
Negative Predictive Value	0.9450	0.9348	0.9749	0.8667
Prevalence	0.1538	0.4211	0.1437	0.2814
Detection Rate	0.1073	0.3846	0.1235	0.1761
Detection Prevalence	0.1538	0.4413	0.1943	0.2105
Balanced Accuracy	0.8212	0.9078	0.8882	0.7890

Figure 14. Overall performance of the rankCMS-38 classifier in the TCGA cohort (fresh frozen samples). Upper table: confusion matrix; lower table: summary of accuracy analysis for each subtype.

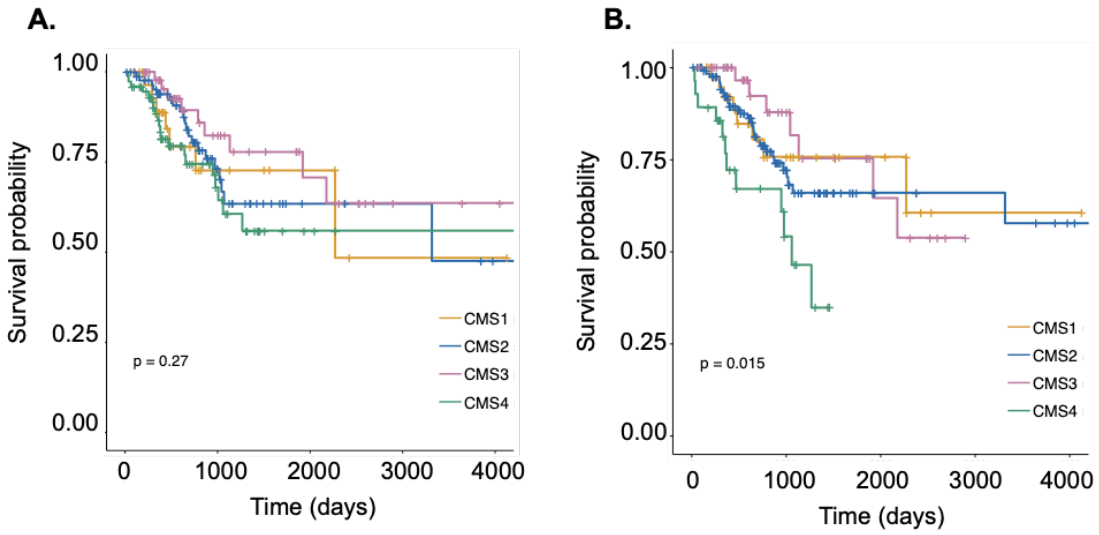

Figure 15. Relapse-free survival according to CMS subtypes (Random-Forest) (A) and rankCMS-38 subtypes (B) in the TCGA cohort (114).

Next, a cohort of FF primary tumour samples (SG-FF) was tested using the newly developed NanoString assay. Of 164 primary tumour samples, 145 had available RNAseq data and CMS classification (Random Forest). Twenty-nine samples unclassified were removed. Hence, 116 samples with known CMS subtype assignment were deployed to further validate the performance of the rankCMS-38 classifier in FF samples (**Figure 16**). The overall accuracy of 89% was in line with the performance demonstrated in FFPE samples.

In summary, when using on-line data from FFPE and FF samples the accuracy of the new rankCMS-38 algorithm was 82% and 79% with overlapping confidence intervals, suggesting the overall performance is comparable across sample-preservation methods. When using the same RNA derived from FF samples and two different platforms (RNAseq and NanoString), the performance of the rankCMS-38 algorithm was 89%; the confidence intervals were overlapping with the on-line data experiments. The numerically higher value may be justified by the smaller number of samples included in the SG-FF dataset (n= 116) compared to the two on-line datasets (n= 454 and n= 494).

Overall Accuracy (95% Confidence Interval): 0.8879 (0.8160 - 0.9390)

		Reference (Random-Forest method)				
RankCMS-38		CMS1	CMS2	CMS3	CMS4	Total
	CMS1	**20**	0	0	0	20
	CMS2	0	**55**	3	0	58
	CMS3	2	2	**21**	2	27
	CMS4	2	1	1	**7**	11
	Total	24	58	25	9	116

	CMS1	CMS2	CMS3	CMS4
Sensitivity	0.8333	0.9483	0.8400	0.7778
Specificity	1.0000	0.9483	0.9341	0.9626
Positive Predictive Value	1.0000	0.9483	0.7778	0.6364
Negative Predictive Value	0.9583	0.9483	0.9551	0.9810
Prevalence	0.2069	0.5000	0.2155	0.0776
Detection Rate	0.1724	0.4741	0.1810	0.0603
Detection Prevalence	0.1724	0.5000	0.2328	0.0948
Balanced Accuracy	0.9167	0.9483	0.8870	0.8702

Figure 16. Overall performance of the rankCMS-38 classifier in the SG-FF cohort. Upper table: confusion matrix; lower table: summary of accuracy analysis for each subtype.

2.4.7 Assessment of the subtype concordance in matched fresh-frozen and FFPE samples

Sample preservation and nucleic acids extraction methods may affect the RNA integrity and consequently subtype classification. In order to evaluate the subtype concordance and the performance of each probe included in the assay, a cohort of samples with RNA extracted from matched FF and FFPE primary tumours was assessed. The matched samples belong to contiguous tumour regions; 58 matched samples were available for the analysis.

As demonstrated in **Figure 17A** in this experiment the overall accuracy in detecting the same subtype dropped to 0.53. Macrodissection of tumour-enriched areas was performed during the extraction from FFPE blocks, while this is not possible in case of FF blocks. Hence, a higher degree of normal tissue contamination is expected in FF-derived RNA samples. As previously demonstrated using the CRCA-38 classifier, in cases of higher normal tissue contamination the classification is slightly biased towards subtypes with expression profiles similar to normal colon epithelium (the enterocyte subtype) (154). Similarly, using the rankCMS-38 a possible over-representation of one of the differentiated subtypes (CMS3) was observed. In **Figure 18** the overexpression (>10) of CMS3 genes in FF samples compared to the matched FFPE (<5) is demonstrated, leading to a Persons' correlation of 0.46 within the CMS3 genes. This bias was previously reported also in the original CMS manuscript, where the vast majority of samples derived from FF cohorts: the CMS3 subtype appeared more "normal-like" from gene expression profiles in the absence of clear greater contamination from normal tissue compared to the other CMS subtypes (148). When selecting for samples with tumour cellularity >70% (in the attempt to reduce the normal tissue contamination) the overall accuracy slightly improved (0.67, **Figure 17B**).

A.

Overall Accuracy (95% Confidence Interval): 0.5345 (0.3987 - 0.6666)

		rankCMS38 FFPE				
		CMS1	CMS2	CMS3	CMS4	Total
rankCMS-38 FF	CMS1	**3**	0	0	3	6
	CMS2	0	**17**	0	7	24
	CMS3	1	7	**2**	7	17
	CMS4	0	1	1	**9**	11
	Total	4	25	3	26	58

	CMS1	CMS2	CMS3	CMS4
Sensitivity	0.7500	0.6800	0.6667	0.3462
Specificity	0.9444	0.7879	0.7273	0.9375
Positive Predictive Value	0.5000	0.7083	0.1177	0.8182
Negative Predictive Value	0.9808	0.7647	0.9756	0.6383
Prevalence	0.0690	0.4310	0.0517	0.4483
Detection Rate	0.0517	0.2931	0.0345	0.1552
Detection Prevalence	0.1035	0.4138	0.2931	0.1897
Balanced Accuracy	0.8472	0.7339	0.6970	0.6418

B.

Overall Accuracy (95% Confidence Interval): 0.6667 (0.4468 - 0.8437)

		rankCMS38 FFPE				
		CMS1	CMS2	CMS3	CMS4	Total
rankCMS-38 FF	CMS1	**1**	0	0	0	1
	CMS2	0	**10**	0	2	12
	CMS3	1	1	**1**	4	7
	CMS4	0	0	0	**4**	4
	Total	2	11	1	10	24

	CMS1	CMS2	CMS3	CMS4
Sensitivity	0.5000	0.9091	1.0000	0.4000
Specificity	1.0000	0.8462	0.7391	1.0000
Positive Predictive Value	1.0000	0.8333	0.1429	1.0000
Negative Predictive Value	0.9565	0.9167	1.0000	0.7000
Prevalence	0.0833	0.4583	0.0417	0.4167
Detection Rate	0.0417	0.4167	0.0417	0.1667
Detection Prevalence	0.0417	0.5000	0.2917	0.1667
Balanced Accuracy	0.7500	0.8776	0.8696	0.7000

Figure 17. Overall performance in matched FF and FFPE samples (n: 58) (A) and in selected samples with high cellularity (n: 24) (B).

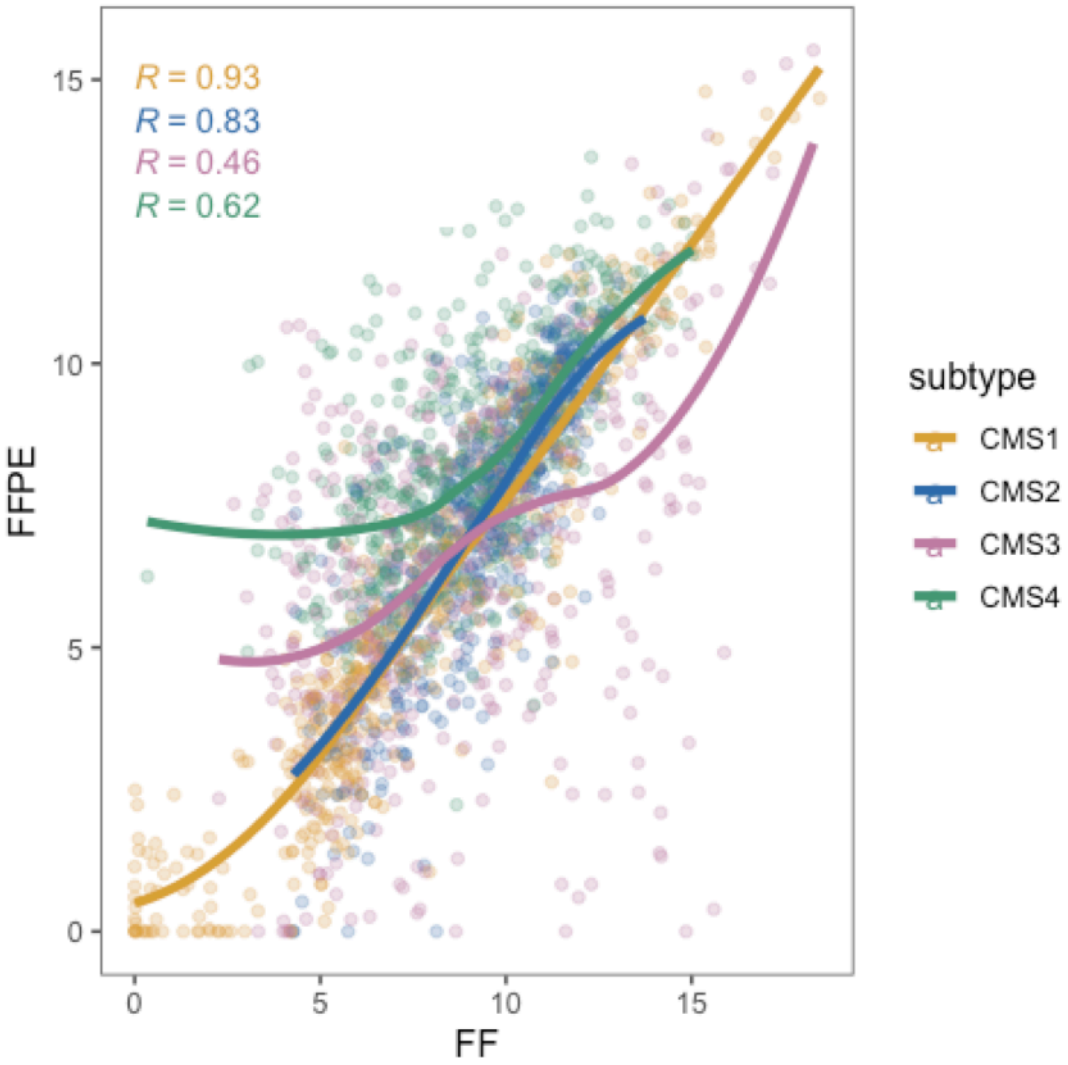

Figure 18. Gene-gene correlation in matched FF and FFPE samples. Each dot represents a gene in each sample and it is coloured based on the subtype the gene belongs to. Four best-fit lines (one for each subtype) are plotted based of the expression of subtype-specific genes in all samples.

2.5 Discussion

In this chapter I have described the development of two new custom assays for NanoString Technologies: one assay, dubbed NanoCMS, formed by 48 genes (38 endogenous and 10 housekeeping) to classify CRC samples into CMS subtypes (rankCMS-38); the second one, formed by 96 genes and created by joining the NanoCMS with the previously developed NanoCRCA, to simultaneously classify samples into CMS (rankCMS-38) and CRCAssigner subtypes (CRCA-38).

After the selection of 38 subtype-specific genes and with the help of Ms Eason, we demonstrated that an ad-hoc algorithm is required when using a reduced panel of genes. We then validated the newly developed algorithm using public microarray and RNAseq data and the standard classification method as a reference.

The signature was used to build new custom biomarker assays for nCounter platform: no technical problems were encountered. The optimal RNA input was established at 100 ng in a titration experiment: this amount was the minimum required to maintain high correlation with higher inputs and allowing us to spare precious tumour material.

A pipeline for data analysis was created to perform quality control assessment and data normalization using the nSolver analysis Software (NanoString Technologies). Each sample was assigned to CRC subtypes using a newly developed algorithm (rankCMS-38) and a previously developed tool (CRCA-38). The CMS subtype distribution was then compared and found to be in line with a cohort from the literature within a similar clinical setting. The CMS subtypes were also compared with the previously validated CRCAssigner subtypes as orthogonal validation: association between the two more prevalent subtypes (CMS2 and CMS4) and their CRCAssigner equivalent was demonstrated. Weaker association between CMS3 and enterocyte plus goblet-like was also demonstrated even if the prevalence of this CMS subtype was as low as 7%.

Lastly, weaker association between the CMS1 subtype and goblet-like was demonstrated: although this subtype was expected to be strongly associated with the inflammatory one, the low prevalence (5%) and also the nature of the sample collection (chemorefractory setting) justifies the possible correlation with the goblet-like.

High overall accuracy of 82% using the selected 38 genes and the rankCMS method was demonstrated using the PETACC-3 dataset (23); similar results were reproduced in the TCGA dataset (114). As expected, in the TCGA dataset the accuracy slightly dropped to 79% in view of the different type of platform (RNAseq) and source of sample (fresh-frozen) compared to PETACC-3. However, the prognostic value of the subtypes was not lost but actually improved. A new RNAseq cohort was then assessed and an aliquot of the same RNA was used for both sequencing and NanoString technologies: also in this case, the overall accuracy between rankCMS-38 and reference RF method was very high, with 89% of the samples correctly classified.

Of note, the source of sample used is very relevant. We demonstrated that the use of RNA extracted from FF or FFPE samples could affect the classification. This may be related to interference with preservation substances or different fragmentation of target RNAs. The exclusion of samples with low cellularity can partially improve performance. However, it is unlikely that selecting for high cellularity could completely address this issue: the RNA extracted from matched FF and FFPE samples derives from different areas of the tumours (although contiguous). These areas may be biologically different because of intra-tumoural heterogeneity.

Once developed, the subtypes defined with the newly developed NanoString assays were studied in more details in different cohorts of samples and correlated with clinicopathological features and outcomes. This was done in order to understand whether the known clinical and prognostic associations originally described in the CMS Subtyping Consortium and in the CRCAssigner manuscripts were equally captured and to also understand the potential clinical utility of the assays. These findings are described in the next chapters.

Chapter 3

Biomarker assay validation using clinico-pathological features

3.1 Introduction

3.1.1 Clinico-pathological features of CMS subtypes

In the original Colorectal Cancer Subtyping Consortium (CRCSC) extensive biological characterization of the CMS subtypes was provided (148). The clearest associations demonstrated were as follows:

- CMS1: hypermutation and hypermethylation, low prevalence of somatic copy number alterations (SCNA); microsatellite instability (MSI) in 75% of cases and overexpression of DNA damage repair proteins; *BRAF* mutation; higher prevalence in the right colon (31%) compared to left (7%) and only 3% of rectal tumours.
- CMS3: *KRAS* mutation; hypermutation and MSI (30% of cases); low SCNA;
- CMS2 and CMS4: high chromosomal instability.

Although enrichment for genomic aberrations in certain subtypes was observed, no genomic alteration was unique to a subtype. In particular, a proportion of CMS1 and CMS3 were very similar in genomic profile as were CMS2 and CMS4. Major differences were explained by gene set enrichment analyses: CMS1 was associated with high immune infiltration, CMS2 with epithelial differentiation and WNT pathway activation, CMS3 with metabolic deregulation and CMS4 with epithelial-to-mesenchymal (EMT) upregulation and angiogenesis and complement-mediated inflammation. This analysis

highlighted the fact that the four subtypes summarise distinctive biological entities with differentially active pathways potentially targetable with subtype-specific therapies, hence, supporting the need of a suitable assay for clinical exploitation.

3.1.2 Challenges due to technical differences in subtype assessment

After the publication of the CRCSC paper, the scientific community used the CMS classification to perform multiple retrospective analyses of clinical trial cohorts to further investigate the potential role of the CMS subtypes as biomarkers for treatment decisions. Unfortunately, inconsistent results across studies created some confusion instead of clarification; we recently published a review article explaining how technical factors need to be taken into account when applying the classification to trial data (153).

In particular, the context of application of the CMS classification matters and the expected proportion of the different subtypes can vary in at least four different contexts:

1. Stage: the classification was developed in early stage disease, hence its application in the metastatic setting may not be optimal;
2. Sample source: only primary tumour samples collected before any treatment were originally analysed, limiting the potential application of the classifier to samples of metastatic lesions or samples collected after chemotherapy or radiotherapy;
3. Trial versus off-trial sample collections: given the clinical trial inclusion criteria usually excluding patients with poor performance status or heavily symptomatic, patients with high disease burden and aggressive biology may be underrepresented;
4. In case of enrichment by genomic or clinical variables: in view of expected associations between certain subtypes and genomic variables as example *RAS* mutational status, the distribution of CMS

subtypes may vary and be enriched of a particular subtype because of genomic selection.

Beyond different contexts, confounding factors may affect the classification, as example, intra-tumoural heterogeneity with more than one subtype within the same tumour, technical factors like the algorithm used to predict the subtypes, different gene sets and assays. Some concrete examples from recent *post-hoc* analyses of clinical trials are described below.

Gene expression datasets derived from multiple types of platforms (Affymetrix, Agilent microarrays and RNAseq) were included in the CRCSC analysis (148). The portability of the CMS classifier across different platforms was demonstrated; hence the type of platform used is unlikely to affect the classification. Conversely, the number of genes and the algorithm may affect the classification. For example, two correlative analyses of first-line clinical trials both assessing the effect of bevacizumab or cetuximab together with chemotherapy were recently performed (CALGB 80405, FIRE-3) (149,150). Discordant results were described, with CMS2 in one study and CMS4 in the other one as potential predictive biomarkers of response to cetuximab. In the FIRE-3 study the CMS subtypes were assessed using microarray technology, more than 600 genes and Random Forest classifier, in line with the CRCSC analysis. Conversely, in the CALGB 80405 study the CMS classification was performed with NanoString Technologies: because of the lack of overlapping genes analysed in the original CRCSC analysis, the CMS classifier was retrained based on the available genes (number unspecified) and a logistic regression model used as an algorithm (149). This may at least partially explain these discordant results. Similarly, in 2014 the CMS analysis of an adjuvant study (NSAPB-C07) suggested that adding oxaliplatin to fluorouracil was particularly beneficial in the CMS2-enterocyte subtype (166). The CMS analysis was performed using NanoString Technologies and gene panels developed before the publication of the CRCSC analysis. Thirty-seven genes were overlapping with the CRCSC signature (without specific selection criteria established). Recently, the same authors could not replicate the same results in another adjuvant study (MOSAIC); the assay deployed was altered since the

previous analysis without demonstrating the concordance with that one used in the first study (166,167).

This evidence supports once again the need for technical consistency in the evaluation of the subtypes in order to obtain reproducible and comparable results across studies.

3.1.3 Possible biological variation across different populations

The CRCSC included primarily Caucasian patient samples. Hence, the applicability of the classifier in non-Caucasian populations remained to be established. Recently a Japanese study evaluated the CMS distribution within samples from Japanese patients with metastatic disease (168). Technically, no major flaws were described in the CMS classification: the source of samples was the primary tumour from FFPE blocks; data were generated using the Agilent microarray platform and the algorithm was the single-sample-prediction one from the original CRCSC manuscript. The authors found enrichment for CMS3 tumours (69 out of 193 cases representing 35.8%) compared to the CRCSC population, in which the CMS3 subtype represented 13% of the cases. This suggests a potential diversity of subtype distribution in different ethnic groups.

Ethnicity is an important factor in gastrointestinal cancers. Significantly different prognosis (better in Asian patients) is well known in gastric cancer: this was historically attributed to early diagnosis and more extensive surgical approaches in Asian versus non-Asian populations (169). However, recent studies demonstrated how biological factors play a major role in pathogenesis and molecular characteristics. As an example, different strains of *Helicobacter pylori* with different carcinogenesis capacity or different incidence of Ebstein-Barr virus infections across countries have an impact on the distribution of the genomic subtypes of gastric cancer (170, 171). Similarly, a recent gene expression study demonstrated differentially expressed gene signatures

between Asian and non-Asian patients with gastric cancer, in particular signatures related to immune functions and inflammation (171).

In order to identify potential subtype difference across populations it is important to deploy the same assay, thus minimising any technical artefacts. Understanding potential differences or similarities across populations has particular relevance in the context of biomarker-driven clinical trials, which are frequently developed on a global scale. This knowledge may help rationalising screening efforts and expected outcomes from new drugs.

3.2 Specific aims

1. Evaluate the existing associations between clinico-pathological features and CMS subtypes as orthogonal validation of the rankCMS-38 assay in FFPE samples
2. Compare the association between rankCMS-38 subtypes and clinico-pathological features in Caucasian and Asian populations

3.3 Methods

3.3.1 Patient samples

Two clinically annotated cohorts of patient samples were analysed in this chapter:

1. The INCLIVA-Valencia cohort: FFPE samples and patients' data were prospectively collected at the Research Institute INCLIVA, Valencia, Spain (Comité Etico de Investigacion Clinica del Clìnico Universitario de Valencia: F-CE-GEva-15; named collaborators: Prof. Andrés Cervantes and Dr. Noelia Tarazona).
2. The Singapore FFPE (SG-FFPE) cohort: previously described in chapter 2 (section 2.3.6).

All samples were processed with the same assay for simultaneous classification into rankCMS-38/CRCA-38 subtypes (NanoCRC) as described in chapter 2 (section 2.3.8).

3.3.2 Statistical analyses

Clinico-pathological features of each cohort were analysed using descriptive statistic. Fisher's exact or ANOVA tests were used to assess the association between subtypes and categorical or continuous variables, respectively.

3.4 Results

3.4.1 RankCMS-38 subtypes' distribution in a Caucasian population

The INCLIVA-Valencia cohort was firstly analysed: this cohort included patients with early stage disease prospectively enrolled in an observational study at the time of surgery. Out of 144 samples tested with the NanoCRC assay, 132 passed all the quality control steps. The subtype distribution is presented in **Figure 19A**: the proportion of CMS1 and CMS3 were 7% and 8%, respectively.

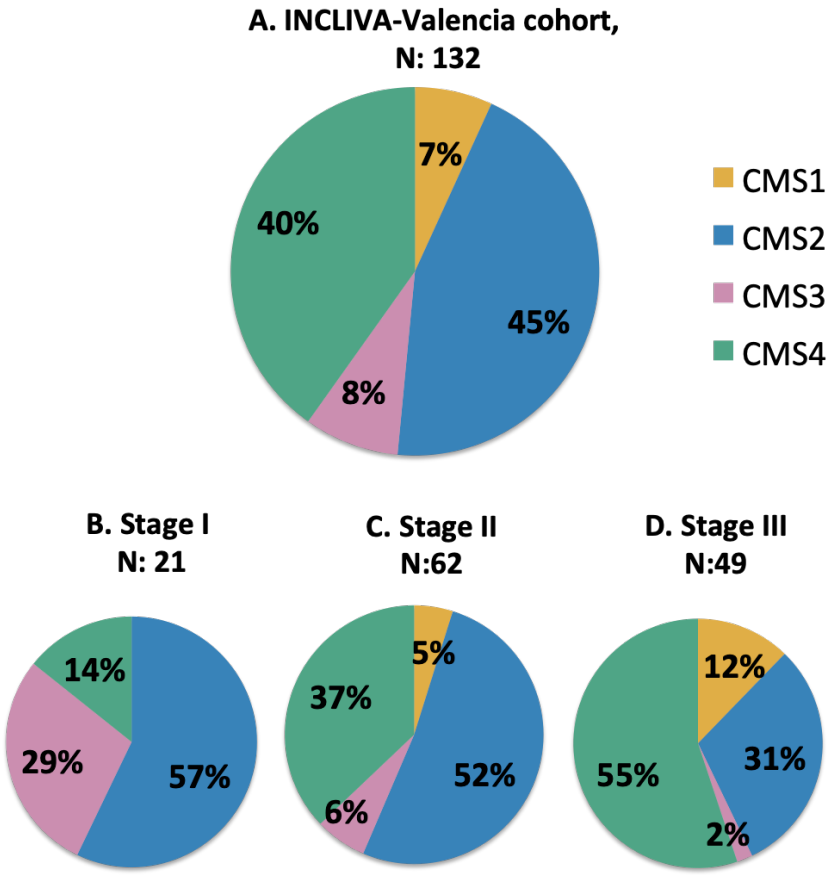

Figure 19. Subtypes' distribution is the INCLIVA-Valencia cohort; overall (A) and by stage at diagnosis (B, C, D).

Based on the CRCSC (including primarily retrospective sample collections), the expected proportion of CMS1 and CMS3 subtypes in early stage is 16% and 15%, respectively (**Figure 20**) (148). To understand whether the lower proportions observed in the INCLIVA cohort was truly related to cohort' characteristics or possibly due to technical misclassification, the subtype proportions were analysed by stage of disease (**Figure 19 B-D**). Of note, in stage III tumours, CMS1 and CMS3 represented 12% and 2% of the subgroup: this was similar to the recently presented PETACC-8 study (CMS1: 17%; CMS3: 4%; Fisher's Exact Test p-value= 0.47), in which patients were prospectively enrolled and the subtypes were assessed with a NanoString panel, hence more similar to the INCLIVA-Valencia cohort than the CRCSC cohort (172). Interestingly, CMS3 tumours were predominantly present in stage I disease: as discussed in chapter 2 and in the CRCSC paper, the expression profile of the CMS3 subtype is the most "normal-like"; the higher proportion observed was in stage I tumours also in the CRCSC work (**Figure 20**) (148). Furthermore, in a recent publication in which adenomas were stratified according to the CMS classification, the proportion of CMS3 was the highest ever observed, with 45 out of 62 adenomas (73%), reinforcing the evidence of association between very early stage disease and "normal-like" CMS3 subtype (173). Overall, the subtype distribution in the INCLIVA cohort was as expected given the available literature.

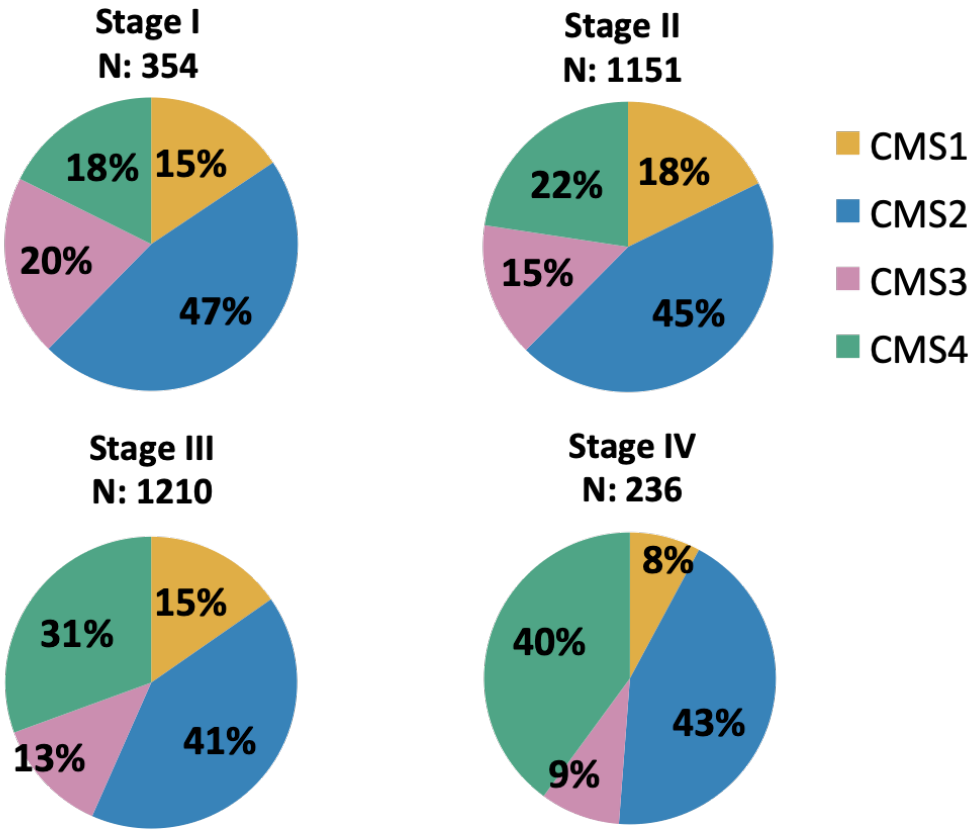

Figure 20. Subtypes' distribution according to stage at diagnosis within the CRCSC cohort (redrawn from supplementary data from Guinney *et al.* (148)).

3.4.2 Associations with clinical features

The next step in the validation of the subtyping results in FFPE samples was to assess whether the known associations between clinico-pathological features and subtypes were present. Given the small number of CMS1 and CMS3 subtypes (expected to be associated with relevant features), the two cohorts (INCLIVA and Singapore SG-FFPE) were analysed together. Firstly, clinical and molecular characteristics of the cohorts were compared to understand whether any significant differences were present (**Table 6**).

Characteristic		Singapore (N: 106)	Spain (N: 132)	*p-value*
		n(%)	n(%)	
Gender	Female	49(46.3)	49(37.1)	0.185
	Male	57(53.7)	83(62.9)	
Age				<0.001
	Median	61	70	
	Range	34-81	41-93	
Sidedness				0.005
	Left	71(67.0)	74(56.1)	
	Right	24(22.6)	58(43.9)	
	NA	11(10.4)	0(0.0)	
Stage				<0.001
	I	2(1.9)	21(15.9)	
	II	10(9.4)	62(47.0)	
	III	36(34.0)	49(37.1)	
	IV	42(39.6)	0(0.0)	
	NA	16(15.1)	0(0.0)	
T stage				0.005
	T1	1(0.9)	10(7.6)	
	T2	3(2.8)	14(10.6)	
	T3	50(47.2)	82(62.1)	
	T4	30(28.3)	25(18.9)	
	Tis	0(0.0)	1(0.8)	
	NA	22(20.8)	0(0.0)	
N Stage				<0.001
	N0	22(20.8)	83(62.9)	
	N1	32(30.1)	34(25.8)	
	N2	30(28.3)	15(11.3)	
	NA	22(20.8)	0(0.0)	

Characteristic		Singapore (N: 106)	Spain (N: 132)	*p-value*
		n(%)	n(%)	
MSI status				0.031
	MSI	2(1.9)	14(10.6)	
	MSS	83(78.3)	118(89.4)	
	NA	21(19.8)	0(0.0)	
RAS status				0.883
	Mut	38(35.8)	57(43.2)	
	WT	38(35.8)	54(40.9)	
	NA	30(28.3)	21(15.9)	
BRAF status				0.379
	Mut	3(2.8)	10(7.6)	
	WT	61(57.6)	101(76.5)	
	NA	42(39.6)	21(15.9)	
rankCMS-38 subtypes				0.859
	CMS1	5(4.7)	9(6.8)	
	CMS2	51(48.1)	59(44.7)	
	CMS3	7(6.6)	11(8.3)	
	CMS4	43(40.6)	53(40.2)	
CRCA-38 subtypes				0.705
	Enterocyte	33(31.1)	36(27.3)	
	Goblet-like	16(15.1)	29(22.0)	
	Inflammator	17(16.0)	22(16.7)	
	Stem-like	16(15.1)	20(15.1)	
	TA	24(22.6)	25(18.9)	

Table 6. Characteristics of patients included in the INCLIVA-Valencia and Singapore FFPE cohorts. NA: not available.

As expected, the stage distribution was significantly different; in fact only the Singapore cohort included cancers diagnosed in stage IV disease. Furthermore, a smaller number of stage I disease were included compared to the INCLIVA cohort. Interestingly, patients in the Singapore cohort were ten years younger than those in the Spanish cohort. The proportion of MSI high patients was also

significantly smaller in the Singapore cohort, although the number of samples with not-available data was higher. There were no differences in the distribution of both CRCA-38 subtypes and ramkCMS-38 subtypes; also *RAS* and *BRAF* mutational statuses were comparable. Given the stage imbalance, a further comparison including exclusively stage II-III cancers in the two groups was performed (**Table 7**).

Characteristic		Singapore (N:46)	Spain (N:111)	p-value
		n(%)	n(%)	
Gender				0.589
	Female	19(41.30	40(36.0)	
	Male	27(58.7)	71(64.0)	
Age				<0.001
	Median	61	71	
	Range	44-79	49-93	
	NA	2	0	
Stage				<0.001
	II	10(21.7)	62(55.9)	
	III	36(78.3)	49(44.1)	
	NA	0	0	
Sidedness				0.012
	Left	35(76.1)	60(54.1)	
	Right	11(23.9)	51(45.9)	
	NA	0	0	
MSI status				0.116
	MSI	1(2.2)	13(11.7)	
	MSS	38(82.6)	98(88.3)	
	NA	7(15.2)	0(0.0)	

Characteristic		Singapore (N:46)	Spain (N:111)	p-value
		n(%)	n(%)	
RAS status				1.000
	Mutant	16(34.8)	48(43.2)	
	Wild-type	17(36.9)	50(45.1)	
	NA	13(28.3)	13(11.7)	
BRAF status				0.456
	Mutant	1(2.2)	10(9.0)	
	Wild-type	25(54.3)	88(79.3)	
	NA	20(43.5)	13(11.7)	
CMS				0.917
	CMS1	3(6.5)	9(8.1)	
	CMS2	18(39.1)	47(42.3)	
	CMS3	3(6.5))	5(4.5)	
	CMS4	22(47.8)	50(45.1)	
CRCA				0.392
	Enterocyte	16(34.8)	27(24.3)	
	Goblet-like	6(13.0)	2421.6)	
	Inflammatory	5(10.9)	21(18.9)	
	Stem-like	10(21.7)	20(18.0)	
	TA	9(19.6)	19(17.1)	

Table 7. Comparisons of the characteristics of the INCLIVA-Valencia and Singapore FFPE cohorts in patients with stage II-III cancers

No significant genomic or transcriptional differences were present between the two cohorts considering the same stages of disease. Hence, in view of the apparently similar molecular characteristics the two datasets were merged to evaluate the association between rankCMS-38 subtypes and features minimising possible sample-size issues.

Multiple significant associations were demonstrated (**Figure 21**). CMS1 tumours were associated with MSI-high status, right side and *BRAF* mutations; CMS3 were associated with *KRAS* mutations; stage IV disease were predominantly represented by CMS2 and CMS4, while CMS3 was associated with early stage disease.

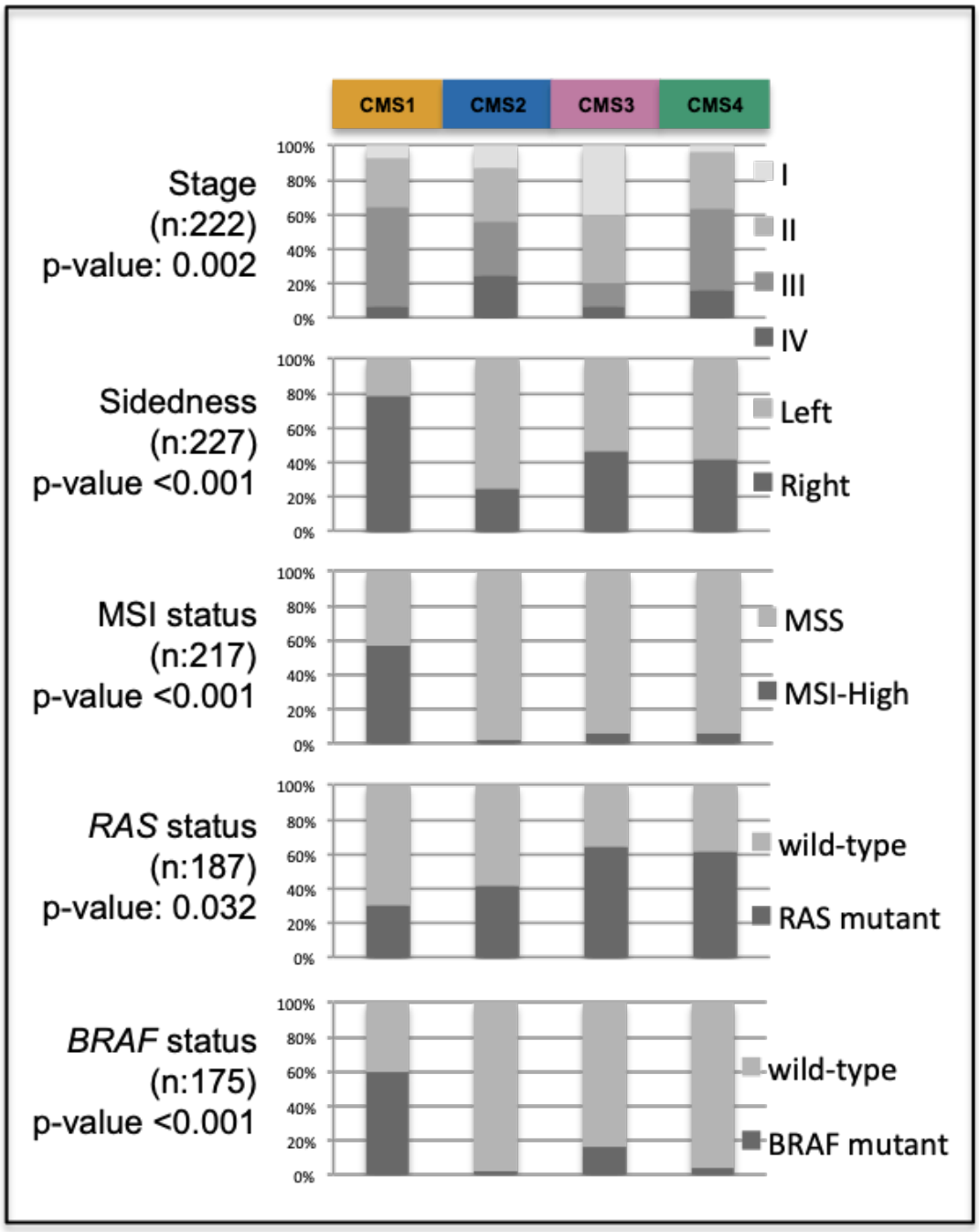

Figure 21. Associations between clinico-pathological features and rank-CMS-38 subtypes in a cohort of 238 primary CRC samples preserved in FFPE blocks.

Figure 22 represents the proportions of subtypes according to the tumour location: as expected CMS1 tumours were predominantly located in the caecum and ascending colon, while only one CMS1 tumour was located in the rectum.

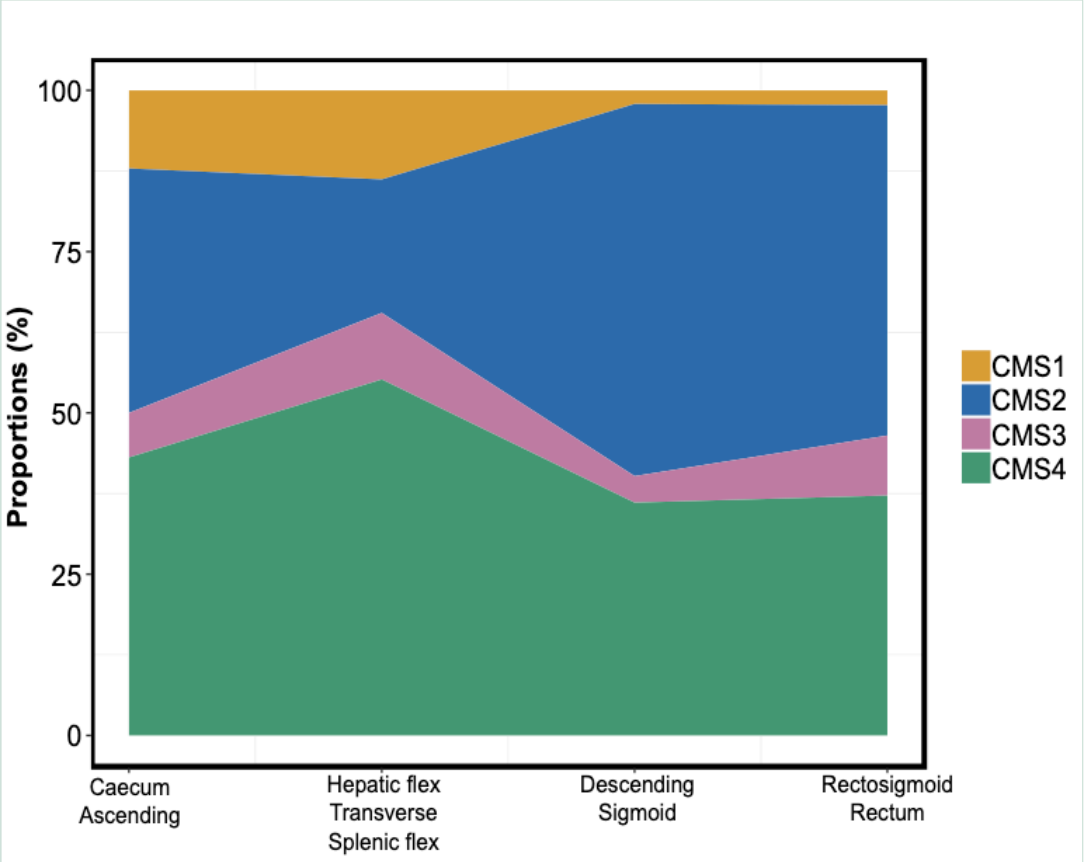

Figure 22. Distribution of the rankCMS-38 subtypes according to tumour location.

3.4.3 Comparison between Caucasian and Asian populations

In the previously presented **Table 7**, the Caucasian and Asian populations with similar stage of disease at diagnosis were directly compared. No significant differences between molecular characteristics were identified.

Associations between clinico-pathological features and rankCMS-38 subtypes were evaluated in the two cohorts, separately (**Table 8**). This to understand whether the molecular features of rankCMS-38 subtypes were similar in both populations.

In both cohorts, sidedness and *BRAF* mutation were significantly associated with the subtypes; similarly, gender, age and *RAS* mutation were not significantly associated with the subtypes in both cohorts. The only difference observed was related to the highly significant association between MSI status and CMS1 subtype in the Caucasian population, but not in the Asian one. This was likely due to the low incidence of MSI-high tumours (n: 2) in the Asian cohort.

A.

Characteristic		CMS1	CMS2	CMS3	CMS4	p-value
		n(%)	n(%)	n(%)	n(%)	
Gender						0.953
	Female	3(60)	23(45)	3(43)	20(47)	
	Male	2(40)	28(55)	4(57)	23(53)	
Age						0.105
	Median	70	61	70	59	
Sidedness						0.006
	Left	2(40)	41(80)	4(57)	24(56)	
	Right	3(60)	6(12)	0(0)	15(35)	
	NA	0(0)	4(8)	3(43)	4(9)	
MSI status						0.102
	MSI	1(20)	0(0)	0(0)	1(2)	
	MSS	4(80)	43(84)	5(71)	31(72)	
	NA	0(0)	8(16)	2(29)	11(26)	
RAS status						0.257
	Mut	1(20)	16(31)	3(42)	18(42)	
	WT	1(20)	24(47)	2(29)	11(26)	
	NA	3(60)	11(22)	2(29)	14(32)	
BRAF status						0.009
	Mut	1(20)	0(0)	1(14)	1(2)	
	WT	1(20)	33(65)	2(29)	25(58)	
	NA	3(60)	18(35)	4(57)	17(40)	

B.

Characteristic		CMS1	CMS2	CMS3	CMS4	p-value
		n(%)	n(%)	n(%)	n(%)	
Gender						0.508
	Female	5(55)	22(37)	5(45)	17(32)	
	Male	4(45)	37(63)	6(55)	36(68)	
Age						0.323
	Median	77	68	74	70	
Sidedness						0.008
	Left	1(11)	39(66)	4(36)	30(56)	
	Right	8(89)	20(34)	7(64)	23(44)	
MSI status						0.000
	MSI	7(78)	2(4)	1(9)	4(8)	
	MSS	2(22)	57(96)	10(91)	49(92)	
RAS status						0.130
	Mut	2(22)	21(36)	6(54)	28(53)	
	WT	6(66)	27(46)	3(27)	18(34)	
	NA	1(12)	11(18)	2(19)	7(13)	
BRAF status						0.000
	Mut	5(55)	2(4)	1(9)	2(4)	
	WT	3(34)	46(78)	8(73)	44(83)	
	NA	1(11)	11(18)	2(18)	7(13)	

Table 8. Associations between clinico-pathological characteristics and rankCMS-38 in Singapore-FFPE (A) and INCLIVA-Valencia cohort (B).

3.5 Discussion

In this chapter the validity of the rankCMS-38 assay was evaluated in FFPE samples. In the absence of an alternative method to assess the expression of the signature, clinico-pathological features were used to determine whether known subtype-specific associations could be reproduced using the new assay. The rankCMS-38 subtypes maintained the subtype-specific features, supporting the robustness of the assay.

Although in line with recent literature, the evaluation of subtype distributions demonstrated the presence of a small number of samples belonging to CMS1 and CMS3 subtypes in both the cohorts. It is possible that a small proportion of these subtypes is misclassified as CMS4 by the assay given the reduced sensitivity of the CMS4 group (chapter 2, section 2.4.2). However, this may not be completely related to assay performance but rather to the CMS classifier itself. In fact, recently Dunne *et al.* demonstrated how the performance of the CMS classification is challenged by intra-tumoural heterogeneity, with discordant subtyping results from different areas of the same tumour (115). In particular, the presence of stromal/fibrotic areas may interfere with the classification with consequent overestimation of the CMS4 (mesenchymal, fibroblast-enriched) subtype. Other classifiers primarily based on cancer-intrinsic genes/epithelial genes have been developed, though their robustness has still not been tested on a large scale (174,175). Furthermore, the expected subtype distribution in different settings is difficult to define: the vast majority of the published studies so far reported the results of the Random-Forest classifier (148,153). The classification derived from this algorithm is partially affected by intra-cohort normalization and therefore by the type of cohort analysed. Conversely, using a single-sample predictor (SSP) algorithm each sample is classified independently of the context. The rankCMS-38 classifier was developed as SSP, possibly representing a more realistic distribution of the CMS subtypes. Nevertheless, biologically and clinically distinctive subgroups of patients can be identified, supporting its further prospective evaluation.

When assessing potential biological differences between Caucasian and Asian CRC, no significant differences were demonstrated in terms of subtypes' distribution and subtype-specific characteristics. Interestingly, Asian patients were much younger than Caucasians. When considering stage II and III tumours only, a significantly higher proportion of Asian patients were diagnosed with a stage III CRC: it is possible that this association could be due to selection biases or reflection of delayed diagnosis (in view of the younger median age possibly outside screening programs). However, this may also be an indicator of a more aggressive disease, in line with the lower incidence of MSI-high tumours (typically associated with stage II and favourable prognosis in Caucasian population).

Interestingly, a previous systematic study of a Singaporean population fulfilling the Amsterdam clinical criteria for Lynch Syndrome highlighted how all pathogenic defects were confined to two MMR genes, *MLH1* and *MSH2*, but not to *MSH6* and *PMS2* (176). Furthermore, out of 15 pathogenic variants in *MLH1* and *MSH6*, 6 were novel. This study demonstrated the molecular heterogeneity of Lynch Syndrome and how both Amsterdam and Bethesda criteria (developed in Caucasian populations) may not completely apply to Asian populations (177-178). In view of the increasingly recognised role of MSI and defective mismatch-repair mechanisms as predictive biomarker of response to immunotherapy, a thorough assessment of these biomarkers in different populations is essential (179). Given the similar phenotypic profile of Caucasian and Asian population identified in the current analysis despite the difference in MSI status, assessing the association between subtypes and response to immunotherapy across populations is worth noting.

Chapter 4 Assessment of NanoCRC biomarker assay to predict treatment response in CRC

4.1 Introduction

4.1.1 The epidermal growth factor receptor (EGFR) signalling pathway

Located on the chromosome 7p, the *EGFR* (or *ErbB-1*) gene encodes for a transmembrane tyrosine kinase receptor protein (180). Similarly to the other 3 members of the family (ERBB2, ERBB3 and ERBB4), the receptor undergoes a conformational change after the interaction with its ligands (including the epidermal growth factor (EGF), amphiregulin (AREG) and heregulin (EREG)), with activation of downstream signalling pathways involved in cellular survival, proliferation, differentiation and migration (180). In some cancers the activation of the receptor is ligand-independent as a result of alterations of the extracellular domain with consequent constitutive receptor activation or as consequence of cellular stresses such as radiation (181). Upon activation, key tyrosine residues of the intracellular domain are phosphorylated, becoming docking sites for intracellular proteins (Grb2 and Sos). These proteins form a complex able to activate at least two intracellular cascades, one is the RAS/RAF/MAPK pathway and the other is the PIK3CA/AKT/mTOR pathway. Both pathways lead to the translocation of transcriptional factors into the nucleus with activation of proliferation, survival and invasion genes (181).

The EGFR pathway plays a critical physiological role during embryogenesis of vertebrates (182). The members of the family are expressed in the vast majority of cells with the exception of hematopoietic cells (182). In animal models, gene knock out results in embryonic or perinatal lethality due to abnormal brain, lung, skin and gastrointestinal development. The four family members are very similar

in structure but associated with slightly different body distribution and mechanism of activation and signalling. As example, while EGFR activation is crucial for the central nervous system and mammary glands maturation, ERBB2 and ERBB3 are active in the cardiac formation (182). EGFR is also crucial in skin maturation, hair follicles and hair cycling development. These functions explain typical side effects of anti-EGFR drugs (skin toxicities) or anti-HER2 agents (cardio-toxicity).

Hot-spot mutations of the EGFR gene may result in aberrant domains of the receptor, which becomes constitutionally active; in glioblastomas, the extracellular domain is the portion more frequently mutated while in lung cancer the aberrant domain is typically the intracellular one, with consequent activation of the tyrosine kinase domain (182). The L585R point mutation and the exon 19 in-frame deletion are the most commonly activation mutations observed in lung cancer which became positive predictive biomarker of response to tyrosine kinase inhibitors (TKIs) like gefinitib or erlotinib (183). Conversely, the presence of the T790M mutation has been associated with resistance to TKIs (183).

Activating mutations are rarely found in CRC, where the wild type gene is overexpressed in 25% to 80% of cases (184). Gene amplification has been reported inconsistently in CRC: in some studies the amplification is uncommon while in other reports a moderately increased copy number may be present in up to 50% of the cases (184). Recently, an integrated genomic analysis of CRC development and progression highlighted how epigenetic modifications may play a key role in up-regulating the EGFR signalling pathway: during the progression from adenoma to carcinoma increased expression of the EGFR ligand EREG was demonstrated following demethylation of two sites of the *EREG* promoter (185).

4.1.2 Targeting EGFR in colorectal cancer

The EGFR pathway was the first one recognised as oncogenic driver in human epithelial cancer. In 1984 John Mendelsohn and Gordon Sato described for the first time how monoclonal antibodies against EGFR were able to inhibit the growth of human tumour cells implanted in athymic mice (186). These studies led to the development of monoclonal antibodies and tyrosine kinase inhibitors in human cancers. Cetuximab is a human-murine chimeric antibody with high affinity for the EGFR external domain. It works as competitive antagonist of EGFR ligands. Following ligand binding, the complex is internalized and degraded with consequent down-regulation of EGFR on the cell surface. In this way, the intracellular signal is down-regulated and arrests in the G1 phase of the cell cycle is triggered with initiation of the apoptotic cascade (187). As immunoglobulin (Ig) G1, cetuximab is able to promote antibody-dependent cell-mediated cytotoxicity (ADCC): after binding EGFR on the cancer cell surface, its Fc region is recognised by the Fcy receptor (R) of Natural Killer and macrophages (187). Polymorphisms in FcyR have been associated with different activity of the drug leading to distinctive patient outcomes, although controversial results have been reported in multiple retrospective studies in CRC (187).

Another monoclonal antibody targeting EGFR, panitumumab, has a similar mechanism of action with the advantage of a minor immunogenicity in view of its fully humanised structure (188). This property reduces the risks of allergic reactions during the infusion of the antibody, however, as IgG2 the cytotoxic activity due to ADCC mechanisms is unlikely trigger, opposite to cetuximab (187).

Both cetuximab and panitumumab were initially compared to best supportive care in patients with metastatic disease after progression to standard chemotherapy options (189-190). Both drugs demonstrated activity in molecularly unselected populations, with objective responses in about 10% of the patients and survival prolongation of about 1.5 months (from about 4.5 to 6 months) (189-190) (**Table 9**). The two drugs were also compared in a non-

inferiority phase III trial, demonstrating overlapping efficacy results and minor differences in the toxicity profiles (191). Subsequent studies aimed to determine the effect of anti-EGFR agents in earlier settings in combination with different chemotherapy backbones (**Table 9**). Although an increase in response rate was observed in some of the studies, the majority of the patients still did not benefit from these expensive drugs. Therefore, the identification of biomarkers of response became crucial.

Study	Study interventions	Molecular selection	N	ORR	mPFS (months)	mOS (months)
Anti-EGFRs monotherapy in chemorecfractory setting						
CO.17 (189,192)	Cetuximab + BSC vs BSC	Unselected	572	8% / 0%	NR	6.1 / 4.6
		KRAS exon 2 wt	230	13% / 0%	3.7 / 1.9	9.5 / 4.8
CO.20 (193)	Cetuximab + brivanib vs Cetuximab + placebo	*KRAS* exon 2 wt	750	14% / 7%	5.0 / 3.4	8.8 / 8.1
/ (190,194)	Panitumumab + BSC vs BSC	Unselected	463	10% / 0%	2.0 / 1.8	NR
		KRAS exon 2 wt	243	17% / 0%	3.1 / 1.8	8.1 / 7.6
ASPECCT (191)	Panitumumab vs Cetuximab	*KRAS* exon 2 wt	1010	22% / 20%	4.2 / 4.4	10.2 / 9.9
2nd line and beyond trials with anti-EGFR agents						
BOND (195)	Cetuximab -/+ Irinotecan	Unselected	329	11% / 23%	1.5 / 4.1	6.9 / 8.6
PICCOLO (196)	Irinotecan +/- Panitumumab	*KRAS exon 2, 3* wt	460	34% / 12%	NR	10.4 / 10.9
EPIC (197)	Irinotecan +/- Cetuximab	Unselected	1298	16% / 4%	4.0 / 2.6	10.7 / 10.0
20050181 (198)	FOLFIRI +/- Panitumumab	*KRAS exon 2*	1186	36% / 10%	6.7 / 4.9	14.5 / 12.5
		RAS wt	1014	41% / 10%	NR	NR
1st line trials with anti-EGFR agents						
OPUS (199)	FOLFOX +/- Cetuximab	Unselected	337	46% / 36%	7.2 / 7.2	18.0 / 18.3
		KRAS exon 2 wt	179	57% / 34%	8.3 / 7.2	22.8 / 18.5
		KRAS, BRAF wt	164	60% / 36%	8.3 / 7.2	22.8 / 19.5
COIN (200)	FOLFOX +/- Cetuximab	*KRAS* exon 2, 3 wt	729	64% / 57%	8.6 / 8.6	17.0 / 17.9
		KRAS exon 2, 3, *NRAS, BRAF* wt	581	NR	NR	19.9 / 20.1
CRYSTAL (201, 202)	FOLFIRI +/- Cetuximab	Unselected	1217	47% / 39%	8.9 / 8.0	19.9 / 18.6
		KRAS exon 2 wt	666	57% / 40%	9.9 / 8.4	23.5 / 20.0
		KRAS exon 2, *BRAF* wt	566	61% / 43%	10.9 / 8.8	25.1 / 21.6
PEAK (203)	FOLFOX + Panitumumab vs FOLFOX + Bevacizumab	*KRAS* exon 2 wt	285	58% / 54%	10.9 / 10.1	34.2 / 24.3
		RAS wt	170	64% / 61%	13.0 / 9.5	41.3 / 28.9
PRIME (204)	FOLFOX +/- Panitumumab	*KRAS* exon 2 wt	656	55% / 48%	9.6 / 8.2	23.8 / 19.4
		RAS wt	512	NR	10.1 / 7.9	25.8 / 20.2
		RAS, BRAF wt	446	NR	10.8 /9.2	28.3 / 20.9
FIRE3 (89,90)	FOLFIRI + Cetuximab vs FOLFIRI + Bevacizumab	*KRAS* exon 2 wt	592	62% / 58%	10.0 / 10.3	28.7 / 25.0
		RAS wt	400	72% / 56%	8.4 / 9.7	33.1 / 25.0
CALGB80405/ SWOG (41)	FOLFOX or FOLFIRI + Cetuximab vs FOLFOX or FOLFIRI + Bevacizumab	*KRAS* exon 2 wt	1137	60% / 55%	10.5 / 10.6	30.0 / 29.0
		RAS wt	526	67% / 54%	11.2 / 11.0	32.0 / 31.2

Table 9. Summary of multicentre randomised clinical trials assessing the benefit of anti-EGFR therapy as a single agent compared to best supportive care (BSC) or placebo or in combination with standard chemotherapy regimens in first and second-line setting in CRC. Overall response rates (ORR) and survival outcomes are presented based on treatment arm. NR: not reported.

4.1.3 Molecular biomarkers to predict benefit from anti-EGFR agents

In view of the mechanism of action of the antibodies, binding the receptor on the cell surface, EGFR expression level was the first biomarker investigated as potential indicator of activity. Unfortunately, multiple studies failed to demonstrate any correlation between EGFR expression measured by IHC and cetuximab or panitumumab benefit (180).

The high level of expression of the ligands EREG and AREG has been associated with increased response to cetuximab in retrospective analyses of clinical trials (205,206). However, the lack of validated assays to systematically assess the expression of the ligands halted their potential clinical application. Similarly, high EGFR copy number gain was associated with better outcomes in CRC patients treated with anti-EGFR therapy in retrospective studies mainly lacking of control groups and of standardized and reproducible methods to evaluate the biomarker (207).

In 2006 Lievre and colleagues reported for the first time that mutations in *K-RAS* gene were associated with primary resistance to anti-EGFR therapy (208). This gene is part of the EGFR downstream signalling pathway; when mutated, KRAS is constitutively active, leading to cell proliferation independently from the EGFR signal (208). Hence, blocking the EGFR receptor becomes futile. The anti-EGFR therapy was initially restricted to *KRAS* exon 2 wild-type population (29). Further retrospective analyses demonstrated that other mutations in *KRAS* (exons 3 and 4) and *NRAS* (Neuroblastoma RAS Viral oncogene homolog) gene (exons 2, 3 and 4) were equally effective in preventing the effect of anti-EGFR therapies (188). In 2013, both the Food and Drug Administration (FDA) and The European Medicine Agency (EMA) restricted the use of anti-EGFR monoclonal antibodies to patients with metastatic CRC with extended *RAS* (*KRAS* and *NRAS* exons 2,3 and 4) wild type tumours (188).

Increasing evidence suggest that the V600E mutation in the *BRAF* gene (present in about 12% of metastatic CRC patients) is not only a prognostic factor of poor prognosis, but also negatively predicts the benefit from anti-EGFR therapy in late lines of therapy (29). However, conflicting evidence from meta-

analyses of first and second line studies have been reported (29). Hence, the presence of *BRAF* mutation is not an absolute contraindication to cetuximab or panitumumab. Increased activity has been reported when these agents are combined with *BRAF* and *MEK1* (Mitogen Activating Protein Kinase) inhibitors (130).

Multiple less frequent molecular events have been indicated as mechanisms of primary resistance to anti-EGFR therapy. These include *HER2* alterations, *MET* amplification, *PIK3CA* mutations and rare rearrangement of *NTRK, ROS, ALK* or *RET* genes (209). Cremolini *et al.* recently used a panel of genomic alterations to demonstrate how the presence of any of the selected alterations are significantly more frequent in patients showing primary resistance than among patients who benefitted from anti-EGFR therapy. The study included 47 patients with *RAS/BRAF* wild-type tumour resistant to therapy in a chemorefractory setting and further 47 patients who responded to the treatment in the same setting (209).

4.1.4 Gene expression subtypes to predict benefit from anti-EGFR targeted agents

Following the identification of the five CRCAssigner subtypes, Sadanandam *et al*. asked whether increased anti-EGFR benefit was associated with any of the subtypes using publicly available data from the Khambata-Ford dataset (139,205). Microarray data generated from metastatic CRC lesions (the majority from liver metastases) collected from patients prior to cetuximab therapy were analysed. Three (TA, stem-like and goblet-like) out of five subtypes were identified using an unsupervised method (Non-negative Matrix Factorizations) and the 786 CRCAssigner gene signature (139, 210). Only 23% of patients with stem-like and goblet-like benefitted (complete, partial or stable disease) from cetuximab. In contrast, 54% of the TA subtype benefitted. This TA partition was confirmed in cell lines and xenograft models, leading to the functional sub-classification of the TA subtype into cetuximab sensitive (CS-TA) and cetuximab resistant (CR-TA) (139). Although not significant, *KRAS* wild-type tumours were

numerically higher in the CS-TA group compared with CR-TA. Whether these two sub-subtypes were significantly associated with extended *RAS* mutational profiles is unknown, given that the only *KRAS* exon 2 mutational status was available.

4.2 Hypotheses and aims

Hypotheses

The CRC subtypes identified with the newly developed assay (NanoCRC) and algorithm (chapter 2) are clinically meaningful because they are associated with distinctive prognosis and differential response to anti-EGFR therapies. In view of its potential clinical applicability, the NanoCRC assay may serve as a stratification tool for prospective patient selection for anti-EGFR therapy.

Specific aims

1. Evaluate (a) the CRCA-38 subtypes and (b) a derivative biomarker (lately dubbed TA classes) identified using the NanoCRC assay in patients samples and in experimental cohorts (cell lines and patient-derived xenografts) to understand their clinical relevance and whether an association with response to anti-EGFR therapy exists;
2. Evaluate the rankCMS-38 subtypes identified using the NanoCRC assay to understand their clinical relevance and potential association with anti-EGFR benefit.

4.3 Methods

4.3.1 Sample collection

A first cohort of patients' samples was identified within two different ethically approved translational studies at The Royal Marsden Hospital (RMH) (The RETRO-C and FOrMAT, described below); three further cohorts were identified, two via Italian collaborators and one via the Canadian Cancer Trial Group. These were the details of the studies and cohorts:

1. The RETRO-C study (ethic committee reference: 10/H0308/28): A retrospective translational study: characterisation of molecular predictors of response to cetuximab or panitumumab in patients with colorectal cancer (Principal Investigator, PI: Professor David Cunningham). In this study, formalin-fixed paraffin embedded (FFPE) samples from patients who received cetuximab or panitumumab at the RMH between January 2004 and January 2014 were retrospectively collected. Link-anonymised clinical data were reviewed (initially by Dr Francesco Sclafani, clinical research fellow in the Gastrointestinal Unit, RMH, and then by myself). Only patients who received anti-EGFR therapy as a single agent or in an irinotecan-refractory (chemorefractory) setting were included. Patients were considered chemorefractory if they progressed during or within 3 months from the last dose of irinotecan. All patients must have received at least one cycle of anti-EGFR therapy. This cohort included a proportion of patients with *RAS* or *BRAF* mutant tumour. This is because some of the patients were treated before the UK implementation of *KRAS* testing (August 2009) and extended *RAS* testing (December 2011) (211,212). In April 2017, I amended the protocol in order to include the current analysis, which was approved by the Trial Management Group.
2. The FOrMAT feasibility study (ethic committee reference: 13/LO/1274RM): Feasibility of a Molecular characterisation Approach to Treatment (Principal Investigator: Dr Naureen Starling). In this study,

FFPE samples from patients with gastrointestinal cancer who received (or were about to receive) at least one line of therapy in the advanced setting were prospectively collected (213). Patients with metastatic CRC treated with single agent anti-EGFR therapy between January 2014 and January 2016 were identified. Clinical data were collected in a link-anonymised fashion and merged to the RETRO-C clinical data.

3. The PRESSING case-control study (ethic committee reference: 1333/17 Area Vasta Nord Ovest): the design and results of this study were previously described (209). I successfully established a collaboration and material transfer agreements between The Institute of Cancer Research and The National Institute of Cancer (PI Dr Filippo Pietrantonio, Medical Oncology Department, Fondazione IRCCS Istituto Nazionale dei Tumori, Milan, Italy). A cohort of patients with extended RAS wild-type CRC previously included in the PRESSING study and with available FFPE samples were identified. The FFPE blocks and link-anonymised clinical information were transferred to our lab. After review of the clinical information, only patients who received anti-EGFR therapy as a single agent or in combination with chemotherapy but in a chemorefractory setting were included.
4. The CO.20 clinical trial cohort (ClinicalTrials.gov identifier NCT00640471): In this clinical trial, patients with metastatic CRC received single agent cetuximab or cetuximab in combination with the anti-angiogenic agent brivanib after progression from standard chemotherapy (193). Here, I successfully developed a research proposal submitted to the Canadian Cancer Trial Group and Australasian Gastrointestinal Trial Group (CCTG/AGITG) Gastrointestinal Correlative Science and Tumour Biology Committee. The research proposal was approved by the Committee in May 2017. Material transfer and collaboration agreements were established. In collaboration with the CCTG statistician (Dr Dongsheng Tu) and the CCTG Pathology coordinator (Dr Shakeel Virk), FFPE cancer samples of patients who received at least one cycle of treatment in the control arm of the trial (cetuximab only) were selected for further analysis.

5. The “Cases” cohort: in this cohort, RNA extracted from *KRAS*, *NRAS*, *BRAF* and *PIK3CA* wild type CRC liver metastases (pre-implantation samples) and correlated patient-derived xenografts (PDXs; six mice treated with cetuximab and six mice treated with placebo) was collected from a well-established biobank of patient samples with matched xenograft lines (214-215). Each pre-implantation sample and the two linked PDXs cohorts together were considered as a “case”, as per previous publications (214-215). Xenopatients’ tumour volume variation data at 3 weeks after cetuximab treatment initiation were collected. The RNA and response data were provided by Dr Livio Trusolino (Department of Oncology, University of Torino Medical School and Translational Cancer Medicine, Candiolo Cancer Institute, Candiolo, Torino, Italy).

For cohorts 1,2,3 and 4, the FFPE block of the primary tumour sample collected prior to any treatment was retrieved whenever available. If the primary tumour block was not available, any other available block containing metastatic lesions was retrieved. The information related the type of sample and whether pre- or post-treatment was carefully reviewed in the patient notes and taken into account for downstream analyses.

4.3.2 Publicly available data

1. Affymetrix Human Genome U133A 2.0 Array gene expression files (.CEL) of metastatic biopsies from 80 CRC patients who received single agent cetuximab within a phase II study were downloaded from Gene Expression Omnibus (GEO, accession number GSE5851) and Robust Multiarray Averaging (RMA) normalised (this step was performed by Ms Katherine Eason) (205). Clinical data, mutational status, response to treatment and PFS data were downloaded from the on-line supplementary Table1 of the same publication (205).
2. Illumina array-based mRNA expression profiles for 155 CRC cell lines were downloaded from GEO (accession GSE59857) (Ms Katherine

Eason)(216). The mutational status, “AUX index” and the percentage of growth inhibition with different cetuximab concentrations were recovered from the on-line Supplementary Data 1 of the same manuscript (216).

4.3.3 Nucleic acid extraction

All FFPE blocks from the different cohorts were processed by myself with the same protocol described in Chapter 2.

The RNA received from cohort 5 (the cases) was extracted in Italy with protocols previously published (214,215). For the CO.20 cohort, nucleic acids from about half of the samples were extracted in Canada using an automated extractor and shipped in dry ice. The samples not suitable for automated extraction due to small dimensions were extracted by myself (with the help of Dr Patrick Lawrence, Scientific Officer) with the same methods (chapter 2, section 2.3.7). Technical difference between different extraction batches were taken into account and corrected if required (see batch effect assessment section 4.3.9).

4.3.4 Mutational profiling

- For cohort 1 (RETRO-C), the assessment of the mutational status of 5 frequently mutated genes in CRC was an on-going project described in the RETRO-C protocol; the project was lead by Dr Francesco Sclafani (GI unit). The mutational analysis was performed by Ms Sanna Hullki (High Scientific Officer) in the Department of Molecular Pathology, RMH. I shadowed Ms Hullki during the analysis and recovered the data for the relevant samples.

  KRAS, *NRAS*, *BRAF, PIK3CA* and *TP53* mutational status were evaluated with a TruSeq custom panel amplicon next generation sequencing (TSCA NGS) previously validated for routine clinical use in the Department of Molecular Pathology (accredited laboratory). Up to 20 ng of DNA were processed using TSCA NGS including 35 amplicons optimised for DNA extracted from FFPE (following extensive internal

validation with over 200 specimens, unpublished data). Hotspot regions for *KRAS* (exons 2-4), *NRAS* (exons 2-4), *PIK3CA* (exons 2, 10 and 21) and *BRAF* (exon 15) and all the coding exons of *TP53* (exons 2-10) were targeted with >3% allele frequency as limit of detection. Amplicons of 60-130bp were obtained. A positive control quantitative multiplex DNA reference standard (Horizon Discovery) and a no template control (NTC) were used as internal controls. The TSCA NGS products were sequenced using MiSeq (Illumina Inc.) according to manufacturer's instructions. For data analysis, two separate pools were combined into a single output file and annotated for the variants using Variant Studio (Illumina Inc.). Variant results from BAM files and amplicon coverage were visualised and assessed in Integrative Genomic Viewer (Broad Institute).

- The mutational status of *KRAS*, *NRAS*, *BRAF and PIK3CA* of the samples in the FOrMAT cohort was already available as part of the main project (213).
- For the Italian cohort, oncogenic mutations of 50 cancer-related genes were previously published in the PRESSING case-control study (209). Only *KRAS*, *NRAS*, *BRAF and PIK3CA (*quadruple wild type) samples with available FFPE material were selected for the current study.
- For the CO.20 cohort, high sensitivity mutational profile data were generated in an on-going project using nested polymerase chain reaction (PCR) (this analysis was performed by Prof. Paul Waring's group at the University of Melbourne, Australia). Methods were provided by our collaborators and included a DNA repair step (New England Biolabs PreCR repair mix) and an in-house customised protocol for nested ICE COLD PCR kit (Precipio ICEme). Sequencing was performed with Illumina MiSeq platform. In view of the high sensitivity of this protocol each sample was analysed in triplicate and considered mutant only if: a) the mutation appeared in all the replicates at approximately equal frequency, b) the mutational signal was significantly stronger than the baseline or the ICE COLD PCR induced and with strong signal compared to baseline.

4.3.5 Gene expression analysis

In this project I used the 96-genes assay (NanoCRC assay – **Appendix 1**), which was developed as previously described in chapter 2. RNA in the region of 100 ng were hybridized with the custom probes of the NanoCRC assay using the Elements XT protocol for NanoString Technologies as manufacturer' instructions. Hybridization temperature and duration was in line with the protocol previously optimised in the lab (154). The hybridized products were immobilised on a cartridge; each barcode was counted and recorded in an ".RCC file" using the Max Analysis System from NanoString Technologies as described in chapter 2, section 2.3.8.

4.3.6 Data quality control and batch effect assessment

Each ".RCC" file download from the Digital Analyzer was then up-loaded in the nSolverTM 3.0 Analysis Software provided by NanoString Technologies. After standard quality control steps (as per chapter 2, section 2.3.9), normalization of the raw data was performed using 8 negative and 6 positive controls. The performance of the 10 housekeeping genes included in the panel was evaluated with the geNorm algorithm integrated in the nCounter Advance Analysis protocol version 2.0. Only housekeeping genes selected by the algorithm were used for data normalization. The possible batch effect in each cohort was visually assessed using Principal Component Analysis (PCA). The PCA plots were generated directly using the Advance Analysis Software. In view of the expected presence of significant batch effect in the CO.20 cohort (where the nucleic acid extraction was performed partially in Canada and partially in our Lab), batch correction was performed with the exploBatch method, previously developed and published by Dr Gift Nyamundanda (Bioinformatics Postdoctoral Fellow in The Sadanandam Lab) (217). Log2 transformed normalised data were exported in .txt file for downstream analyses.

4.3.7 Biomarkers prediction

Log2 normalised data for each cohort were used to classify each sample according to three possible classifications:

1. CRCA-38 subtypes, using the published CRCA-38 classifier (154);
2. RankCMS-38 subtypes, using the new classifier described in chapter 2;
3. Transit-Amplifying (TA) class-1 and TA class-2, using the CRCA-38 classifier with a modification in sample assignment described in details in the results section.

4.3.8 Study design

1. Objective: to identify whether CRC gene expression subtypes (or the newly defined biomarkers TA class-1 and TA class-2) are associated with distinctive outcomes in CRC patients who received anti-EGFR therapy as single agent or in combination with chemotherapy in a chemorefractory setting.

2. Endpoints:
    a. Primary: progression-free survival (PFS) between patients with the candidate molecular subtype (TA or CMS2 or TA class-1) and those with other subtype. The PFS was defined as the time measured from the date of the first cycle of anti-EGFR therapy to the date of radiological or clinically documented progression of disease or death from any cause. Patients with no documented progression and alive at the time of analysis were censored at the last follow-up.

    b. Secondary:
        i. Overall survival (OS), defined as the time measured from date of the first cycle of anti-EGFR therapy to date of death

from any cause. Patients alive at the time of analysis were censored at the last follow-up.

ii. Disease control rate (DCR), defined as complete, partial or stable disease according to RECIST (Response Evaluation Criteria In Solid Tumours) criteria version 1.1;

iii. Overall response rate (ORR), defined as complete or partial response according to RECIST criteria version 1.1.

c. Exploratory endpoints:

i. To measure the distribution of the biomarkers in the different cohorts of patients;

ii. To examine the association between biomarkers and clinical and pathological characteristics;

iii. To further confirm that the assessment of the proposed classifications using the established NanoCRC assay is feasible;

3. Study populations

Three main cohorts analysed for the first time in this work were defined: a test cohort, formed by all patients whom tumour was collected between retrospective, non-trial protocols (RETRO-C, FOrMAT and PRESSING); a validation cohort, represented by the CO.20 clinical trial cohort; an experimental cohort, represented by “the cases” cohort, where both patients liver metastatic samples and preclinical models were profiled (details in section 4.3.1).

4. Statistical analyses

The analyses related to the test and “the cases” cohorts were performed by me or by Dr Gift Nyamundanda under my guidance. The analyses related to the CO.20 cohort were performed by Dr Dongsheng Tu (senior biostatistician at The Canadian Cancer Trial Group) under my guidance and as per the analysis protocol submitted to the CCTG Committee. Clinical characteristics were analysed according to biomarker of interest using

descriptive statistics. Within the CO.20 cohort, patients' characteristics were compared to those of the original trial population to identify whether selection biases were present. To test the association between categorical variables Fisher's exact test was used, whilst for continuous variables T-test or non-parametric equivalent were deployed. Pearson's correlation was also used where appropriate.

For the survival endpoints, the Kaplan-Meier method was used to summarise the survival estimate, while Cox proportional hazards models were used to compare the survival rate between the biomarkers adjusted for the effect of known prognostic variables. Hazard ratios along with 95% confidence intervals (CI) were reported. The DCR and ORR were calculated and presented according to molecular subtypes. Logistic regression was used to assess the effect of different biomarkers adjusted for the effect of known prognostic variables. Odds ratio were presented with 95% CI. To assess the accuracy of the biomarkers in defining DCR a receiver operating characteristic (ROC) curve was built.

5. Analysis of publicly available data

To further validate the findings, two publicly available data (previously described in section 4.3.2) were downloaded. Biomarker prediction using the same methods described above in section 4.3.7 was performed.

4.4 Results

4.4.1 Sample identification, nucleic acid extraction and NanoString analysis

Within the retrospective tissue collections (RETRO-C, FOrMAT and PRESSING studies), up to 132 tumour blocks were retrieved and reviewed by different pathologists (at the Royal Marsden and at The National Institute of Cancer in Milan). Due to low tumour content in the block or low RNA yields after attempted extraction, 25 samples were excluded. In the PRESSING study, 17 patients were excluded after review of the clinical information; those patients received anti-EGFR therapy in both first-line and after progression following irinotecan within a re-challenge strategy, and were therefore not suitable for the current analysis.

The RCC files from Royal Marsden (RETRO-C and FOrMAT) and Italian samples (PRESSING) were analysed separately with the nSolver Analysis Software. This was in line with previously published multi-cohorts studies, for example the Consensus Molecular Subtype Consortium analysis (148). For all cohorts, the 10 housekeeping were selected for normalization by the geNorm algorithm. No evident batch effect was observed in these cohorts (**Figure 23**). After normalization, 6 Royal Marsden samples were excluded because of a “content normalization” flag. Hence, 84 samples passed all the quality control steps and were included in the test cohort.

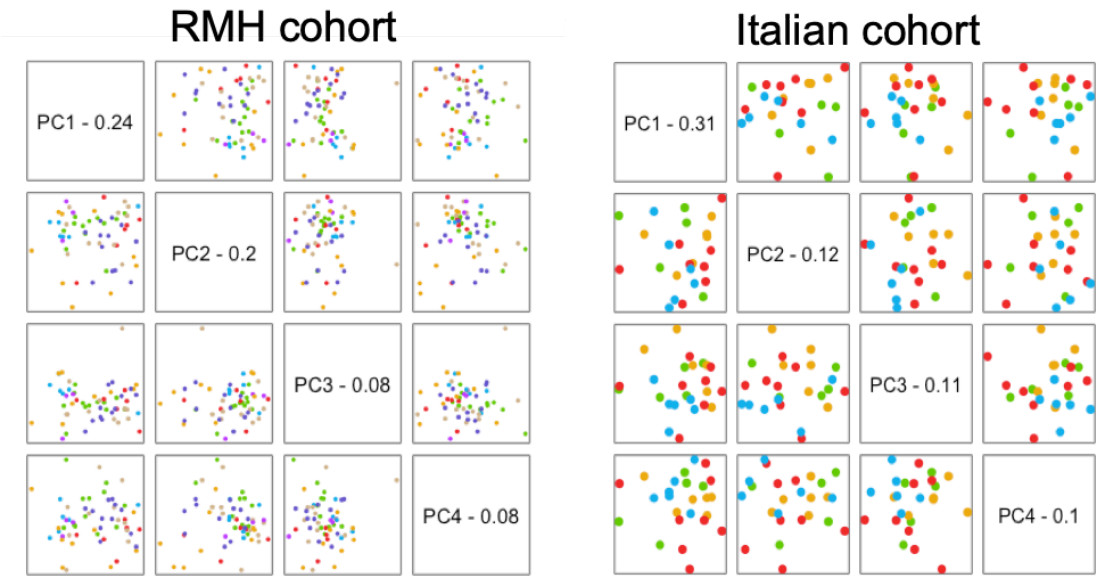

Figure 23. Principal component analysis performed to rule out potential batch effect due to different run of NanoString in the RMH cohort (left) and Italian cohort (right) from the PRESSING case-control study. Each dot represents a sample and each colour a batch. Samples with the same colour were processed in the same NanoString batch. No batch was separated from the others, excluding the present of potential technical effect.

For the validation cohort, 163 patients who received at lest one cycle of cetuximab and with sample available in the Canadian Cancer Trial Group Biobank were identified. Seventeen samples were excluded because of insufficient RNA after extraction. After NanoString analysis, 146 samples were analysed with the nSolver Analysis Software. All 10 housekeeping genes were selected; 123 samples passed the quality control analysis; 23 were excluded because of “content normalization” flag. **Figure 24** represents a consort diagram summarizing the samples identified and selected within each cohort.

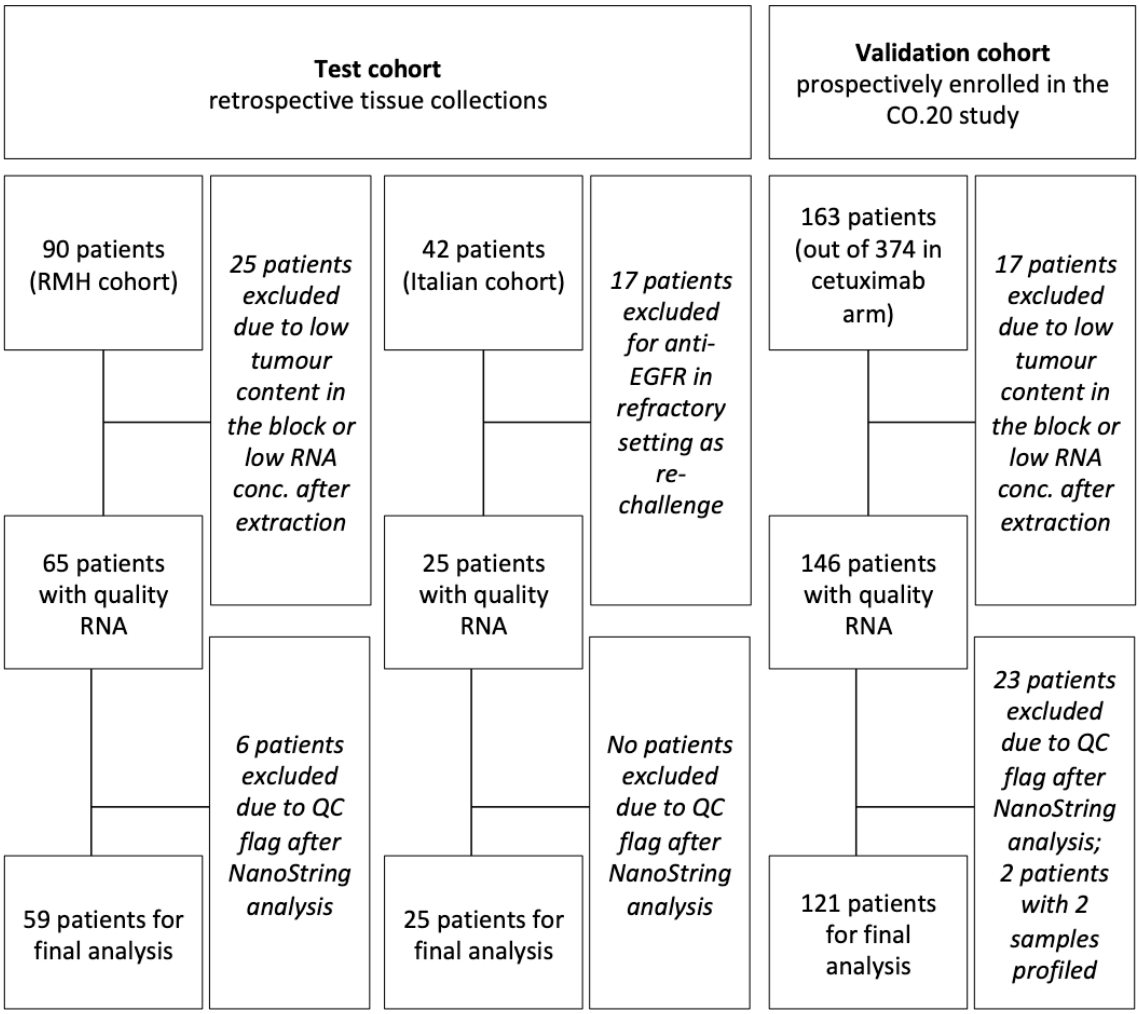

Figure 24. Consort diagram of samples included in the Test (retrospective samples from the RMH and Italian cohort) and Validation (from CO.20 trial sample collection) cohorts.

Because of the different protocols used for RNA extraction in this cohort, with the risk of introducing technical variation, the normalised data were assessed with exploBatch (Dr Nyamundanda) (217). Significant batch effect was demonstrated and therefore corrected (**Figure 25**). After the sample identifiers were cross-checked with the clinical data (Dr Dongsheng Tu), two further samples (with the same subtype class) were excluded because belonging to the same patient. Hence, 121 patients were finally included in the validation cohort.

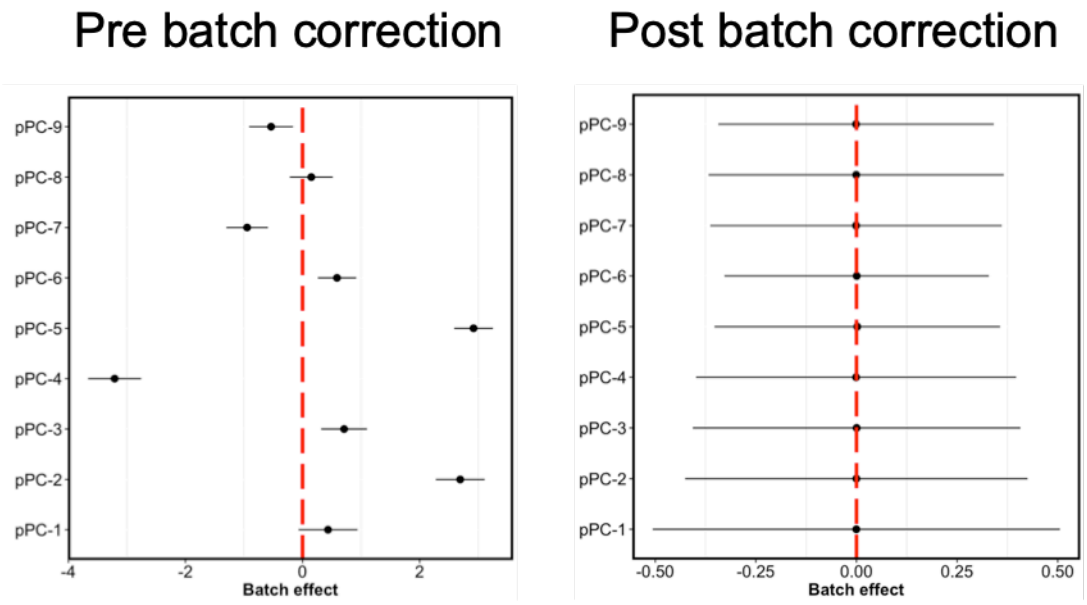

Figure 25. Batch effect assessment and correction using exploBatch method for gene expression data from the test cohort. X-axis represents regression co-efficients from the method and Y-axis represents different probabilistic principal components (pPC) for the Validation cohort data. The 95% confidence interval for each of the pPC has been shown. If the 95% confidence interval touches zero, then there is no batch effect. The left side figure shows the existence of batch effect, whereas the right side figure shows no batch effect after correction.

4.4.2 Patients' characteristics, response and survival data

1. Test cohort: **Table 10** summarises the main characteristics of patients of this cohort. The majority of the patients were male; the median age at diagnosis was 59. This was slightly lower than the median age for colon

cancer (72 in men, 68 in women); however, patients with rectal cancer were also included (median age around 63 for both sexes according to literature) (218). In the majority of cases the primary tumour sample was available for the analysis; in 74% of patients the sample was collected before any type of systemic or radiation therapy. Of note, nearly 26% of the patients carried a mutation in *RAS* or *BRAF* genes. Overall response rate was 26%; disease control rate was 61%; median PFS and OS were 5.30 (95%CI, 3.13 - 6.37) and 10.40 (95%CI, 8.17 - 15.03) months, respectively.

Variable	***Level***	***Overall n(%)***
		84(100)
Sex	*Male*	53(63)
	Female	31(36)
Age<65	*Yes*	54(64)
	No	30(36)
	median (range)	59 (24-88)
Sidedness	*Left*	58(69)
	Right	26(31)
RAS/BRAF mutational status	*Extended wild-type*	47(56)
	KRAS wild-type	8(9.5)
	RAS mutant	13(15.5)
	BRAF mutant	9(11)
	NA	7(8)
Stage at diagnosis	*I-III*	44(52)
	IV	38(45)
	NA	2(3)
Type of samples	*Primary*	64(76)
	Metastatic	29(24)
Sample retrieval time-point	*Pre-treatment*	62(74)
	Post-treatment	22(26)
Anti-EGFR therapy	*single agent*	28(45)
	with chemo	46(55)
Response to anti-EGFR	*Partial response*	22(26)
	Stable disease	29(35)
	Progression	26(31)
	Not available	7(8)
Median PFS (months)	5.30 (95%CI, 3.13 - 6.37)	
Median OS (months)	10.40(95%CI 8.17 - 15.03)	

Table 10. Characteristics of patients included in the Test cohort.

2. Validation cohort: **Table 11** summarises the main characteristics of this cohort. Statistical comparison with the characteristics of the entire CO.20 trial population was performed (Dr Tu) in order to exclude any potential selection biases. With the exception of sex, enriched for female patient in the current study, no significant differences with the entire population enrolled in the CO.20 study were found.

Characteristic	All randomized patients (N = 750)	Current study (N = 121)	p-value
Age – median (range) in year	63.6 (27 – 87.9)	63.7 (27- 87.9)	0.8
<65	406 (54.1)	67 (55.4)	
>=65	344 (45.9)	54 (44.6)	
Gender			0.02
Female	269 (35.9)	57 (47.1)	
Male	481 (64.1)	64 (52.9)	
ECOG performance status			0.3
0	239 (31.9)	47 (38.8)	
1	436 (58.1)	64 (52.9)	
2	75 (10.0)	10 (8.3)	
Type of Malignancy			0.3
Colon only	438 (58.4)	79 (65.3)	
Rectum Only	227 (30.3)	29 (24.0)	
Colon and Rectum	85 (11.3)	13 (10.7)	
Any prior radiotherapy	250 (33.3)	34 (28.1)	0.3
Prior chemotherapy			
Number of regimens 0	1 (0.1)	0 (0.0)	0.9
1-2	8 (1.1)	0 (0.0)	
3	52 (6.9)	9 (7.4)	
4	102 (13.6)	15 (12.4)	
≥5	587 (78.3)	97 (80.2)	
Prior thymidylate synthase inhibitor	747 (99.6)	121 (100.0)	1
Prior irinotecan	728 (97.1)	118 (97.5)	1
Prior oxaliplatin	742 (98.9)	119 (98.3)	0.9
Any prior VEGFR target therapy	310 (41.3)	51 (42.1)	0.6
Any liver metastasis	538 (71.7)	85 (70.2)	0.8
Number of sites of disease			0.3
1	137 (18.3)	24 (19.8)	
2	242 (32.3)	47 (38.8)	
3	198 (26.4)	28 (23.1)	
≥4	173 (23.1)	22 (18.2)	

Table 11. Characteristics of patients in the validation cohort and comparison with the CO.20 clinical trial population (129).

Overall, test and validation cohorts included a similar population in terms of clinical characteristics (although slight variation in the type of data collected does not allow a perfect comparison). The major differences between the cohorts included the mutational status of *KRAS* (all wild-type in the validation cohort, although a few mutations were subsequently identified using high sensitivity techniques) and the fact that all the patients in the validation cohort received anti-EGFR as single agent. Conversely, 55% of the patients in the test cohort received anti-EGFR in combination with chemotherapy. This difference may explain the fact that a higher response rate was observed in the test cohort compared to the validation cohort (ORR: 26% test; ORR: 5% validation).

4.4.3 Analysis of CRCA-38 subtypes

4.4.3.1 Subtypes assignment

Following quality control assessment of the gene expression data, the log2-normalised file generated using the nSolver Analysis Software was used to predict the CRCA-38 subtypes according to the published method (154). The algorithm was applied using RStudio and a user-friendly *R* code. This was specifically developed by Dr Sadanandam to serve the purpose. The algorithm consists of Pearson's correlation of gene-wise median-centred expression profiles for each sample with the recently developed CRCA-38 centroids for each subtype. The subtype with highest correlation is assigned to the sample.

Caution is required in interpreting the associations found between subtypes and clinical characteristics and outcomes; in fact both test and validation cohorts included non-primary samples or samples collected after treatment, while the subtypes were originally developed in primary untreated tumours.

4.4.3.2 Test cohort: clinical characteristics

The pie chart in **Figure 26** represents the distribution of the CRCA-38 subtypes in the test cohort, while **Table 12** summarises the associations between

subtypes and clinical characteristics. With the limitation of the small numbers in each group, no association between subtypes and sex was demonstrated; the median age at diagnosis for TA, stem-like and inflammatory was lower than that in the differentiated subtypes (enterocyte and goblet-like). Right-sided tumours were enriched for goblet-like and inflammatory subtypes. As expected, mutations in *RAS* genes were mainly found in goblet-like and enterocyte, while *BRAF* mutations were distributed between goblet-like and inflammatory. Of note and not surprisingly, a significant association with the type of sample was demonstrated: the highly differentiated subtypes (enterocyte and goblet-like) were predominantly found when the primary tumour was profiled but very rarely in metastatic samples. The expression profiles of these two subtypes are very similar to normal colonic tissue. Either over-estimation in primary tumour samples exists due to normal tissue contamination or whether this is due to biological switch-off of their differentiated signature during metastasization (epithelial-to-mesenchymal transition) may be plausible explanations. Although not readily discernable in the current study, the type of sample deployed in the analysis is an important variable to be taken into account.

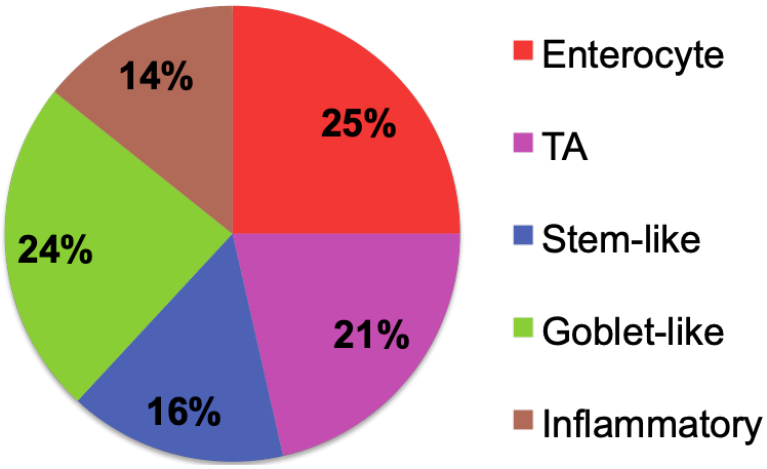

Figure 26. Pie chart showing the CRCA-38 subtype distribution in the Test cohort (N: 84)

		CRCA subtypes n: 84					
Variable	**Level**	**Enterocyte n(%)**	**TA n(%)**	**Stem-like n(%)**	**Goblet-like n(%)**	**Inflammatory n(%)**	**p-value**
		21(25)	**18(21)**	**13(15)**	**20(24)**	**12(14)**	
Sex	Male	12(57)	14(78)	10(77)	11(55)	6(50)	3.52E-01
	Female	9(43)	4(22)	3(23)	9(45)	6(50)	
Age<65	Yes	14(67)	13(72)	13(100)	8(40)	6(50)	3.61E-03
	No	7(34)	5(28)	0(0)	12(60)	6(50)	
	median (range)	62(41-76)	57(31-88)	57(34-64)	61(32-74)	58(24-76)	
Sidedness	Left	18(86)	13(72)	11(85)	10(50)	6(50)	4.84E-02
	Right	3(14)	5(28)	2(15)	10(50)	6(50)	
RAS/BRAF mutational status	Extended wild-type	10(48)	16(88)	9(69)	6(30)	6(50)	2.00E-03
	KRAS wild-type	1(5)	0(0)	2(15)	4(20)	1(8)	
	RAS mutant	6(28)	1(6)	1(8)	5(25)	0(0)	
	BRAF mutant	1(5)	0(0)	0(0)	5(25)	3(25)	
	NA	3(14)	1(6)	1(8)	0(0)	2(17)	
Stage at diagnosis	I-III	10(48)	5(28)	11(85)	12(60)	6(50)	3.27E-02
	IV	10(48)	13(72)	2(15)	8(40)	5(42)	
	NA	1 (4)	0(0)	0(0)	0(0)	1(8)	
Type of samples	Primary	20(95)	11(61)	10(77)	17(85)	6(50)	1.44E-02
	Metastatic	1(5)	7(39)	3(23)	3(15)	6(50)	
Sample retrieval time-point	Pre-treatment	18(86)	9(50)	11(85)	16(80)	8(67)	1.01E-01
	Post-treatment	3(14)	9(50)	2(15)	4(20)	4(33)	
Anti-EGFR therapy	single agent	10(48)	9(50)	4(31)	9(45)	6(50)	8.54E-01
	with chemo	11(52)	9(50)	9(69)	11(55)	6(50)	

Table 12. Characteristics of the CRCA-38 subtypes in the Test cohort.

4.4.3.3 Test cohort: treatment outcomes

A significant association between subtypes and type of response to treatment was demonstrated. Treatment response and disease stability were predominantly seen in the TA, stem-like and enterocyte (**Figure 27**). Conversely, the majority of the goblet-like and inflammatory tumours progressed to anti-EGFR treatment. In view of the association between subtypes and *RAS/BRAF* mutational status (with goblet-like and inflammatory enriched for mutant tumours and TA and stem-like enriched for wild-type), these types of response were expected.

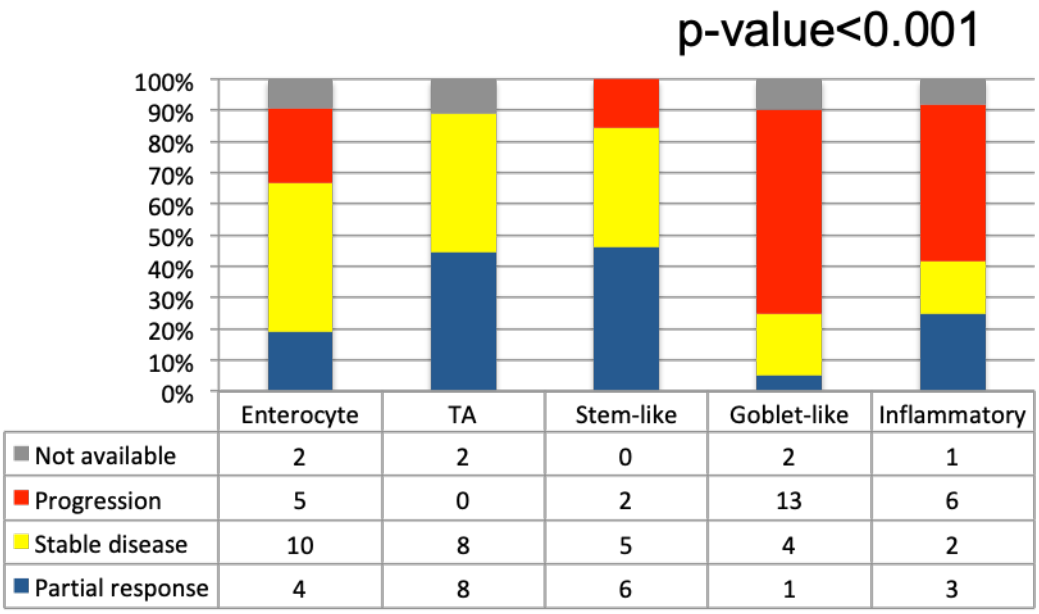

	Enterocyte	TA	Stem-like	Goblet-like	Inflammatory
Not available	2	2	0	2	1
Progression	5	0	2	13	6
Stable disease	10	8	5	4	2
Partial response	4	8	6	1	3

Figure 27. Stacked columns showing the percentage of type of response to anti-EGFR therapy according to CRCA-38 subtypes in the Test cohort.

After 80 events for PFS and 74 for OS, significantly different survival outcomes were demonstrated (**Figure 28**). The risk of progression for inflammatory and goblet-like tumours was 3.96 and 1.70 significantly higher compared to TA tumours, respectively (**Table 13**). Similarly, the risk of death was 2.27 and 4.45 significantly higher for the same comparison. Of note, no significant difference in outcomes was observed between TA and stem-like subtypes.

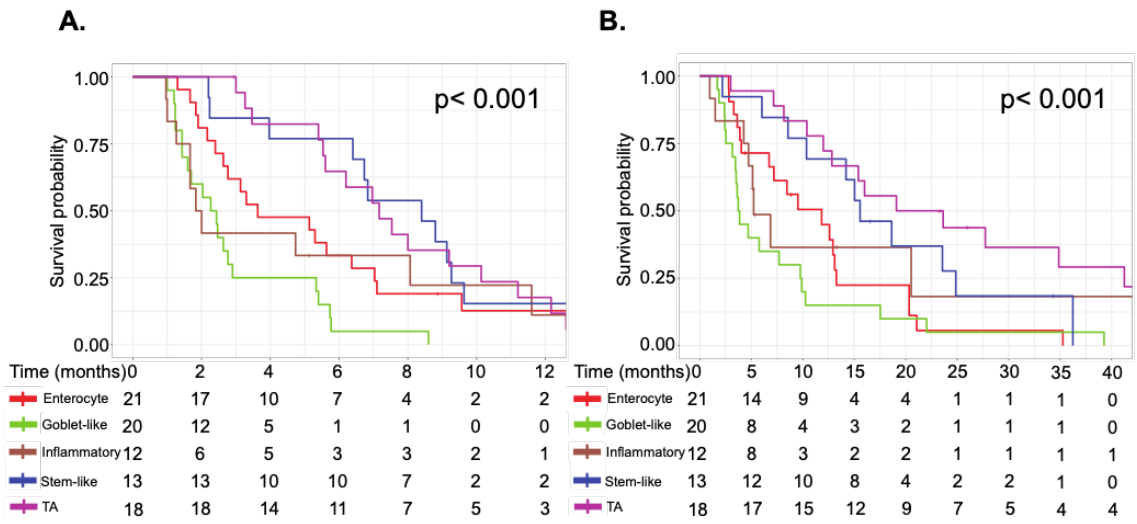

Figure 28. Kaplan Meir curves for progression-free survival (A) and overall survival (B) according to CRCA-38 subtypes – Test cohort

Hazard for progression (Reference subtype: TA)

Subtype	HR	95% CI lower limit	95%CI upper limit	p-value
Enterocyte	1.52	0.79	2.92	0.209
Stem.like	0.87	0.41	1.83	0.716
Inflammatory	1.70	0.78	3.73	0.185
Goblet.like	3.96	2.00	7.84	<0.001

Hazard for death (Reference subtype: TA)

Subtype	HR	95% CI lower limit	95%CI upper limit	p-value
Enterocyte	2.86	1.39	5.89	0.004
Stem.like	1.59	0.71	3.57	0.262
Inflammatory	2.27	0.97	5.28	0.058
Goblet.like	4.45	2.19	9.07	<0.001

Table 13. Hazard ratios for progression and death of the different CRCA-38 subtypes compared to the TA subtype (Test cohort). HR: Hazard Ratio; CI: Confidence Interval.

4.4.3.4 Validation cohort: clinical characteristics

The 121 patient samples available for validation within the CO.20 clinical trial cohort were analysed; a summary of the patients' characteristics was previously presented in **Table 11**.

The distribution of the subtypes was in line with the test cohort; a smaller proportion of goblet-like subtype was present possibly explained by the fact that this was a *KRAS* exon 2 wild type cohort. In **Table 14** the clinical characteristics of the different subtypes are described.

Characteristic	Enterocyte (N = 26)	Goblet-like (N = 23)	Inflammatory (N = 16)	Stem-like (N = 33)	TA (N = 23)	p-value
Age – median (range)	64.3 (40.2-87.9)	66.1 (40.7- 85.2)	61.9 (32.9- 78.2)	63.2 (27- 87.7)	62.1 (40.3- 78.2)	0.29
<65	13 (50.0)	9 (39.1)	9 (56.3)	20 (60.6)	16 (69.6)	
>=65	13 (50.0)	14 (60.9)	7 (43.8)	13 (39.4)	7 (30.4)	
Gender						0.56
Female	13 (50.0)	14 (60.9)	6 (37.5)	15 (45.5)	9 (39.1)	
Male	13 (50.0)	9 (39.1)	10 (62.5)	18 (54.5)	14 (60.9)	
Performance status						0.10
0	12 (46.2)	6 (26.1)	2 (12.5)	15 (45.5)	12 (52.2)	
1	10 (38.5)	15 (65.2)	13 (81.3)	16 (48.5)	10 (43.5)	
2	4 (15.4)	2 (8.7)	1 (6.3)	2 (6.1)	1 (4.3)	
Any prior radiotherapy	8 (30.8)	3 (13.0)	4 (25.0)	10 (30.3)	9 (39.1)	0.36
Number of prior regimens						0.76
1-2	0 (0.0)	0 (0.0)	0 (0.0)	0 (0.0)	0 (0.0)	
3	4 (15.4)	1 (4.3)	1 (6.3)	2 (6.1)	1 (4.3)	
4	1 (3.8)	3 (13.0)	2 (12.5)	6 (18.2)	3 (13.0)	
≥5	21 (80.8)	19 (82.6)	13 (81.3)	25 (75.8)	19 (82.6)	
Prior irinotecan	26 (100.0)	22 (95.7)	15 (93.8)	33 (100.0)	22 (95.7)	0.39
Prior oxaliplatin	25 (96.2)	23 (100.0)	16 (100.0)	33 (100.0)	22 (95.7)	0.67
Prior VEGFR therapy	14 (53.8)	11 (47.8)	10 (62.5)	9 (27.3)	7 (30.4)	0.07
Any liver metastasis	19 (73.1)	15 (65.2)	12 (75.0)	21 (63.6)	18 (78.3)	0.76
Number of disease sites						0.93
1	8 (30.8)	5 (21.7)	2 (12.5)	4 (12.1)	5 (21.7)	
2	10 (38.5)	8 (34.8)	6 (37.5)	14 (42.4)	9 (39.1)	
3	5 (19.2)	4 (17.4)	5 (31.3)	9 (27.3)	5 (21.7)	
≥4	3 (11.5)	6 (26.1)	3 (18.8)	6 (18.2)	4 (17.4)	

Table 14. CRCA-38 subtypes' characteristics in the Validation cohort.

4.4.3.5 Validation cohort: treatment outcomes

As demonstrated in the test cohort, the subtypes were associated with a significantly different PFS (overall p-value 0.04); this difference was mainly due to the short PFS of the goblet-like subtype of less than 2 months compared to the others where the PFS was at least 3.5 months (**Figure 29**). Significantly different OS was also demonstrated, with TA and stem-like subtypes showing the longest median OS of 13.4 and 12.3 months, respectively. As expected the response rate was low with single agent cetuximab, ranging from 0% in goblet-like and 11% in the enterocyte and with overlapping confidence intervals.

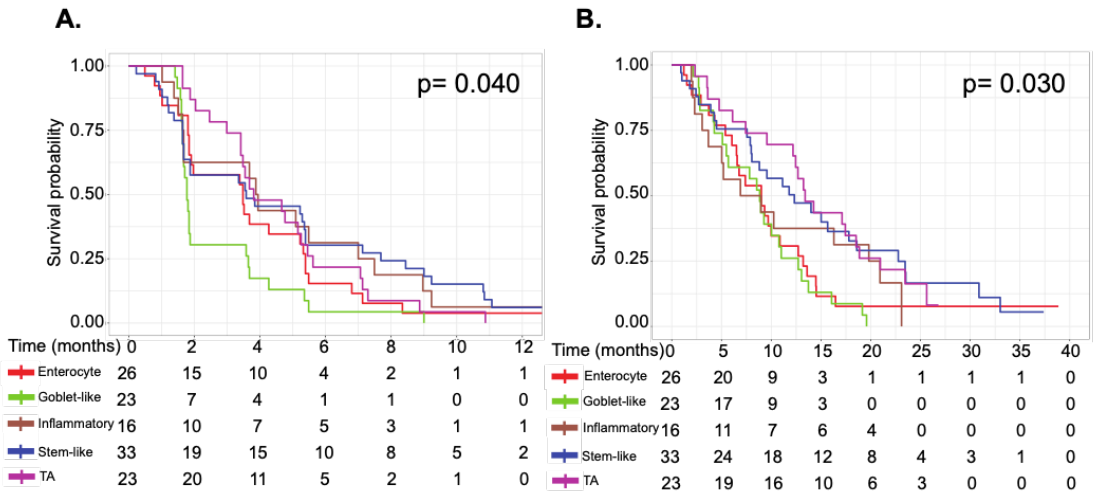

Figure 29. Kaplan Meier curves for progression-free survival (A) and overall survival (B) according to CRCA-38 subtypes (Validation cohort).

A borderline significance for PFS, but not for OS, was observed after adjustment for multiple variables in Cox regression models (**Table 15**).

Prognostic analysis for progression-free survival						
	N	Univariate Analysis			Multivariate Analysis[1]	
Biomarker		Median PFS (Months)	Hazard Ratio[2] (95% CI)	p-value	Hazard Ratio[2] (95% C.I.)	p-value
CRCA-38 group				0.040[3]		0.054[3]
Enterocyte	26	3.48	0.62 (0.35, 1.10)	0.103[4]	0.51 (0.26, 0.99)	0.047[4]
Inflammatory	16	3.91	0.49 (0.25, 0.99)	0.046[4]	0.36 (0.15, 0.90)	0.029[4]
Stem-like	33	3.58	0.51 (0.29, 0.92)	0.024[4]	0.45 (0.22, 0.94)	0.033[4]
TA	23	3.81	0.46 (0.25, 0.83)	0.001[14]	0.36 (0.15, 0.87)	0.023[4]
Goblet-like	23	1.77				
Prognostic analysis for overall survival						
	N	Univariate Analysis			Multivariate Analysis[1]	
Biomarker		Median Survival (Months)	Hazard Ratio[2] (95% CI)	p-value	Hazard Ratio[2] (95% C.I.)	p-value
CRCA-38 group				0.030[3]		0.290[3]
Enterocyte	26	9.00	0.88 (0.49, 1.56)	0.656[4]	0.90 (0.46, 1.77)	0.764[4]
Inflammatory	16	7.93	0.56 (0.27, 1.18)	0.126[4]	0.56 (0.23, 1.40)	0.215[4]
Stem-like	33	12.32	0.47 (0.26, 0.85)	0.013[4]	0.45 (0.21, 0.95)	0.036[4]
TA	23	13.4	0.39 (0.20, 0.74)	0.004[4]	0.45 (0.18, 1.10)	0.079[4]
Goblet-like	23	8.84				

(1) Cox regression including the following covariates: ECOG performance status (0-1 vs. 2), gender (male vs. female), age (65 or older vs. younger than 65), baseline LDH level (higher than UNL vs. UNL or less), baseline alkaline phosphatase (higher than UNL vs. UNL or less), baseline hemoglobin (CTC grade 1 or higher vs. CTC grade 0), number of disease sites (more than 2 vs. 2 or less), number of previous chemotherapy drug classes (more than 2 vs. 2 or less), prior VEGFR target therapy (yes vs. no), presence of liver metastases (yes vs. no);
(2) Hazard ratio over Goblet-like group;
(3) Comparison among all classes;
(4) Comparison with Goblet-like group.

Table 15. Uni and multi-variate prognostic analyses (Validation cohort)

The highest DCR was observed in TA tumours (82%), significantly better compared to goblet-like tumours (26%). Enterocyte and stem-like subtypes also showed high DCRs (57%). Overall, the DCR was not significantly different across the subtypes; however, as expected, the TA subtype maintained a significantly higher DCR after adjusting form multiple variables when compared to the goblet-like (**Table 16**). No significant difference was observed in response rate; the response rate observed in the enterocyte subtype was numerically higher (11.5%) followed by inflammatory (6.25%), TA (4.35%), stem-like (3.03) and lastly, goblet-like subtype (0%).

Prognostic analysis for Disease Control Rate						
	N		Univariate Analysis		Multivariate Analysis[1]	
Biomarker		DCR (%)	Odds Ratio[2] (95% CI)	Fisher's exact p-value	Odds Ratio[2] (95% C.I.)	p-value
CRCA group				0.183[3]		0.181[3]
Enterocyte	26	57.69	3.86 (1.15, 13.0)	0.042[4]	30.1 (2.65, 342.5)	0.006[4]
Inflammatory	16	62.50	4.72 (1.19, 18.68)	0.046[4]	NA (NA, NA)	0.912[4]
Stem-like	33	57.58	3.85 (1.21, 12.3)	0.029[4]	14.3 (1.99, 103.5)	0.008[4]
TA	23	82.61	13.46 (3.24, 55.9)	<0.001[4]	29.8 (1.86, 481.2)	0.017[4]
Goblet-like	23	26.09				
Prognostic analysis for response						
	N		Univariate Analysis		Multivariate Analysis[1]	
Biomarker		Response Rate (%)	Odds Ratio[2] (95% CI)	Fisher's exact p-value	Odds Ratio[2] (95% C.I.)	p-value
CRCA-38 group				0.455[3]		0.905[3]
Enterocyte	26	11.54	4.17 (0.41, 42.69)	0.311[5]	NA (NA, NA)	0.618[5]
Goblet-like	23	0	NA (NA, NA)	1.00[5]	NA (NA, NA)	0.992[5]
Inflammatory	16	6.25	2.13 (0.13, 36.47)	1.00[5]	NA (NA, NA)	0.845[5]
TA	23	4.35	1.46 (0.09, 24.51)	1.00[5]	1.14 (0.01, 160.39)	0.960[5]
Stem-like	33	3.03				

(1) Logistic regression including the following covariates: ECOG performance status (0-1 vs. 2), gender (male vs. female), age (65 or older vs. younger than 65), baseline LDH level (higher than UNL vs. UNL or less), baseline alkaline phosphatase (higher than UNL vs. UNL or less), baseline hemoglobin (CTC grade 1 or higher vs. CTC grade 0), number of disease sites (more than 2 vs. 2 or less), number of previous chemotherapy drug classes (more than 2 vs. 2 or less), prior VEGFR target therapy (yes vs. no), presence of liver metastases (yes vs. no);
(2) Odds ratio over Stem-like group;
(3) Comparison among all groups;
(4) Comparison with Goblet-like group.
(5) Comparison with Stem-like group.

Table 16. Logistic regression models for disease control rate (DCR) and response rate (Validation cohort).

4.4.4 Analysis of TA classes

4.4.4.1 Background

Although the CRCA-38 subtypes identified significantly different prognostic groups, only a trend towards significance was identified when the TA subtype was compared to the non-TA group (HR 0.61[95%CI, 0.34-1.09], p: 0.09) (**Figure 30**).

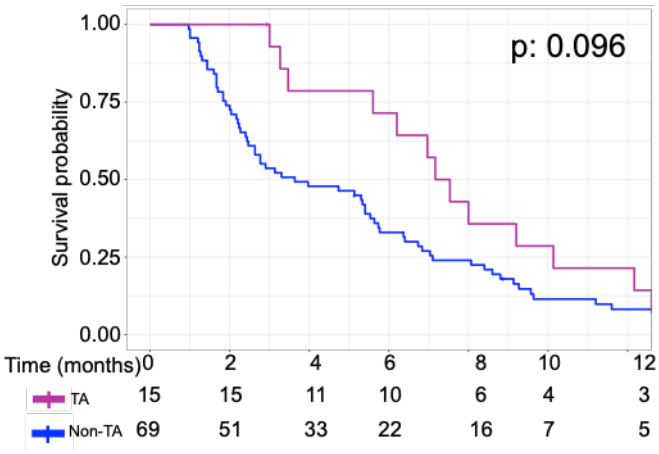

Figure 30. Kaplan Meier curve for progression-free survival comparing the TA subtype versus other non-TA subtypes (Test cohort).

This was possibly due to the small sample size of the TA group. However, as previously shown in **Figure 28**, response and disease stability were observed also in non-TA subtypes. Interestingly, in patients with non-TA tumour, which responded to anti-EGFR therapy, the correlation with the TA centroid was high, although not the highest one (in fact these samples belonged to other subtypes). Conversely, the correlation with the TA centroid was low in samples of patients that did not benefit from the treatment. Hence, we hypothesised that not only tumours strictly assigned to the TA subtype but also those belonging to different subtypes but with high correlation with the TA centroid may benefit from anti-EGFR therapy. This may potentially reflect the intra-tumoural heterogeneity of CRC with more than one subtype co-existing in the same tumour.

4.4.4.2 Correlation between centroids and PFS

Positive linear correlation was demonstrated when the TA-centroid correlation values of each sample were correlated with PFS (**Figure 31A**). Conversely, no linear correlation was demonstrated using the correlation values with inflammatory, enterocyte or stem-like centroids. Not surprisingly, negative linear relationship was demonstrated using the goblet-like-centroid correlation values (**Figure 31B**). This subtype is enriched for *RAS* mutant tumours. When only *RAS/BRAF* wild-type samples were considered for the same analysis, the TA-centroid and goblet-like-centroid correlations maintained significance (**Figure 31C-D**).

A.

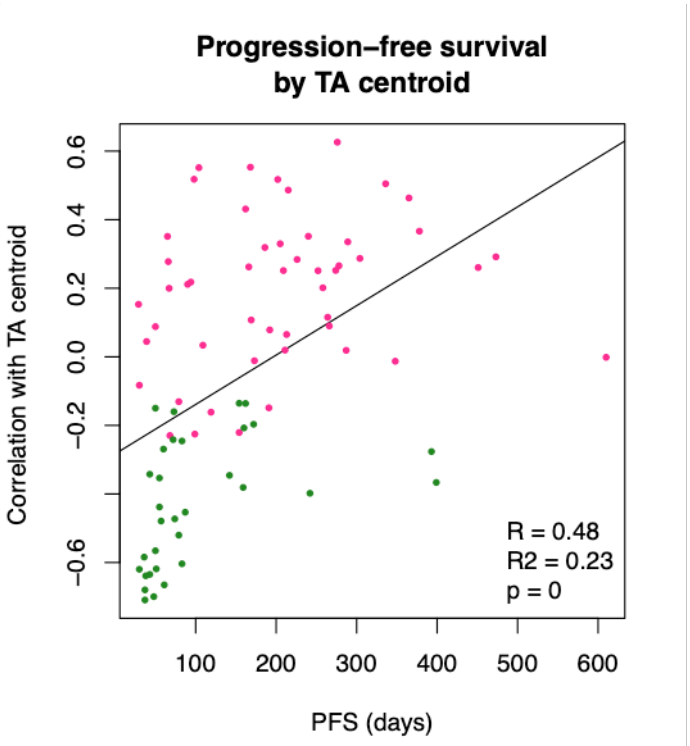
Progression–free survival
by TA centroid
Correlation with TA centroid
0.6
0.4
0.2
0.0
−0.2
−0.6
100
200
300
400
500
600
PFS (days)
R = 0.48
R2 = 0.23
p = 0

B.

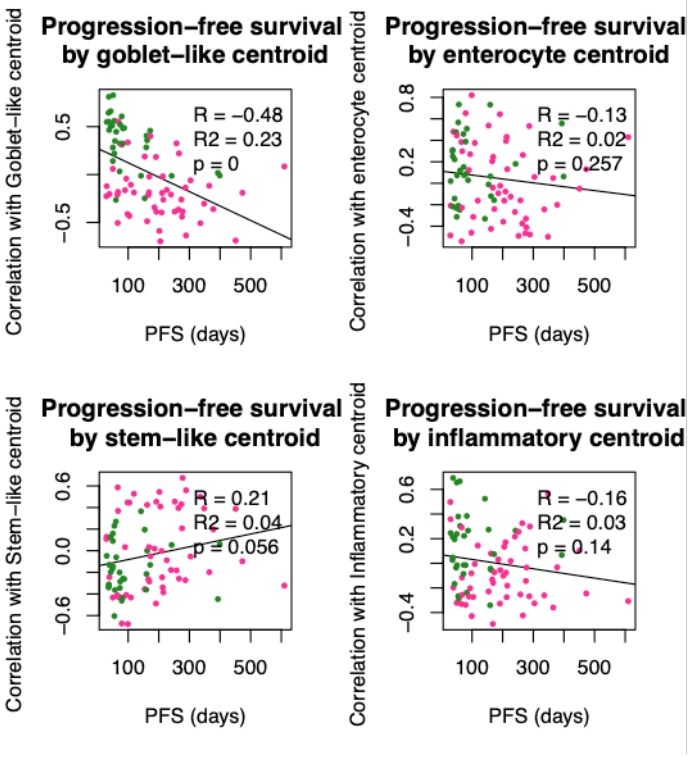
Progression–free survival
by goblet–like centroid
Correlation with Goblet–like centroid
0.5
−0.5
100
300
500
PFS (days)
R = −0.48
R2 = 0.23
p = 0
Progression–free survival
by enterocyte centroid
Correlation with enterocyte centroid
0.8
0.2
−0.4
100
300
500
PFS (days)
R = −0.13
R2 = 0.02
p = 0.257
Progression–free survival
by stem–like centroid
Correlation with Stem–like centroid
0.6
0.0
−0.6
100
300
500
PFS (days)
R = 0.21
R2 = 0.04
p = 0.056
Progression–free survival
by inflammatory centroid
Correlation with Inflammatory centroid
0.6
0.2
−0.4
100
300
500
PFS (days)
R = −0.16
R2 = 0.03
p = 0.14

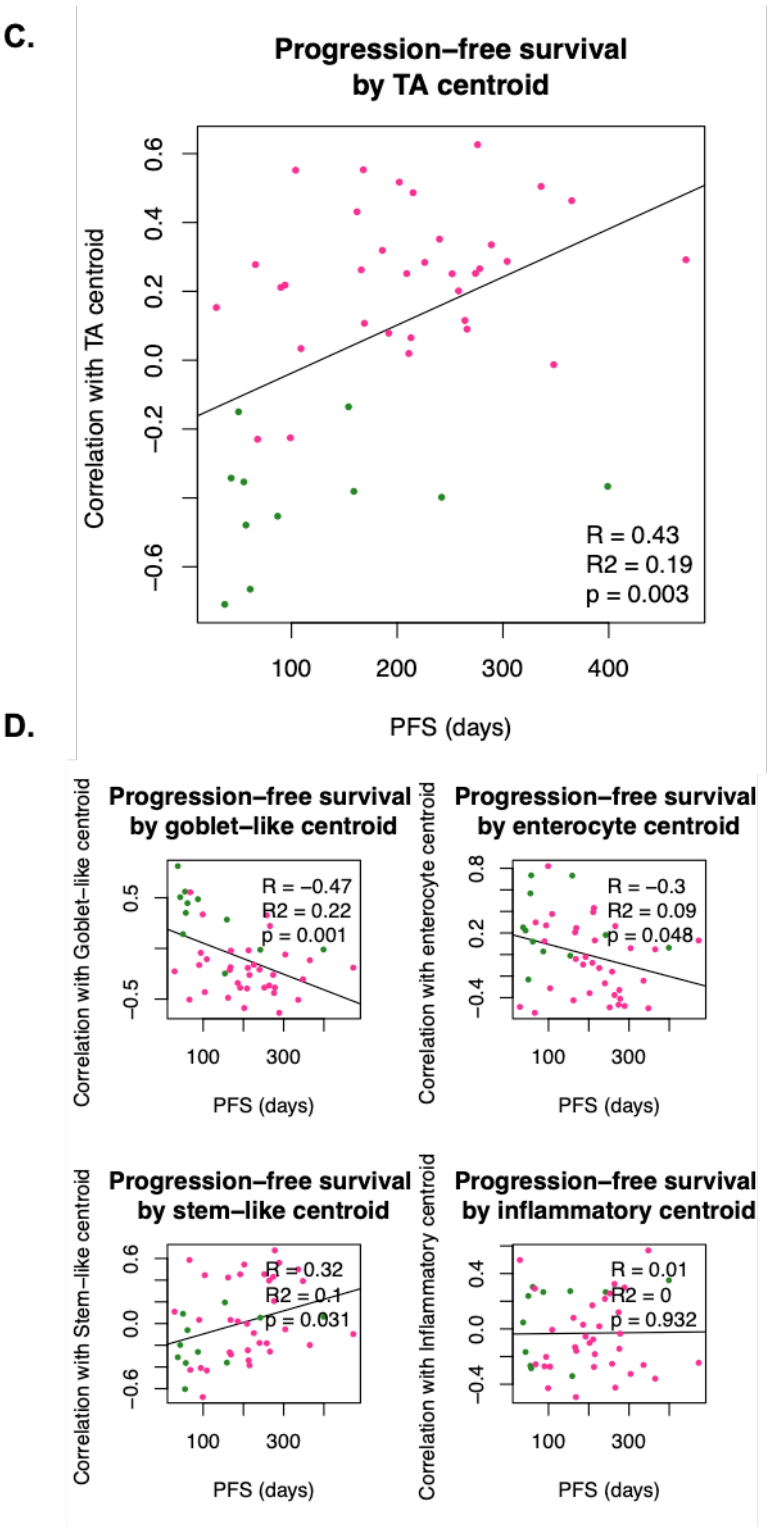

Figure 31. Correlation between centroids and progression-free survival: (A) TA-centroid correlation values of each sample (Y-axis) and PFS associated with the same sample (X-axis); the line of best-fit and the correlation value demonstrate direct correlation between the two continues variables. (B) The four correlation plots demonstrate the correlation between PFS (X-axis) and the other non-TA centroids. Test cohort (A-B); and *RAS/BRAF* wild-type subgroup within the Test cohort (C-D).

Although interesting, the use of the TA-centroid correlation values to potentially predict anti-EGFR benefit posed some challenges in terms of reproducibility due to: a) the values are affected by the number and type of samples simultaneously analysed; and b) cut-off optimization (being the correlation a continuous variable). Furthermore, these findings suggested that the TA signature is prognostic; however, whether the better prognosis is an intrinsic characteristic of samples with high TA-centroid correlation or whether this is due to the effect of anti-EGFR therapy could not be demonstrated in the absence of a control group.

Hence, the next steps aimed to dichotomise the TA-centroid correlation values into categorical variables, dubbed TA class-1 and TA class-2, and demonstrate whether these were associated with response to anti-EGFR therapy.

4.4.4.3 Association between rank of the TA-centroid correlation value and type of response to anti-EGFR therapy

By using the CRCA-38 assigner algorithm, each sample profile is correlated with the five different CRCA-38 centroids. The 5 correlation values are then ordered from the highest to the lowest value. The rank of the TA-centroid correlation values compared to the other subtype centroids were graphically visualised using a tile plot (**Figure 32**).

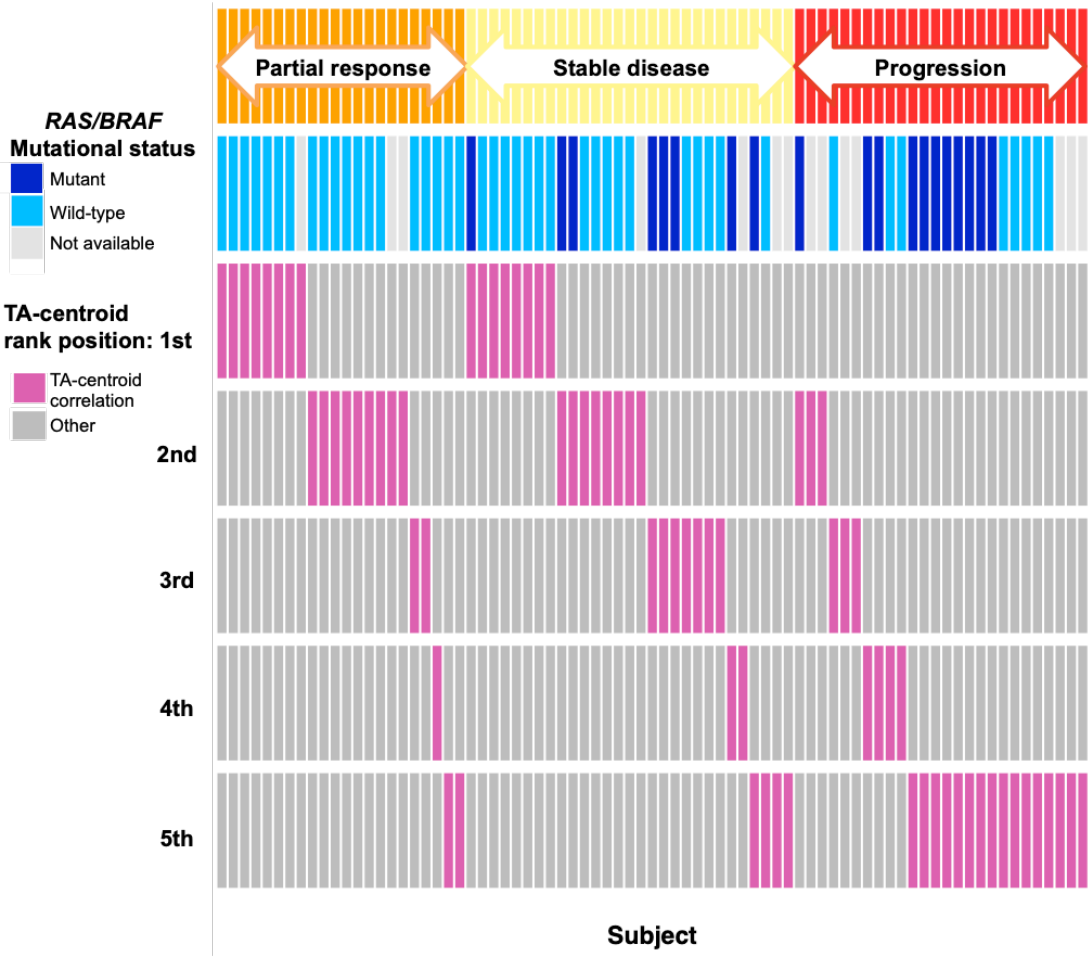

Figure 32. Tile plot showing the rank of the TA-centroid correlation compared with the correlation value with non-TA centroids. This plot also shows *RAS/BRAF* mutational status.

Samples were ordered based on the rank and type of response to anti-EGFR. Of note, the majority of tumours in which the TA-centroid correlation value was the highest, or second or third highest responded or had disease stability with anti-EGFR therapy. Conversely, when the value was the lowest or second-last, tumours progressed throughout the treatment. With the help of Dr Nyamundanda, an ROC curve was built to identify the best cut-off associated with disease control (response and disease stability). As demonstrated in **Figure 33**, the higher area under the curve (AUC) was demonstrated by dichotomising the cohort into two classes: TA class-1 (rank= 1°, 2°, 3°), which included the TA tumours (rank = 1°) and non-TA tumours expressing the TA genes (rank= 2°, 3°); and to TA class-2 (rank = 4°, 5°), representing tumours with no or very low expression of the TA genes.

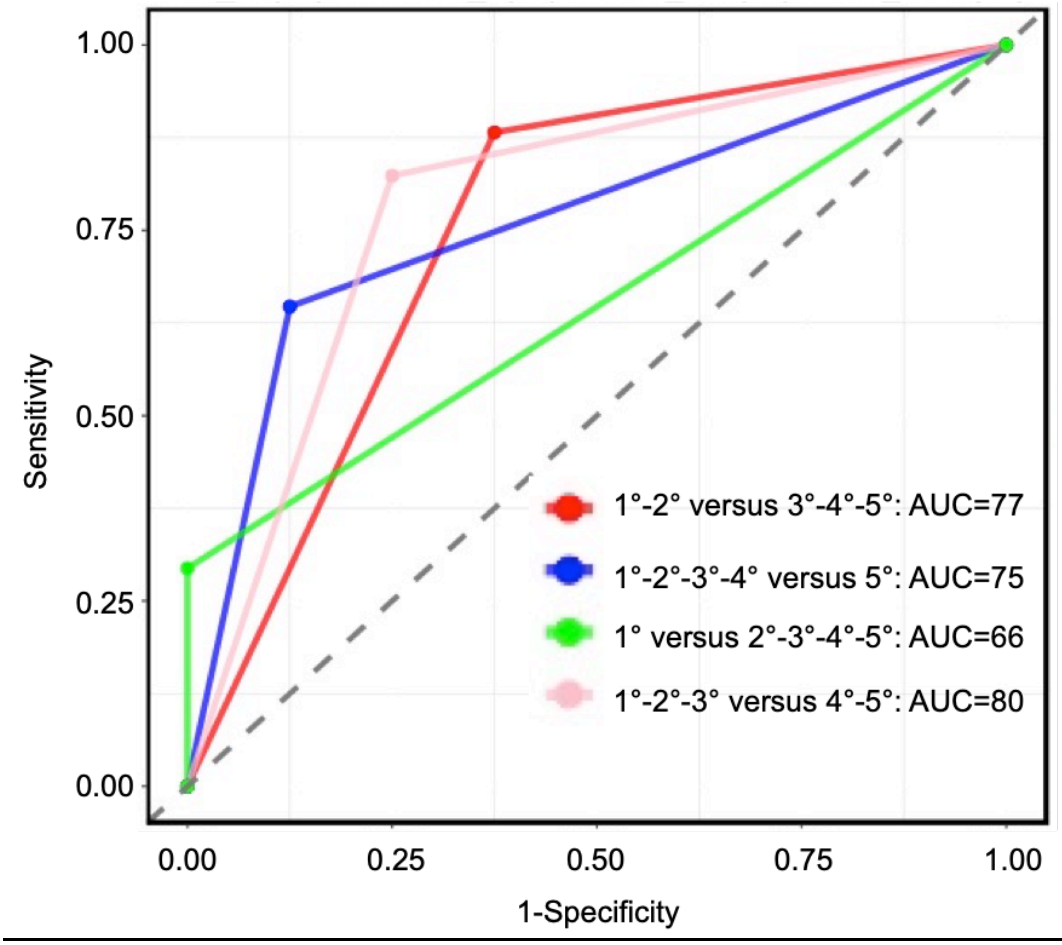

Figure 33. Receiver operating characteristic curve demonstrating the accuracy of different cut-offs in defining disease control.

4.4.4.4 Association between TA classes, patients' characteristics and treatment outcomes

Fifty-two out of 84 (62%) samples in the test cohort were classified as TA class-1 tumours. In this retrospective cohort (possibly subject to selection biases), TA class-1 tumours were significantly associated with male, age<65 and left sidedness when compared to TA class-2. Significant association between the TA classes and *RAS/BRAF* mutational status was demonstrated: TA class-1 was enriched for wild-type tumours (**Table 17**). Importantly, no association with the type of sample profiled (whether primary tumour or metastatic lesion) and whether the sample was collected before or after any treatment (other that anti-EGFR, since all samples were collected before anti-EGFR therapy) was present.

		TA classes n:84		
Variable	***Level***	***Class 1 n(%)***	***Class 2 n(%)***	***p-value***
		52(62)	***32(38)***	
Sex	*Male*	38(73)	15(47)	0.020
	Female	14(27)	17(53)	
Age<65	*Yes*	42(81)	12(37)	<0.001
	No	10(19)	20(62)	
	median (range)	58 (24-88)	62 (32-76)	
Sidedness	*Left*	41(79)	17(53)	0.016
	Right	11(21)	15(47)	
RAS/BRAF mutational status	*Extended wild-type*	36(69)	11(34)	<0.001
	KRAS wild-type	3(6)	5(16)	
	RAS mutant	7(13)	6(19)	
	BRAF mutant	0(0)	9(28)	
	NA	6(12)	1(3)	
Stage at diagnosis	*I-III*	24(46)	20(62)	0.171
	IV	27(52)	11(35)	
	NA	1(2)	1(3)	
Type of samples	*Primary*	38(73)	26(81)	0.441
	Metastatic	14(24)	6(19)	
Sample retrieval time-point	*Pre-treatment*	38(73)	24(75)	1
	Post-treatment	14(27)	8(25)	
Anti-EGFR therapy	*single agent*	19(37)	19(59)	0.046
	with chemo	33(63)	13(41)	
Response to anti-EGFR	*Partial response*	19(36)	3(9)	<0.001
	Stable disease	23(44)	6(19)	
	Progression	6(12)	20(63)	
	Not available	4(8)	3(9)	

Table 17. Characteristics of patients in the Test cohort according to TA classes.

As expected since the cut-off for the two classes was determined using disease control as outcome, significant association with type of response to treatment was also demonstrated and graphically presented in the hypergeometric test in **Figure 34**.

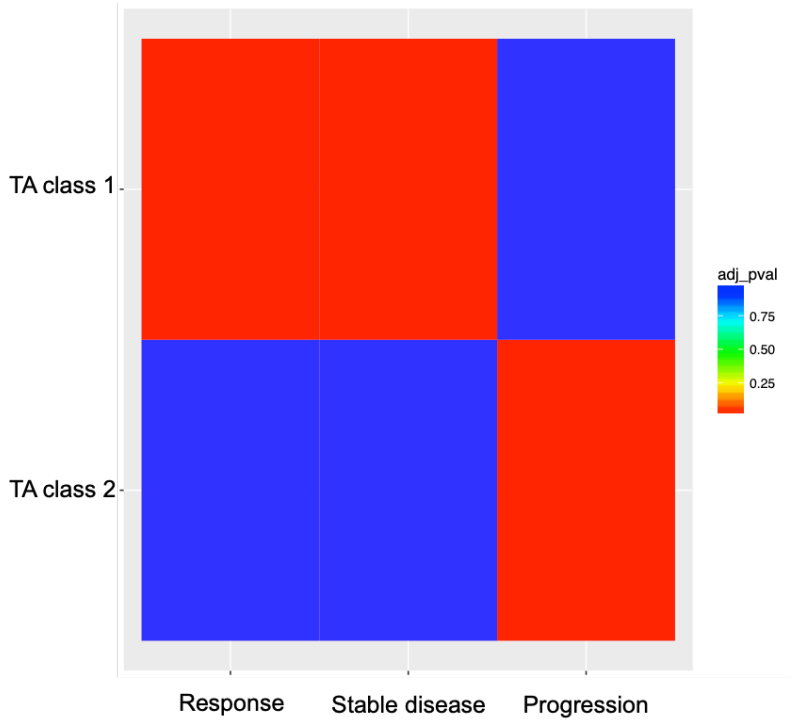

Figure 34. Hypergeometric test demonstrating significant association between TA classes and type of response to anti-EGFR therapy.

Overall p-value = 2.033e-06

A significant association between TA class-1 and PFS was observed [HR: 0.4 (95%CI, 0.25-0.64), p<0.001] (**Figure 35A**). Similarly, significant association with OS was demonstrated [HR: 0.48 (95%CI, 0.29-0.79), p: 0.003] (**Figure 35B**). The TA class-1 group was associated with higher DCR [OR: 14.8 (95%CI, 4.30-59.54), p<0.001]. Importantly, the association between TA class-1 and both PFS and DCR remained significant after adjusting for multiple variables including age, sex, sidedness and mutational status (**Table 15**). Cox and logistic regression models were performed with the help of Dr Nyamundanda.

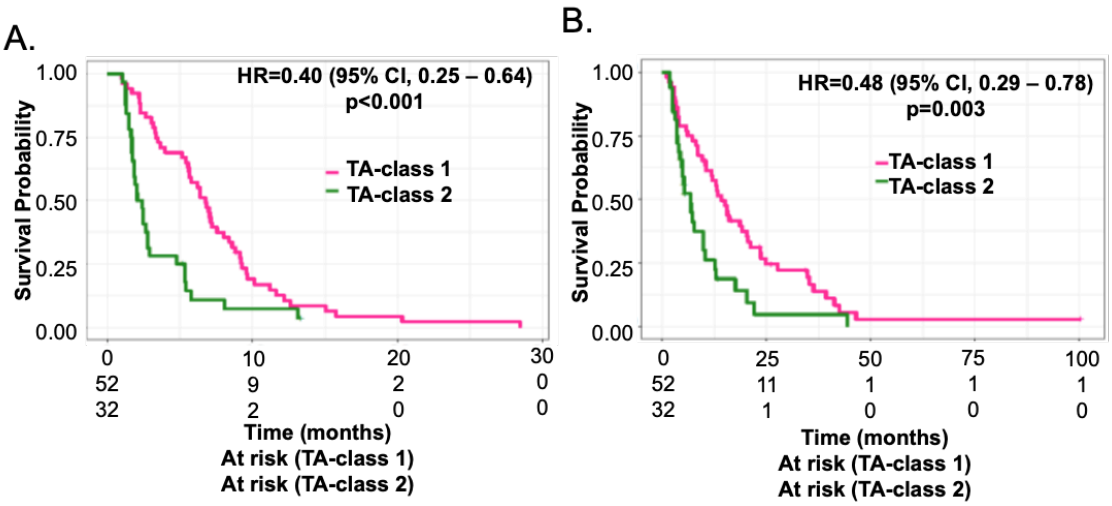

Figure 35. Progression-free survival (A) and overall survival (B) according to TA classes in the Test cohort

Biomarker	N	Median survival (Months)	Univariate Analysis: Hazard Ratio[2] (95% CI)	Log-rank p-value	Multivariate Analysis[1]: Hazard Ratio[2] (95% C.I.)	p-value Cox regression
Prognostic analysis for progression-free survival						
				<0.0001		0.01
TA-class 1	52	6.73	0.40		0.49	
TA-class 2	32	2.22	(0.25, 0.64)		(0.29, 0.84)	
Prognostic analysis for overall survival						
				0.003		0.11
TA-class 1	52	14.20	0.48		0.62	
TA-class 2	32	6.73	(0.29, 0.78)		(0.35, 1.10)	

Biomarker	N	Rate (%)	Univariate Analysis: Odds Ratio[2] (95% CI)	Fisher's exact p-value	Multivariate Analysis[1]: Odds Ratio[2] (95% C.I.)	p-value logistic regression
Prognostic analysis for disease control						
				<0.001		<0.001
TA-class 1	48	87.5	14.8		26.8	
TA-class 2	29	31.0	(4.30, 59.54)		(4.78, 150.6)	
Prognostic analysis for response						
				0.008		0.11
TA-class 1	48	39.6	5.56		3.46	
TA-class 2	29	10.3	(1.40, 32.70)		(0.76, 15.7)	

(1) Cox and logistic regression including the following covariates: age (as a continuous variable), gender (male vs. female), type of treatment (single agent vs. with chemo), sidedness (right vs. left), mutational status (wild-type vs. mutant) (2) Hazard ratio of TA-class 1 over TA-class 2

Table 18. Univariate analyses and Cox/Logistic regression models (Test cohort)

For a subset of patients (n: 33), serial computed tomography scan measurements were reviewed with the help of a consultant radiologist (Dr Maria Bali): significant association with the depth of response and TA classes was demonstrated (Wilcoxon test p<0.001) and graphically shown with a waterfall plot (**Figure 36**).

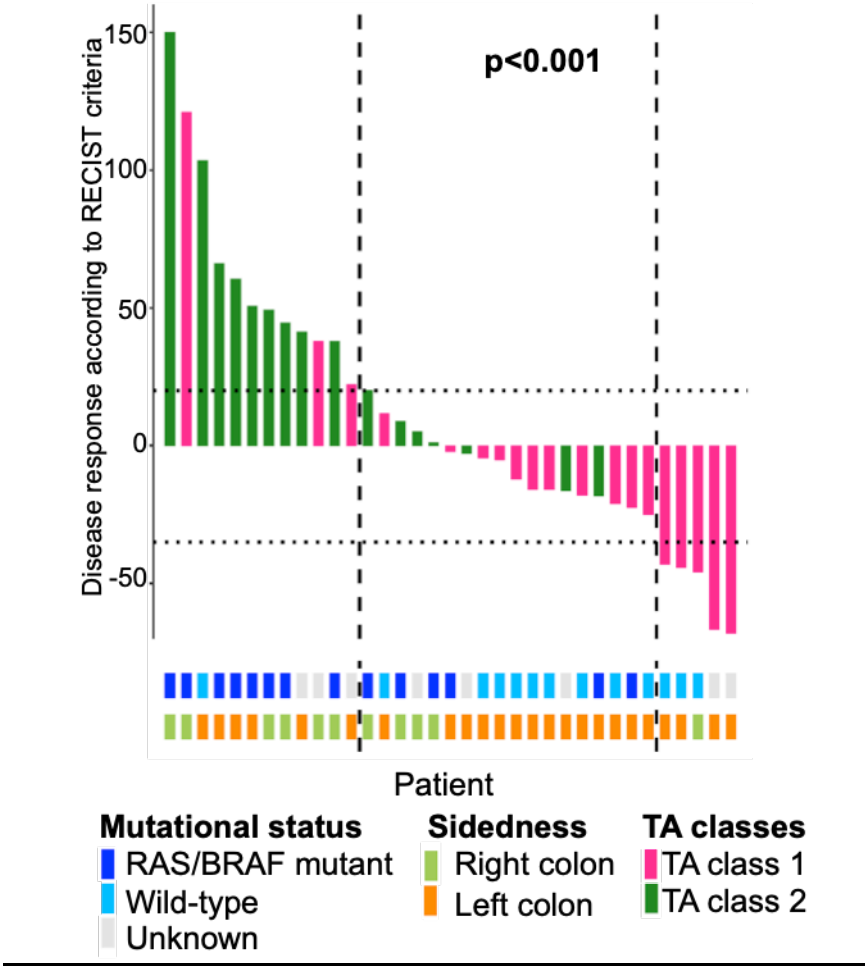

Figure 36. Waterfall plot demonstrating the association between TA classes and RECIST (Response Evaluation Criteria In Solid Tumours) in a subgroup of the Test cohort. The tile plot at the bottom of the figure shows the *RAS/BRAF* mutational status and tumour sidedness for each patient.

The cut-off for TA class definition was determined based on sample and response of patients included in the test cohort. Therefore, the validation of these results in an independent cohort was essential.

4.4.4.5 Validation of the TA classes in the CO.20 trial cohort

The 121 patient samples were now classified into the two TA classes: 66 (55%) and 55 (45%) samples were classified as TA class-1 and TA class-2, respectively. As per CRCA-38 analysis, the TA class data were transferred to Dr Dongsheng Tu who performed the rest of the analyses blinded to the results of the Test cohort. In line with this cohort, PFS and DCR were significantly associated with TA classes: HR for PFS 0.65 (95%CI, 0.45-0.93), p: 0.018 (**Figure 37**); OR for DCR 4.35 (95%CI, 2.00-9.09), p<0.001. The significance was maintained after adjusting for multiple variables (**Table 19**). Longer OS for TA class-1 patients was also observed [HR 0.67 (95%CI, 0.46-0.98), p: 0.04; as expected, only a trend was maintained after multivariate analysis.

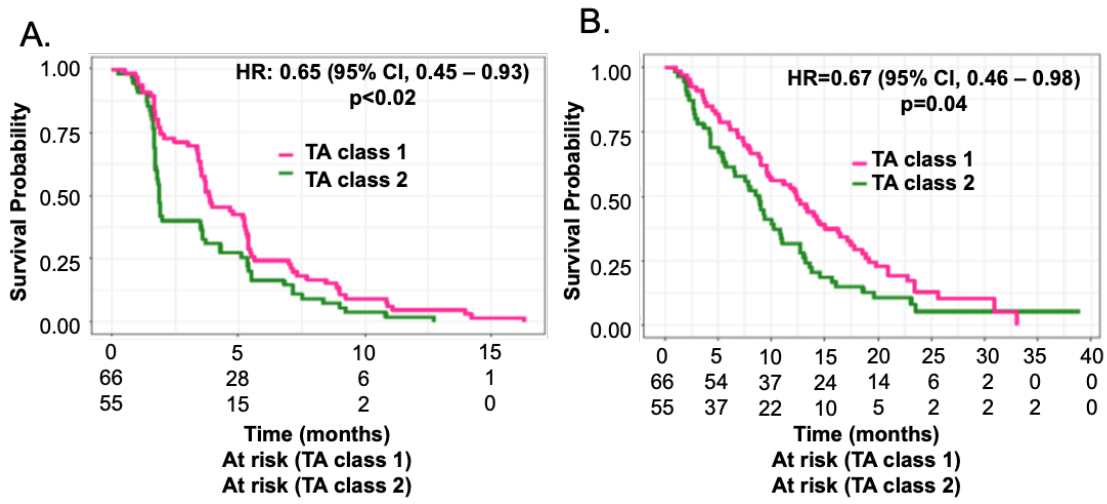

Figure 37. Progression-free survival (A) and overall survival (B) (Validation cohort).

Biomarker	N	Univariate Analysis			Multivariate Analysis[1]	
		Median survival (Months)	Hazard Ratio[2] (95% CI)	Log-rank p-value	Hazard Ratio[2] (95% C.I.)	p-value Cox regression
Prognostic analysis for progression-free survival						
				0.018		0.021
TA-class 1	66	3.83	0.65		0.63	
TA-class 2	55	1.84	(0.45, 0.93)		(0.42, 0.93)	
Prognostic analysis for overall survival						
				0.04		0.06
TA-class 1	66	12.39	0.67		0.68	
TA-class 2	55	8.84	(0.46, 0.98)		(0.45, 1.02)	

Biomarker	N	Univariate Analysis			Multivariate Analysis[1]	
		Rate (%)	Odds Ratio[2] (95% CI)	Fisher's exact p-value	Odds Ratio[2] (95% C.I.)	p-value logistic regression
Prognostic analysis for disease control						
				<0.0001		0.0009
TA-class 1	66	72.7	4.35		4.35	
TA-class 2	55	38.2	(2.00, 9.09)		(1.85, 11.1)	
Prognostic analysis for response						
				0.30		0.32
TA-class 1	66	3.03	0.40		0.33	
TA-class 2	55	7.27	(0.07, 2.27)		(0.04, 2.86)	

(1) Cox and logistic regression including the following covariates: Eastern Cooperative Oncology Group (ECOG) performance status (0-1 vs. 2), gender (male vs. female), age (65 or older vs. younger than 65), baseline LDH level (higher than UNL vs. UNL or less), baseline alkaline phosphatase (higher than UNL vs. UNL or less), baseline hemoglobin (CTC grade 1 or higher vs. CTC grade 0), number of disease sites (more than 2 vs. 2 or less), number of previous chemotherapy drug classes (more than 2 vs. 2 or less), prior VEGFR target therapy (yes vs. no), presence of liver metastases (yes vs. no); (2) Hazard ratio of TA class 1 over TA class 2.

Table 19. Univariate analyses and Cox/Logistic regression models (Validation cohort)

In view of the well-defined value of *RAS/BRAF* wild-type status and left sidedness in predicting benefit form anti-EGFR therapy, I sought to test whether the TA classes could further refine the selection of patients beyond these established markers. Firstly, 71 patients with extended *RAS/BRAF* wild-type tumour were identified between Test and Validation cohorts. Fifty-five patients had a left-sided tumour: 42 (76%) belong to TA class-1 and 13 (24%) to TA class-2. Although the number of patients was small, longer PFS for TA class-1 patients was demonstrated [HR 0.53 (95%CI, 0.28-1.00), p: 0.049] (**Figure 38**). The significance was lost after correction for age and sex; however, neither age nor sex were previously associated with PFS, making the correction of

questionable value (**Table 20**). Only 16 cases were found to be wild-type and right-sided, limiting any powerful statistical comparison. However, the accuracy of the TA classes was compared to sidedness using an ROC curve in 71 wild-type patients (**Figure 39**): the TA classes demonstrated a higher accuracy compared to sidedness, although not statistically significant (AUC 0.70 versus 0.59, p: 0.2).

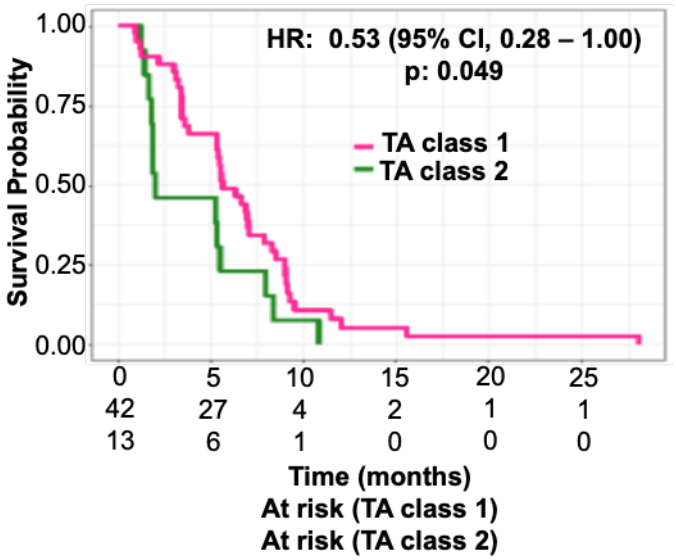

Figure 38. Progression-free survival in 55 patients with RAS/BRAF wild-type and left-sided tumour.

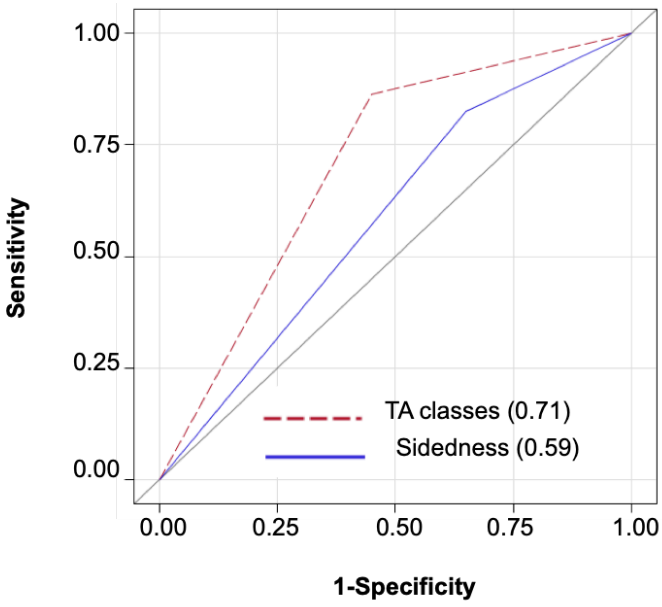

Figure 39. Receiver operating characteristic curve comparing the accuracy of the TA classes and sidedness in defining disease control rate (N: 71 cases with *RAS/BRAF* wild-type tumours).

Biomarker	N	Univariate Analysis			Multivariate Analysis[1]	
		Median survival (Months)	Hazard Ratio[2] (95% CI)	Log-rank p-value	Hazard Ratio[2] (95% C.I.)	p-value Cox regression
Prognostic analysis for progression-free survival						
(1) **All patients**				0.191		0.503
TA-class 1	53	5.62	0.68		0.81	
TA-class 2	18	2.43	(0.39, 1.20)		(0.43, 1.52)	
(2) **Left-sided**				0.049		0.224
TA-class 1	42	5.62	0.53		0.64	
TA-class 2	13	2.00	(0.28, 1.00)		(0.31, 1.32)	
(3) **Right-sided**				0.650		0.605
TA-class 1	11	4.67	1.35		1.43	
TA-class 2	5	2.86	(0.37, 5.00)		(0.37, 5.56)	
Prognostic analysis for overall survival						
(1) **All patients**				0.887		0.799
TA-class 1	53	13.24	0.95		1.10	
TA-class 2	18	12.75	(0.51, 1.79)		(0.54, 2.22)	
(2) **Left-sided**				0.741		0.769
TA-class 1	42	14.00	0.89		1.12	
TA-class 2	13	12.75	(0.45, 1.75)		(0.52, 2.44)	
(3) **Right-sided**				0.773		0.957
TA-class 1	11	10.22	1.27		0.95	
TA-class 2	5	17.28	(0.26, 6.25)		(0.16, 5.56)	
Biomarker	**N**	**Univariate Analysis**			**Multivariate Analysis[1]**	
		Rate (%)	**Odds Ratio[2] (95% CI)**	**Fisher's exact p-value**	**Odds Ratio[2] (95% C.I.)**	**p-value logistic regression**
Prognostic analysis for disease control						
(1) **All patients**				<0.001		0.003
TA-class 1	53	83.02	7.69		7.14	
TA-class 2	18	38.89	(2.33, 25.0)		(1.92, 25.0)	
(2) **Left-sided**				<0.001		0.003
TA-class 1	42	88.10	12.5		12.5	
TA-class 2	13	38.46	(2.78, 50.0)		(2.33, 50.0)	
(3) **Right-sided**				0.60		0.63
TA-class 1	11	63.64	2.63		1.79	
TA-class 2	5	40.00	(0.30, 25.0)		(0.17, 20.0)	
Prognostic analysis for response						
(1) **All patients**				0.24		0.43
TA-class 1	53	32.08	2.38		1.82	
TA-class 2	18	16.67	(0.60, 9.09)		(0.42, 7.69)	
(2) **Left-sided**				0.09		0.14
TA-class 1	42	33.33	5.88		5.26	
TA-class 2	13	7.69	(0.71, 4.55)		(0.58, 4.55)	
(3) **Right-sided**				1.00		0.36
TA-class 1	11	27.27	0.56		0.25	
TA-class 2	5	40.00	(0.06, 5.26)		(0.01, 4.76)	

(1) Cox and logistic regression including the following covariates: age (65 or older vs. younger), gender (male vs. female) (2) Hazard ratio of TA-class 1 over TA-class 2

Table 20. Univariate and multi-variate analyses in 71 cases with *RAS/BRAF* wild-type tumours.

4.4.4.6 Validation of the TA classes in *RAS/BRAF* wild-type cohorts

To further validate the potential role of the TA classes in an independent experimental setting including *RAS/BRAF* wild-type tumours, the "Cases" cohort (patients liver metastases and mouse-propagated tumours treated with vehicle or cetuximab, described in Methods section) was deployed. Thirty liver metastases (pre-implantation samples) were classified into TA class-1 (n: 16) and TA class-2 (n: 14). The depth of response to cetuximab in the mouse-propagated tumours of each case was plotted in a waterfall plot (**Figure 40**). Significant association between TA classes and depth of response was demonstrated using Wilcoxon test (p: 0.042). The mouse-propagated samples were also classified into TA classes and graphically visualised on the waterfall plot: interestingly, out of 11 responders, 10 (91%) belonged to TA class-1. In 7 (70%) out of 10 responders the TA class-1 signature was lost upon treatment.

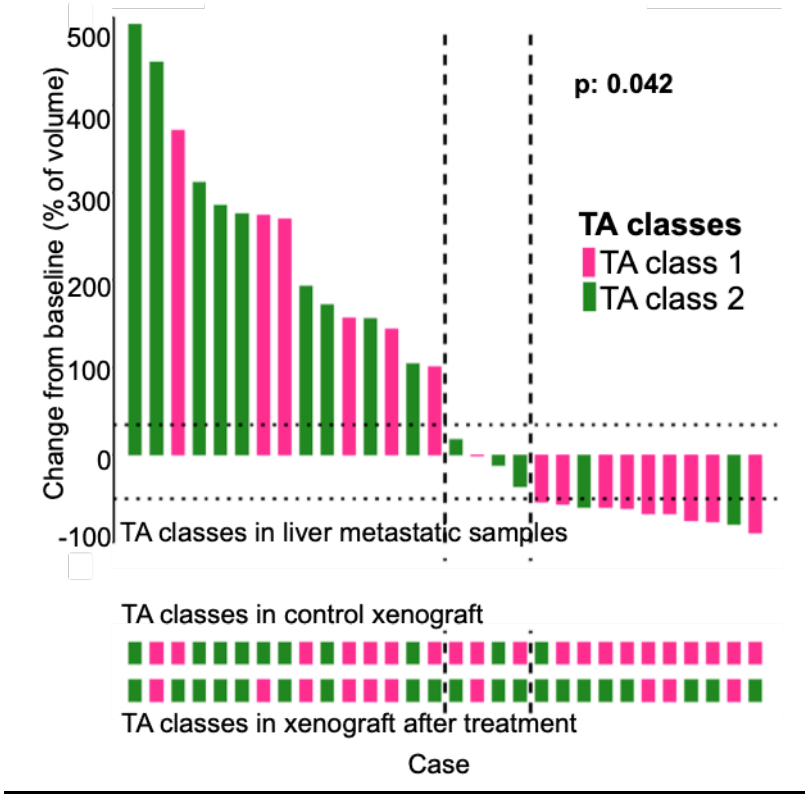

Figure 40. Waterfall plot demonstrated the association between the TA class profile of the liver metastatic samples and the response observed in the mouse-propagated tumour. The tile plot at the bottom shows the TA class profile in matched control and treatment xenografts.

4.4.4.7 Validation of TA classes in publicly available data

As described in Methods, two public gene expression datasets were downloaded and deployed to further validate the TA classes.

Forty-eight of the 155 CRC cell lines available from the GSE59857 gene expression dataset were wild-type for *RAS/BRAS* status. After the TA classes were assigned, significant association with growth inhibition from cetuximab (at a range of concentrations) was demonstrated (Wilcoxon test p: 0.007 with minimal concentration of cetuximab of 0.001 μg/ml and p: 0.042 with maximum concentration of 100 μg/ml) (**Figure 41**).

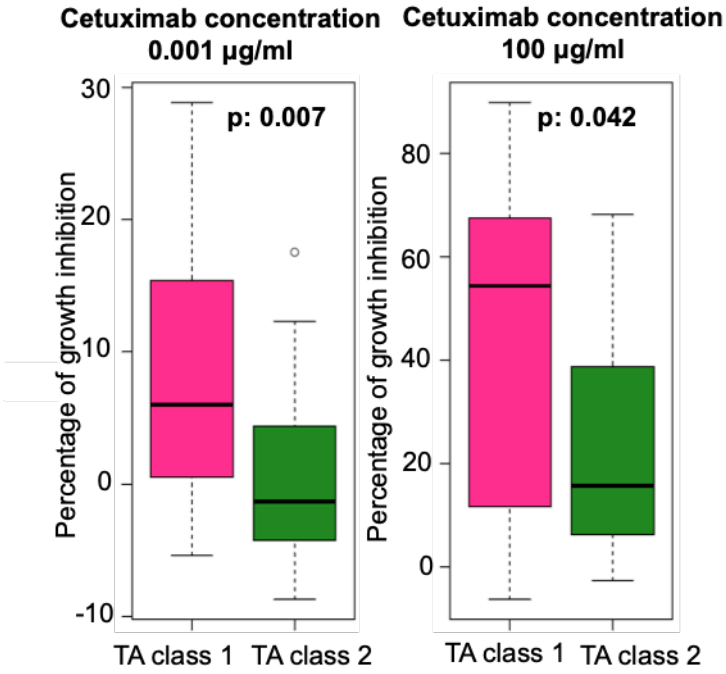

Figure 41. Growth inhibition using different concentrations of cetuximab in *RAS/BRAF* wild-type cell lines of CRC classified into TA classes. TA class 1 cell lines are more sensitive to cetuximab compared to TA class 2 cell lines.

Lastly, the TA classes were assessed in the Khambata-Ford dataset (205). This dataset was generated by profiling CRC metastatic lesions (the majority being liver) using microarrays. Samples were collected with a biopsy before the

beginning of cetuximab treatment and after progression to standard chemotherapy options. Significant association between TA class-1 and longer PFS was demonstrated [HR for PFS 0.36 (95%CI, 0.22-0.56), p<0.001] (**Figure 42**). This analysis demonstrated that:

1. The significant association is retained also using a sample different from the primary tumour collected after different treatments. These results are in line with those in the Test cohort, where a proportion of samples were from metastatic lesions.
2. The results obtained using the newly developed NanoString assay are reproducible using a different platform. This confirmed the existence of non-TA tumours sensitive to anti-EGFR therapy, excluding the possibility that the results demonstrated in the Test and Validation cohorts were due to misclassification of TA tumours into other subtypes by the new assay.

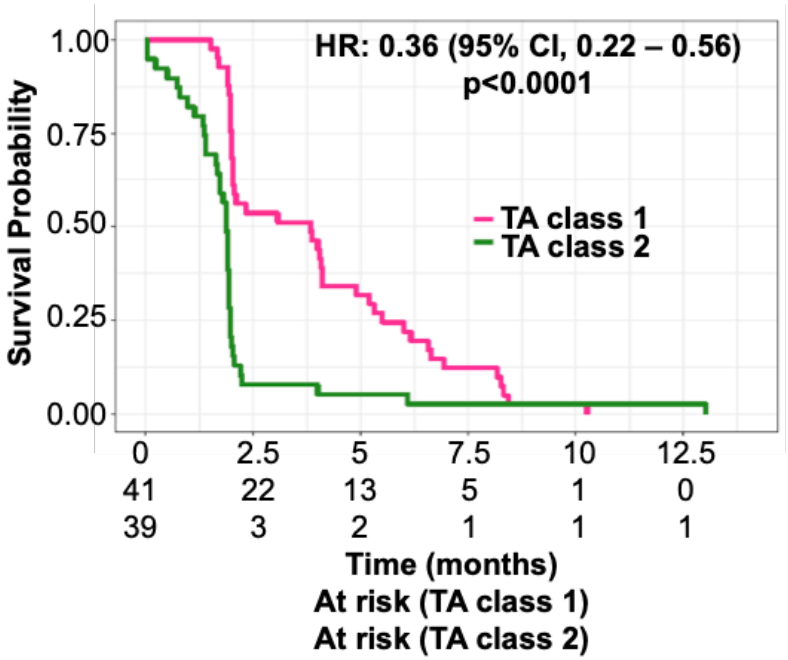

Figure 42. Progression-free survival in the Khambata-Ford dataset (N: 80) according to TA classes.

4.4.5 Analysis of CMS subtypes

4.4.5.1 Biomarkers associations

The 96-gene NanoCRC assay was developed to simultaneously identify CRCA-38 subtypes and rankCMS-38 subtypes, this to provide a better understanding of the subtypes results to the international community (familiar with CMS classification after the Consortium manuscript (148)). In the meantime, the CMS analysis, which deploys a mostly non-overlapping set of genes with CRCA-38, may be considered as an orthogonal validation of the newly developed assays.

Greater anti-EGFR benefit was demonstrated in TA class-1 tumours, which are significantly associated with TA and stem-like tumours and to a lesser extent to enterocyte. Conversely, no benefit was demonstrated in TA class-2 tumours, which are significantly associated with goblet-like and inflammatory subtypes (**Figure 43**).

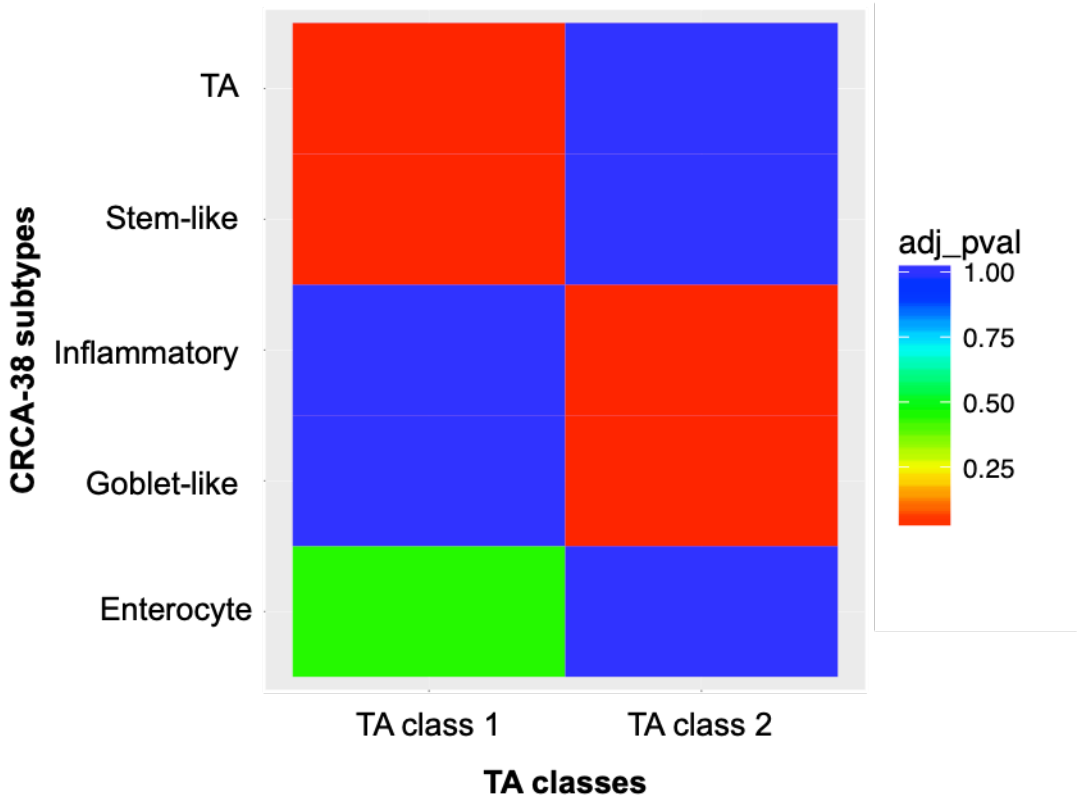

Figure 43. Hypergeometric test demonstrating the associations between CRCA-38 subtypes and TA classes in the Test cohort.

Overall p-value = 5.683e-11

Therefore, based on the previously demonstrated associations between CRCAssigner and CMS subtypes in the consortium manuscript (inflammatory/CMS1, enterocyte and TA/CMS2, goblet-like/CMS3, stem-like/CMS4) (91), the expectation was to demonstrate anti-EGFR benefit in CMS2/CMS4 tumours and no benefit in CMS1/CMS3 tumours.

4.4.5.2 Subtypes assignment

Using the gene-set and algorithm developed in chapter 2, section 2.3.2, each sample of the Test cohort was assigned to the rankCMS-38 subtype. The vast majority of the samples belonged to CMS4 (54%) and CMS2 (32%), with only 8% and 6% of the samples belonging to CMS1 and CMS3, respectively. This distribution is similar to the only known distribution of CMS subtypes in a chemorefractory cohort from the CORRECT clinical trial (Fisher's Exact Test p-value= 0.006) (**Figure 44** and **Figure 11B, chapter 2**).

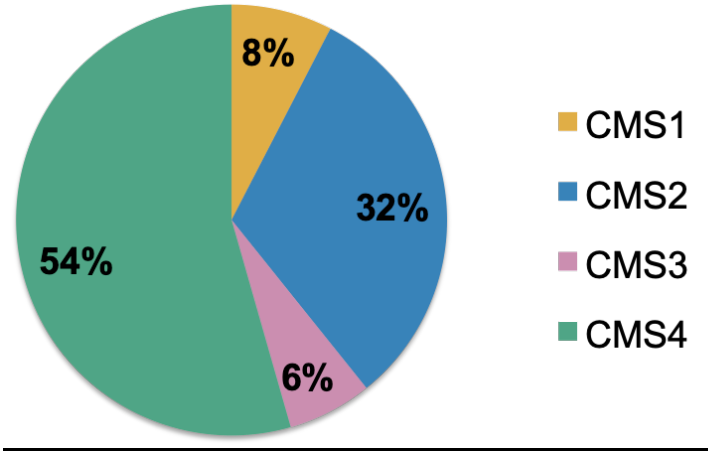

Figure 44. RankCMS-38 subtypes in the Test cohort (n: 79)

4.4.5.3 Test cohort: clinical characteristics

As per CRCA-38 subtypes, the association between CMS subtypes and clinical characteristics need to be interpreted with caution in view of the fact that 36% of the samples were not primary tumours collected pre-treatment.

In line with the CRCSC paper, no association with sex and age was found in the test cohort. Although not significant, enrichment for left-side tumours was

observed in the CMS2 subtype, which was also enriched for *RAS/BRAF* wild-type tumours (**Table 21**).

Variable	Level	CMS1 n(%)	CMS2 n(%)	CMS3 n(%)	CMS4 n(%)	P value
		6(8)	25(32)	5(6)	43(54)	
Sex	Male	3(50)	19(76)	3(60)	26(60)	0.480
	Female	3(50)	6(24)	2(40)	17(40)	
Age<65	Yes	2(33)	16(64)	2(40)	31(72)	0.162
	No	4(67)	9(36)	3(60)	12(28)	
	median (range)	63(49-72)	60(31-88)	59(32-76)	59(24-76)	
Sidedness	Left	3(50)	18(72)	5(100)	28(65)	0.338
	Right	3(50)	7(28)	0(0)	15(35)	
RAS/BRAF mutational status	Extended wild-type	2(33)	18(72)	5(100)	19(44)	0.030
	KRAS wild-type	1(17)	0(0)	0(0)	7(16)	
	RAS mutant	1(17)	5(20)	0(0)	6(14)	
	BRAF mutant	2(33)	0(0)	0(0)	6(14)	
	NA	0(0)	2(8)	0(0)	5(12)	
Stage at diagnosis	I-III	2(33)	5(20)	2(40)	32(74)	<0.001
	IV	3(50)	19(76)	3(60)	11(26)	
	NA	1(17)	1(4)	0(0)	0(0)	
Type of samples	Primary	4(67)	17(68)	4(80)	35(81)	0.550
	Metastatic	2(33)	8(32)	1(20)	8(19)	
Sample retrieval time-point	Pre-treatment	3(50)	15(60)	4(80)	37(86)	0.031
	Post-treatment	3(50)	10(40)	1(20)	6(14)	
Anti-EGFR therapy	single agent	3(50)	11(44)	5(100)	18(42)	0.102
	with chemo	3(50)	14(56)	0(0)	25(58)	
Response to anti-EGFR	Partial response	0(0)	7(28)	1(20)	12(28)	0.419
	Stable disease	2(33)	10(40)	1(20)	16(37)	
	Progression	4(67)	5(20)	3(60)	13(30)	
	Not available	0(0)	3(12)	0(0)	2(5)	

Table 21. Patients' characteristics in the Test cohort according to rankCMS-38 subtypes

4.4.5.4 Test cohort: treatment outcomes

In **Figure 45** PFS and OS Kaplan Meier curves are presented. As expected, CMS2 and CMS4 tumours demonstrated a significantly longer PFS compared to CMS1 and CMS3 tumours. The risk of progression in CMS1/CMS3 tumours was >3 times compared to CMS2 (**Table 22**). A trend for longer OS in CMS2 patients was observed.

Response to treatment was observed in patients with CMS2, CMS3 and CMS4 tumours. The majority of patients with CMS2 and CMS4 tumours experienced a clinical benefit while the majority of patients with CMS1 and CMS3 tumours progressed (**Figure 46**).

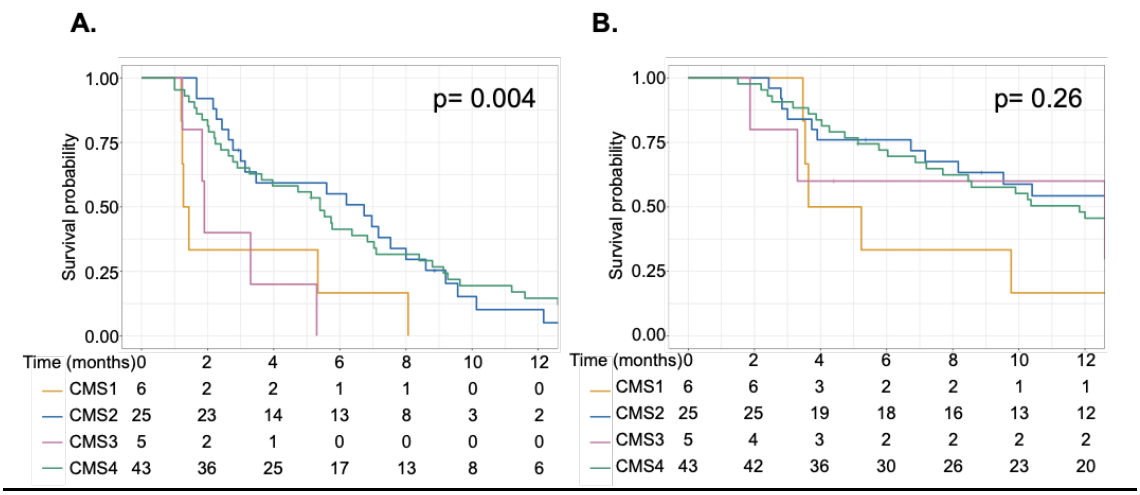

Figure 45. Progression-free survival (A) and overall survival (B) according to rankCMS-38 subtypes in the Test cohort.

Hazard for progression (Reference subtype: CMS2)

Subtype	HR	95% CI lower limit	95%CI upper limit	p-value
CMS1	3.02	1.21	7.50	0.017
CMS3	3.53	1.29	9.60	0.014
CMS4	0.99	0.59	1.66	0.969

Hazard for death (Reference subtype: CMS2)

Subtype	HR	95% CI lower limit	95%CI upper limit	p-value
CMS1	1.75	0.69	4.44	0.242
CMS3	2.60	0.86	7.84	0.089
CMS4	1.44	0.82	2.51	0.201

Table 22. Hazard ratios for progression (top) and death (bottom) in the Test cohort.

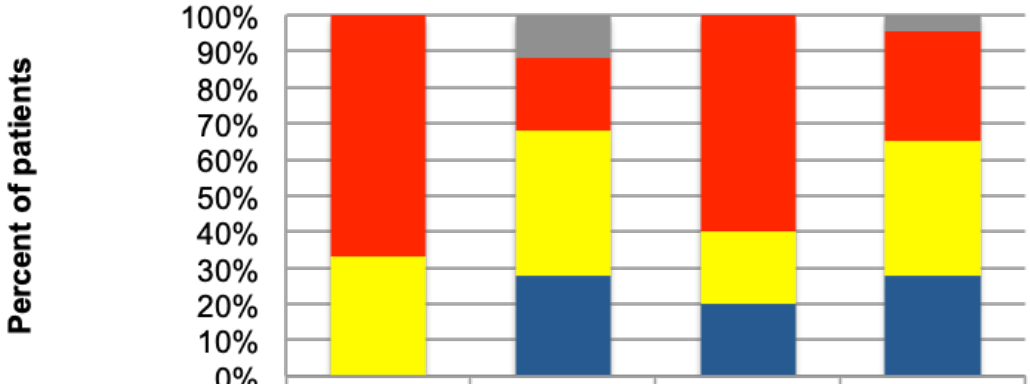

	CMS1	CMS2	CMS3	CMS4
Not available	0	3	0	2
Progression	4	5	3	13
Stable disease	2	10	1	16
Partial response	0	7	1	12

Figure 46. Stacked columns showing the type of response to anti-EGFR therapy according to rankCMS-38 subtypes (Test cohort).

4.4.5.4 Validation cohort: clinical characteristics

Similar to CRCA-38 and TA classes, the CO.20 cohort was deployed as a validation cohort. The distribution of the subtypes once again demonstrated the high prevalence of CMS2 and CMS4 subtypes and low prevalence of CMS3 and CMS1. In particular, CMS2 represented the vast majority of the samples (67%) possibly justified by the enrichment for *KRAS* exon 2 wild type tumours (**Figure 47**). In **Table 23** the main patients' characteristics are presented. As expected the CMS2 tumours were predominantly left-sided.

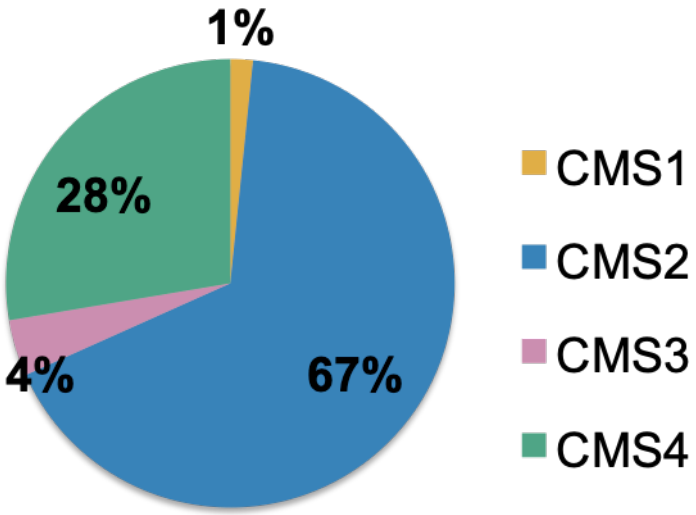

Figure 47. RankCMS-38 subtypes in the Validation cohort.

Characteristic	CMS 1 (N = 2)	CMS 2 (N = 80)	CMS 3 (N = 5)	CMS 4 (N = 34)	p-value
Age – median (range)	65.9 (57.8-74)	63 (32.9- 87.9)	70.3 (49.1-78.1)	64.3 (27- 87.7)	0.388
<65	1 (50.0)	47 (58.8)	1 (20.0)	18 (52.9)	
>=65	1 (50.0)	33 (41.3)	4 (80.0)	16 (47.1)	
Gender					0.162
Female	2 (100.0)	34 (42.5)	4 (80.0)	17 (50.0)	
Male	0 (0.0)	46 (57.5)	1 (20.0)	17 (50.0)	
ECOG performance status					0.532
0	0 (0.0)	34 (42.5)	2 (40.0)	11 (32.4)	
1	2 (100.0)	41 (51.3)	2 (40.0)	19 (55.9)	
2	0 (0.0)	5 (6.3)	1 (20.0)	4 (11.8)	
Any prior radiotherapy	0 (0.0)	23 (28.8)	1 (20.0)	10 (29.4)	1.000
Number of chemotherapy regimens					0.490
1-2	0 (0.0)	0 (0.0)	0 (0.0)	0 (0.0)	
3	0 (0.0)	6 (7.5)	0 (0.0)	3 (8.8)	
4	1 (50.0)	8 (10.0)	0 (0.0)	6 (17.6)	
≥5	1 (50.0)	66 (82.5)	5 (100.0)	25 (73.5)	
Prior irinotecan	2 (100.0)	78 (97.5)	5 (100.0)	33 (97.1)	1.000
Prior oxaliplatin	2 (100.0)	78 (97.5)	5 (100.0)	34 (100.0)	1.000
Any prior VEGFR target therapy	0 (0.0)	36 (45.0)	4 (80.0)	11 (32.4)	0.115
Any liver metastasis	0 (0.0)	62 (77.5)	2 (40.0)	21 (61.8)	**0.013**
Number of sites of disease					0.459
1	0 (0.0)	19 (23.8)	0 (0.0)	5 (14.7)	
2	2 (100.0)	31 (38.8)	2 (40.0)	12 (35.3)	
3	0 (0.0)	15 (18.8)	1 (20.0)	12 (35.3)	
≥4	0 (0.0)	15 (18.8)	2 (40.0)	5 (14.7)	
Sidedness					**0.010**
Left	1 (50.0)	67 (83.8)	3 (60.0)	20 (58.8)	
Right	1 (50.0)	13 (16.3)	2 (40.0)	14 (41.2)	

Table 23. Patients' characteristics according to rankCMS-38 subtypes (Validation cohort).

4.4.5.5 Validation cohort: treatment outcomes

Similar to the test cohort, CMS1 and CMS3 tumours were associated with very short PFS (**Figure 48**). The CMS2 subtype was confirmed to be associated with longer PFS, OS and higher disease control rate. Conversely, the CMS4 subtype demonstrated worse outcomes compared to the Test cohort (**Table 24**). This difference may be related to the effect of chemotherapy (used in combination with anti-EGFR agents) in the Test cohort and not present in the Validation cohort (cetuximab single agent).

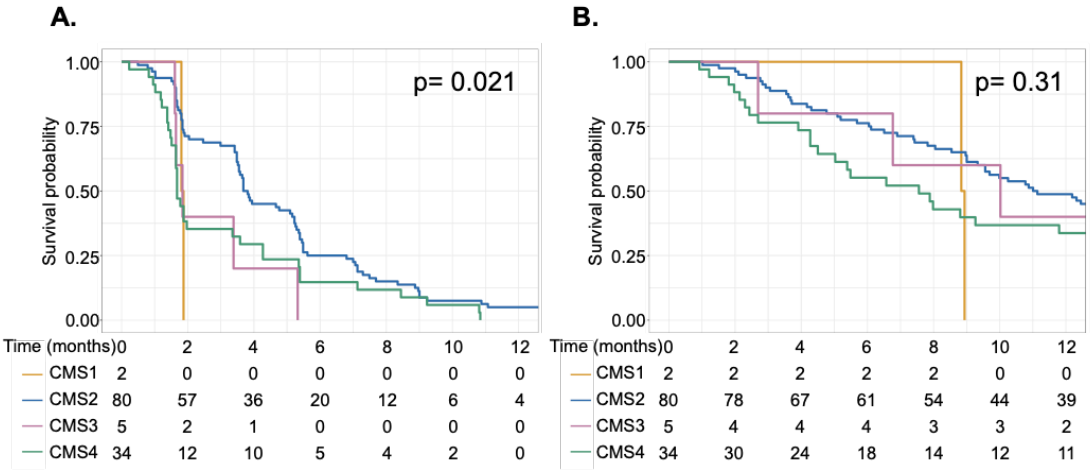

Figure 48. Progression-free survival (A) and overall survival (B) according to rankCMS-38 subtypes (Validation cohort).

A multi-variate analysis directly comparing CMS2 over CMS4 subtypes demonstrated that the significantly longer PFS and higher DCR of the CMS2 subtype were independent from multiple co-variates used for correction (**Table 25**). A trend for longer OS was also observed, highlighting once again the favourable prognosis of CMS2 tumours.

Biomarker	N	Univariate Analysis			Multivariate Analysis[1]	
		Median survival (Months)	Hazard Ratio[2] (95% CI)	Log-rank p-value	Hazard Ratio[2] (95% C.I.)	p-value Cox regression
Prognostic analysis for progression-free survival						
CMS class				0.021[3]		0.007[3]
2	80	3.75	0.28 (0.07, 1.20)	0.086[4]	0.21 (0.04, 0.98)	0.047[4]
3	5	1.84	0.70 (0.12, 4.27)	0.703[4]	NA (0, NA)	1.000[4]
4	34	1.68	0.86 (0.20, 3.66)	0.834[4]	1.54 (0.27, 8.62)	0.625[4]
1	2	1.84	-		-	
Prognostic analysis for overall survival						
CMS class				0.314[3]		0.127[3]
2	80	11.07	0.43 (0.10, 1.79)	0.243[4]	0.17 (0.03, 0.85)	0.031[4]
3	5	10.02	0.46 (0.06, 3.31)	0.440[4]	0 (0, NA)	1.000[4]
4	34	7.56	0.91 (0.21, 3.92)	0.902[4]	1.07 (0.21, 5.49)	0.939[4]
1	2	8.89				
Biomarker	**N**	**Univariate Analysis**			**Multivariate Analysis[1]**	
		Rate (%)	**Odds Ratio[2] (95% CI)**	**Fisher's exact p-value**	**Odds Ratio[2] (95% C.I.)**	**p-value logistic regression**
Prognostic analysis for disease control						
CMS class				<0.001[3]		0.015[3]
2	80	68.75	NA	0.106[4]	NA	0.980[4]
3	5	40.00	NA	1.000[4]	NA	0.911[4]
4	34	35.29	NA	0.543[4]	NA	0.845[4]
1	2	0				
Prognostic analysis for response						
CMS class				0.769[3]		0.911[3]
2	80	6.25	NA	1.000[4]	NA	0.965[4]
3	5	0	NA	NA[4]	NA	NA[4]
4	34	2.94	NA	1.000[4]	NA	0.972[4]
1	2	0				

(1) Cox and Logistic regression including the following covariates: ECOG performance status (0-1 vs. 2), gender (male vs. female), age (65 or older vs. younger than 65), baseline LDH level (higher than UNL vs. UNL or less), baseline alkaline phosphatase (higher than UNL vs. UNL or less), baseline hemoglobin (CTC grade 1 or higher vs. CTC grade 0), number of disease sites (more than 2 vs. 2 or less), number of previous chemotherapy drug classes (more than 2 vs. 2 or less), prior VEGFR target therapy (yes vs. no), presence of liver metastases (yes vs. no); (2) Hazard ratio over CMS1; (3) Comparison among all classes; (4)Comparison with CMS1.

Table 24. Univariate and multivariate prognostic analyses (Validation cohort)

Outcome	Subtype	N	Median PFS (months)	Univariate analysis Hazard Ratio (95%CI)	Log-rank p-value	Multivariate analysis Hazard Ratio (95%CI)	Cox regression p-value
PFS	CMS2	80	3.75	0.61 (0.40-0.91)	0.017	0.46 (0.29-0.73)	0.001
	CMS4	34	1.68				
OS	CMS2	80	11.07	0.74 (0.48-1.13)	0.163	0.63 (0.39-1.00)	0.051
	CMS4	34	7.56				
Outcome	**Subtype**	**N**	**Rate %**	**Univariate analysis Odds Ratio (95%CI)**	**Fisher's exact p-value**	**Multivariate analysis Odds Ratio (95%CI)**	**Logistic regression p-value**
Disease control	CMS2	80	68.75	4.03 (1.73-9.41)	0.002	5.53 (1.93-15.82)	0.001
	CMS4	34	35.29				
Response	CMS2	80	6.25	2.20 (0.25-19.57)	0.667	2.61 (0.21-32.51)	0.456
	CMS4	34	2.94				

Table 25. Uni- and multivariate analyses comparing CMS2 and CMS4 subtypes in the Validation cohort.

4.4.5.6 Further results validation using publicly available data

The Validation cohort suggested increased outcomes in patients with CMS2 subtype tumour over the CMS4. This was different from what was observed in the Test cohort, possibly due to the confounding effect from chemotherapy in the Test cohort and its retrospective patient selection. Hence, the Khambata-Ford dataset was ideal to further validate the prognostic effect of rankCMS-38 subtypes within the context of a phase II study where patients received single-agent cetuximab, in line with the CO.20 clinical trial cohort (193).

As observed in the validation cohort, CMS2 was associated with better prognosis compared to the other subtypes (**Figure 49**). The missing statistical significance was possibly due to the small sample size (n. 80). However, the trend remained the same.

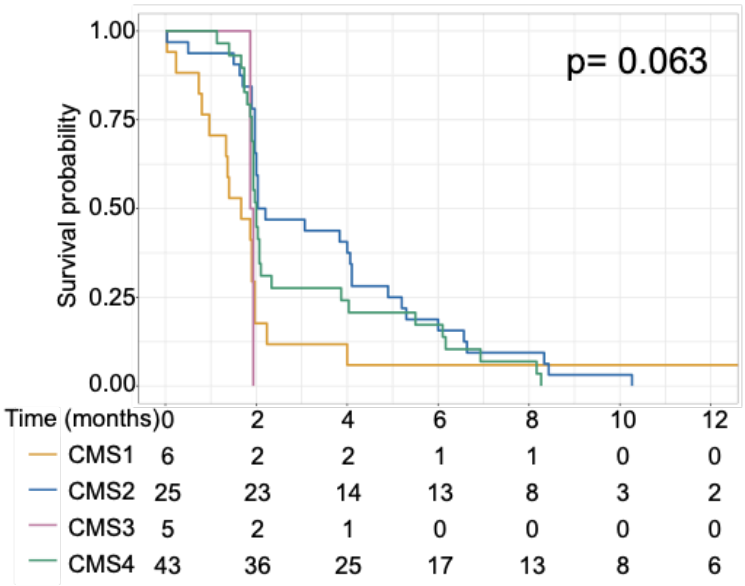

Figure 49. Progression-free survival to single-agent cetuximab according to rankCMS-38 subtypes in the Khambata-Ford dataset.

4.5 Discussion

The primary aims of this chapter were to demonstrate that the subtypes identified with the NanoCRC assay were able to define clinically meaningful subgroups of patients. Both CRCA-38 and rankCMS-38 subtypes demonstrated significantly different outcomes in terms of PFS and OS in three cohorts of patients who progressed after standard chemotherapy treatments for metastatic disease. Hence, one potential clinical utility of the assay was established.

From a technical viewpoint, based on previous evidence (139), the TA subtype of the CRCA-38 classifier was expected to be associated with benefit from anti-EGFR therapy. This was confirmed in both Test and Validation cohorts, conferring further evidence of the validity of the assay. Similarly, CMS2 and CMS4 subtypes were expected to be associated with anti-EGFR benefit based on the subtype analysis of two retrospective analyses of randomised trials in first line setting (149,150). The results of the rankCMS-38 classifier were in line with these studies, once again reinforcing the robustness of the assay and new classifier.

From a clinical viewpoint, these results need to be interpreted with caution. Firstly because not all samples analysed in both test and validation cohorts were from the primary tumour. The concordance between primary tumour and metastatic sites is not completely established. This is difficult to assess especially because it is very common that patients receive chemotherapy between the resection of the primary tumour and metastases. Hence, the expression profiles may be modified by treatments and consequently confound the expected concordance between sources. Also, the tissue available from metastatic samples may have been collected with a biopsy instead of a full resection. Recently, Alderdice *et al.* questioned the robustness of the CMS classification in tissue biopsies, demonstrating a high proportion of unclassified samples (219). The same group demonstrated discordant CMS subtyping

results from different tumour areas within the same sample, possibly due to intratumoural heterogeneity (115).

Nevertheless, three CRCA-38 subtypes (TA, stem-like and enterocyte) and their correlated CMS subtypes (CMS2 and CMS4) demonstrated higher clinical benefit compared to the other two CRCA-38 subtypes (goblet-like and inflammatory) and correlated CMS subtypes (CMS3 and CMS1). However, heterogeneous responses were demonstrated especially in the non-TA subtypes.

To improve the clinical applicability of these classifiers in potentially predicting the benefit from anti-EGFR agents, a new classifier able to dichotomise patient samples into two groups was established. Two different gene expression profiles were identifiable in patient samples based on TA signature: TA class 1 and TA class 2. This TA class assignment has the advantage of providing a qualitative assessment of the TA signature in all the samples, including the non-TA subtypes, overcoming the limitations posed by intra-tumoural heterogeneity in assessing benefit from anti-EGFR therapy. TA class 1 tumours were significantly associated with clinical benefit in patients treated with anti-EGFR therapy; this was validated in a *KRAS* exon 2 wild-type trial cohort, which has the advantage of properly assessing the prognostic value in a homogeneously treated population and in the absence of the confounding effect of chemotherapy. The significant prognostic role of TA class 1 was retained in the *RAS* and *BRAF* left-sided subgroup. Moreover, TA class 2 assignment was enriched for *RAS/BRAF*-mutant tumours, providing a potential alternative method to estimate benefit from anti-EGFR therapy when the mutational status is missing. TA class assignment was also associated with responses in pre-clinical models. Finally, the TA classes retained significance when assessed in either primary tumours or metastatic samples. This is highly clinically relevant, since it means that the signature can be assessed in metastatic lesions when the primary tumour sample is not available; however, intra-patient concordance was not assessed so further validation is required.

Several studies have now evaluated the association between single genes or microRNAs (*EREG/AREG*, *HER2*, *HER3*, *EPHA2*, or mir-31-3p) and responses to anti-EGFR therapy (220). However, establishing single gene assays requires the optimisation of cut-off values for each gene, an approach burdened by several analytical and methodological drawbacks. In contrast, we evaluated a previously derived gene expression signature to identify biologically different CRC subtypes with distinct cellular phenotypes (154). The subtypes summarize a complex network of pathways potentially associated with therapeutic responses, simplifying multiple levels of information derived from heterogeneous samples. Hence, the deployment of subtypes and their signatures, instead of single genes, has the advantage of reducing the dimension of complexity without losing biological information.

With respect to the assessment of the real clinical value of the TA classes, this study has some limitations. First, there were only a small number of extended wild-type patient samples. Second, the study was retrospectively designed on pre-existing tissue collections of patients who had received anti-EGFR therapy. Although association with depth of response was identified in a subgroup of patients and in pre-clinical models, biomarker evaluation in a group of patients who did not receive anti-EGFR therapy may further clarify its prognostic and/or predictive value. The analysis of more contemporary clinical trial cohorts in which patients were upfront selected based on extended *RAS/BRAF* status and with both treatment and control arms available for the analysis may clarify the added value of the TA classes beyond current patient selection in the clinic. Given the robustness of the assay in clinically relevant samples, a prospective assessment would be ideal.

Lastly, the role of CMS subtypes in potentially predicting benefit from anti-EGFR therapy was assessed here for the very first time in patients who received single agent cetuximab. The CMS2 subtype was associated with longer survival and higher disease control rate. The response rate was numerically higher in the CMS2 compared to the CMS4 subtype. However, in view of the low overall

response rate to single agent anti-EGFR therapy, it is challenging to take definitive conclusions. Although interesting, it is not possible to clarify whether the better outcomes observed in the CMS2 subtype are due to its less aggressive biological nature or because of the effect of cetuximab, in the absence of a control group. Future assessment of controlled-studies may clarify this issue.

Chapter 5 Conclusions and future directions

Colorectal cancer is a highly heterogeneous disease at multiple levels (114). In the metastatic setting, limited treatment options are available. A number of clinical trials testing new drugs failed: the lack of biomarkers predictive of response and able to select patients with similar disease biology may have contributed to these failures. To date, genomic biomarkers, namely microsatellite instability and *RAS*/*BRAF* mutational status, are the only molecular features routinely tested in the clinic (29). The recently established gene expression subtypes of CRC helped demonstrating further heterogeneity beyond genomic markers and showed real promise for patient stratification and potential to guide new biomarker-enriched clinical trials (153). However, a number of flaws and challenges are currently holding their prospective evaluation: firstly, the lack of suitable assays for FFPE samples and for routine testing; secondly, the lack of clear value in predicting treatment benefit.

The work presented here aimed to overcome the technical challenges of gene expression subtypes application through the development of new assays similar to others already adopted in the clinic (in breast cancer); then to demonstrate that the established biomarkers have clear clinical utility in defining the likelihood of benefit from one of the most widely used and highly expensive targeted therapy (anti-EGFR) over current risk stratification factors.

Two gene expression assays for nCounter platform (NanoString Technologies) were developed: one assay for the classification of CRC samples into CMS subtypes and one assay for simultaneous classification of CRC samples into CMS and CRCAssigner subtypes. A pipeline for data analysis and quality control assessment was established. Two new algorithms were developed, one (based on a previously validated subtyping method for CRCAssigner subtypes) able to dichotomise samples into two classes with differential sensitivity to anti-EGFR therapy; the other one to classify samples in CMS subtypes using a

limited set of genes, which improved the misclassification error compared to publicly available CMS algorithms.

The subtyping results were validated using various methods: firstly, using publicly available data to test the accuracy of the new algorithms; secondly, using fresh-frozen samples with matched RNAseq data available to use as a reference; and lastly, via orthogonal validation using genomic and clinical data to confirm the presence of known subtype-specific associations.

In chapter 2 I described the technical steps followed to develop the new biomarker assays. Recently, other groups developed similar gene expression assays, as a further evidence of how such assays represent an unmet need for the research community. Piskol and colleagues, all current or former employees of Genentech Inc., developed a CMS classifier using the NanoString Technologies platform and FFPE retrospective tissue collections (164). Similarly to our approach, they used custom designed panels to measure the expression of key genes for CRC biology. The panels included more than 800 genes including 3 housekeeping genes and the analysis required more than 250 ng of total RNA for each sample. A new NanoString-based algorithm to classify samples based on 322 CMS genes included in the custom panels was optimised using publicly available data. The algorithm demonstrated a concordance between 90.5% and 93.8% with the gold-standard CMS classification. To assess the performance of the new algorithm and the NanoString assay 46 high-quality FFPE samples were identified. The classification derived from NanoString platform and from RNAseq data was compared: 35 out of 41 (85.3%) samples successfully profiled with both platforms were assigned to the same CMS subtype. The association between subtypes and mutational and clinical features was also assessed to demonstrate the robustness of the assay results (164).

Given the similarities with our work, the Genentech Inc. study indirectly validates the methodology used in this thesis work. The main differences include the fact that we used a modified protocol for the NanoString platform. This has two significant advantages as direct consequence of using a significantly lower number of genes: firstly, the costs of profiling more than 800

genes versus only 96 genes are significantly cheaper; secondly, the amount of RNA required is 2.5 times lower using our method. This is particularly important in the context of archival FFPE samples where the quality of the RNA may be suboptimal and in presence of a limited tumour content within the sample in case of biopsies or highly fibrotic tumours. In terms of performance, their newly-developed classifier compared favourably with our rankCMS classifier when using public data. Similarly, when the new classifier was coupled with the custom NanoString assay and tested on matched NanoString and RNAseq data their concordance with the gold-standard CMS classification was 85%, which is very similar to what demonstrated by us using fresh-frozen matched data (89%).

Although this high concordance observed in both studies, a recent publication challenged the inter-platform reproducibility of the CMS classification (221). Platform-specific biases were investigated using microarrays and RNAseq approaches in a cohort of 126 primary CRC samples. Of note, systematic technical biases were demonstrated in the presence of short (less than 2000 nucleotides) sequences and lowly expressed genes using RNAseq as well as over-saturation biases in presence of highly expressed genes using microarrays. This study suggests that the selection of the optimal set of genes may require platform-optimization and also justifies the nearly 10% misclassification observed in our study using RNAseq and NanoString platforms.

A further difference between our and the Genentech Inc. assays is related to the number of housekeeping genes, 3 out of 322 (1%) in the Genentech Inc. assay versus 10 out of 96 (10%) in our assay: although a direct comparison of the performance of these two assays has not been done, the higher number of housekeeping genes may be helpful in case of poor quality RNA when a successful measure of all the genes is not warranted (164).

Using a cohort of unmatched primary and metastatic samples the authors wanted to assess the stability of the CMS subtypes during the metastatic process. All the fours subtypes were identified. However, in line with our results (Figure 49 – rankCMS classification in the Khambata-Ford dataset) a

significantly low number of CMS3 tumours were identified in metastatic samples. Once again this supports our subtyping results and suggest a potentially different tropism of CMS3 tumours or a potential misclassification of metastatic samples due to technical effect.

In support of the hypothesis that distinct subtypes may have a preferential tissue tropism, a recent study demonstrated how unsupervised clustering of metastatic liver lesions from CRC identified only two main subtypes in these samples, which recapitulate the CMS2 and CMS4 subtypes (118). This finding once again supports the low prevalence of CMS1 and CMS3 tumours according to rankCMS classification described in this thesis.

These findings have profound clinical implications. While the mutational status of primary tumour and metastatic sites unlikely changes during the metastatic process, the transcriptional profile is possibly more affected. In clinical practice, the RAS mutational status is commonly tested independently of the type of tissue profiled, given the high concordance demonstrated of up to 93% (117). Conversely, the potential discordance between different types of samples from the same patient could highly reduce the applicability of gene expression subtypes in clinical practice where not always the primary tumour sample is available for biomarker analysis. This discordance needs to be systematically assessed and *ad-hoc* classifiers based on the type of sample may be required. A dedicated study of matched primary and metastatic samples is on-going in our lab and will possibly clarify the stability of the rankCMS classification during metastatization.

Concomitantly with the technical validation, the potential clinical utility of the assays was evaluated in this thesis: assays and signatures identified subgroup of patients with significantly different prognosis and with different likelihood of benefit from anti-EGFR therapy. The association between subtypes and anti-EGFR benefit was initially demonstrated in a retrospective cohort. To validate the results a new collaboration with an international clinical trial group (Canadian Cancer Trial Group) was established. The signatures were validated in a clinical trial sample collection from patients who received anti-EGFR therapy as a single agent (193). This study was able to assess the role of the

CMS classification for the very first time in the absence of confounding effect due to chemotherapy. Given the lack of positive predictive biomarkers of response to these drugs, the biomarker assays and the newly defined TA-like signature and rankCMS biomarkers may represent potential companion diagnostic tools for patient selection and precision medicine.

Lastly, for the first time the CMS assay and the rank classifier (which is a single-sample-prediction classifier) were used to study difference and similarities between populations with different ethnicity, overcoming any potential technical artefact. Confirming that the assay is able to capture similar groups across populations justifies its potential application in future international studies.

Overall, these assays have multiple potential implications for clinical practice that may continue to evolve in the near future. The subtypes represent distinctive biological entities, which have been associated with different prognostic values in different stages of disease. Hence, the first clinical use is the possibility to recognise patients with potentially more aggressive disease (as example in presence of stem-like or CMS4 subtype). Secondly, as described in chapter 3, the selection of patients likely to benefit from anti-EGFR therapy can be improved: with further validation some patients may be spared from toxicities of the treatment in case of low likelihood to response; conversely, anti-EGFR therapy could be offered to a proportion of patients with right-sided tumour for whom this treatment is currently not indicated.

Anti-EGFR therapy is one of the most important drugs available for the treatment of CRC patients with metastatic *RAS/BRAF* wild-type disease. Recent evidence suggests a role for the re-challenge in later lines of treatment of cetuximab or panitumumab after progression to these agents. This strategy is supported by the study of Siravegna and colleagues exploiting the dynamic changes of circulating tumour DNA (ctDNA) during anti-EGFR therapy (46). The authors demonstrated how mutant *RAS* clones rise in the blood of patients during anti-EGFR therapy as possible mechanism of acquired resistance. The *RAS* mutant closes decay upon treatment withdrawal and sensitivity to the drug is potentially regained. In this PhD work I demonstrated how gene expression

profiles could help refining the identification of patients with primary resistance to anti-EGFR therapy. In the experimental cohort including xenograft models (Figure 40) the TA-like signature was lost upon treatment, suggesting that dynamic changes are also identifiable using gene expression. While not explored in this current work, whole blood gene expression profiling techniques are rapidly moving into the circulating biomarker space, opening the opportunity to translate our currently tissue-based biomarker into a circulating biomarker (222).

Multiple other projects are on-going in the lab as well as in other institutions. The assays are currently being deployed to assess whether association between subtypes and the intensified chemotherapy regimen FOLFOXIRI plus bevacizumab exists within the context of two randomised clinical trials (TRIBE and TRIBE2) in collaborations with Italian investigators (91,223). Furthermore a new collaboration was recently established to evaluate the subtypes in liver metastatic samples collected within a randomised trial: the aim of the trial was to assess the utility of an antigen-specific cancer vaccine against mucin-1 (MUC-1) as adjuvant therapy after complete hepatic metastasectomy (224).

These ancillary analyses of randomised controlled studies have the possibility to further explore the potential predictive value of the subtypes. Similarly, a new trial investigating a first-in-class bifunctional fusion protein against programmed-death ligand 1 (PD-L1) and the transforming growth factor receptor beta (TGF-beta) in CMS4 tumours is on-going (225). The results of this study may lead to the validation of a subtype-specific treatment, indirectly expanding the clinical utility of the rank-CMS subtypes developed in this project.

In chapter 3, the assays were tested in liver metastatic samples and matched patient-derived xenografts. With the caveat of a small sample size, high concordance between pre and post-implantation samples and association with anti-EGFR benefit were observed. On-going studies in our lab are testing the subtyping results of the assays in patient-derived organoids. The results of these studies may facilitate the future application of the assays as potential research tools for drug screening.

Finally, in view of the characteristics of the assays with potential for commercialization, an accelerator program (The MedTech SuperConnector) was successfully completed and a project for a spin-out company is on-going. This may expedite the future validation of the assays in an accredited laboratory certified for clinical use.

References

1. Schlussel AT, Gagliano Jr RA, Seto-Donlon S, Eggerding F, Donlon T, Berenberg J, Lynch HT. The evolution of colorectal cancer genetics—Part 1: from discovery to practice. Journal of gastrointestinal oncology. 2014 Oct;5(5):326.
2. WARTHIN AS. Heredity with reference to carcinoma: as shown by the study of the cases examined in the pathological laboratory of the University of Michigan, 1895-1913. Archives of Internal Medicine. 1913 Nov 1;12(5):546-55.
3. Lynch HT, Krush AJ. Cancer family "G" revisited: 1895-1970. Cancer. 1971 Jun;27(6):1505-11.
4. Fearon ER, Vogelstein B. A genetic model for colorectal tumorigenesis. cell. 1990 Jun 1;61(5):759-67.
5. Bray F, Ferlay J, Soerjomataram I, Siegel RL, Torre LA, Jemal A. Global cancer statistics 2018: GLOBOCAN estimates of incidence and mortality worldwide for 36 cancers in 185 countries. CA: a cancer journal for clinicians. 2018 Nov;68(6):394-424.
6. Cancer Research UK: https://www.cancerresearchuk.org/health-professional/cancer-statistics/statistics-by-cancer-type/bowel-cancer. September 2019.
7. Arnold M, Sierra MS, Laversanne M, Soerjomataram I, Jemal A, Bray F. Global patterns and trends in colorectal cancer incidence and mortality. Gut. 2017 Apr 1;66(4):683-91.
8. Siegel RL, Fedewa SA, Anderson WF, Miller KD, Ma J, Rosenberg PS, Jemal A. Colorectal cancer incidence patterns in the United States, 1974–2013. JNCI: Journal of the National Cancer Institute. 2017 Feb 28;109(8):djw322.
9. Winawer S, Classen M, Lambert R, Fried M, Dite P, Goh KL, Guarner F, Lieberman D, Eliakim R, Levin B, Saenz R. Colorectal cancer screening world gastroenterology organisation/international digestive cancer alliance practice guidelines. South African Gastroenterology Review. 2008 Mar 1;6(1):13-20.
10. Labianca R, Nordlinger B, Beretta GD, Mosconi S, Mandalà M, Cervantes A, Arnold D, ESMO Guidelines Working Group. Early colon cancer: ESMO Clinical Practice Guidelines for diagnosis, treatment and follow-up. Annals of oncology. 2013 Oct 1;24(suppl_6):vi64-72.
11. Glynne-Jones R, Wyrwicz L, Tiret E, Brown G, Rödel C, Cervantes A, Arnold D. Rectal cancer: ESMO Clinical Practice Guidelines for diagnosis, treatment and follow-up.
12. Böckelman C, Engelmann BE, Kaprio T, Hansen TF, Glimelius B. Risk of recurrence in patients with colon cancer stage II and III: a systematic review and meta-analysis of recent literature. Acta oncologica. 2015 Jan 2;54(1):5-16.
13. National Comprehensive Cancer Network Clinical Practice Guidelines. Available at: https://www.nccn.org/professionals/physician_gls/pdf/colon.pdf. Version 2.2019
14. Ganesan A, Proudfoot J. Analogue-based drug discovery. Fischer J, Ganellin CR, editors. Wiley-VCH; 2010 Jul.
15. Sobrero AF, Aschele C, Bertino JR. Fluorouracil in colorectal cancer--a tale of two drugs: implications for biochemical modulation. Journal of Clinical Oncology. 1997 Jan;15(1):368-81.
16. Twelves C, Wong A, Nowacki MP, Abt M, Burris III H, Carrato A, Cassidy J, Cervantes A, Fagerberg J, Georgoulias V, Husseini F. Capecitabine as adjuvant treatment for stage III colon cancer. New England Journal of Medicine. 2005 Jun 30;352(26):2696-704.

17. André T, Boni C, Navarro M, Tabernero J, Hickish T, Topham C, Bonetti A, Clingan P, Bridgewater J, Rivera F, De Gramont A. Improved overall survival with oxaliplatin, fluorouracil, and leucovorin as adjuvant treatment in stage II or III colon cancer in the MOSAIC trial. J clin oncol. 2009 Jul 1;27(19):3109-16.
18. Schmoll HJ, Tabernero J, Maroun J, De Braud F, Price T, Van Cutsem E, Hill M, Hoersch S, Rittweger K, Haller DG. Capecitabine plus oxaliplatin compared with fluorouracil/folinic acid as adjuvant therapy for stage III colon cancer: final results of the NO16968 randomized controlled phase III trial. Journal of Clinical Oncology. 2015 Aug 31;33(32):3733-40.
19. Yothers G, O'Connell MJ, Allegra CJ, Kuebler JP, Colangelo LH, Petrelli NJ, Wolmark N. Oxaliplatin as adjuvant therapy for colon cancer: updated results of NSABP C-07 trial, including survival and subset analyses. Journal of clinical oncology. 2011 Oct 1;29(28):3768.
20. Sargent DJ, Goldberg RM, Jacobson SD, Macdonald JS, Labianca R, Haller DG, Shepherd LE, Seitz JF, Francini G. A pooled analysis of adjuvant chemotherapy for resected colon cancer in elderly patients. New England Journal of Medicine. 2001 Oct 11;345(15):1091-7.
21. McCleary NJ, Meyerhardt JA, Green E, Yothers G, de Gramont A, Van Cutsem E, O'Connell M, Twelves CJ, Saltz LB, Haller DG, Sargent DJ. Impact of age on the efficacy of newer adjuvant therapies in patients with stage II/III colon cancer: findings from the ACCENT database. Journal of clinical oncology. 2013 Jul 10;31(20):2600.
22. Grothey A, Sobrero AF, Shields AF, Yoshino T, Paul J, Taieb J, Souglakos J, Shi Q, Kerr R, Labianca R, Meyerhardt JA. Duration of adjuvant chemotherapy for stage III colon cancer. New England Journal of Medicine. 2018 Mar 29;378(13):1177-88.
23. Van Cutsem E, Labianca R, Bodoky G, Barone C, Aranda E, Nordlinger B, Topham C, Tabernero J, André T, Sobrero AF, Mini E. Randomized phase III trial comparing biweekly infusional fluorouracil/leucovorin alone or with irinotecan in the adjuvant treatment of stage III colon cancer: PETACC-3. Journal of Clinical Oncology. 2009 May 18;27(19):3117-25.
24. Allegra CJ, Yothers G, O'Connell MJ, Sharif S, Petrelli NJ, Colangelo LH, Atkins JN, Seay TE, Fehrenbacher L, Goldberg RM, O'Reilly S. Phase III trial assessing bevacizumab in stages II and III carcinoma of the colon: results of NSABP protocol C-08. Journal of Clinical Oncology. 2011 Jan 1;29(1):11.
25. de Gramont A, Van Cutsem E, Schmoll HJ, Tabernero J, Clarke S, Moore MJ, Cunningham D, Cartwright TH, Hecht JR, Rivera F, Im SA. Bevacizumab plus oxaliplatin-based chemotherapy as adjuvant treatment for colon cancer (AVANT): a phase 3 randomised controlled trial. The lancet oncology. 2012 Dec 1;13(12):1225-33.
26. Alberts SR, Sargent DJ, Nair S, Mahoney MR, Mooney M, Thibodeau SN, Smyrk TC, Sinicrope FA, Chan E, Gill S, Kahlenberg MS. Effect of oxaliplatin, fluorouracil, and leucovorin with or without cetuximab on survival among patients with resected stage III colon cancer: a randomized trial. Jama. 2012 Apr 4;307(13):1383-93.
27. Taieb J, Tabernero J, Mini E, Subtil F, Folprecht G, Van Laethem JL, Thaler J, Bridgewater J, Petersen LN, Blons H, Collette L. Oxaliplatin, fluorouracil, and leucovorin with or without cetuximab in patients with resected stage III colon cancer (PETACC-8): an open-label, randomised phase 3 trial. The Lancet Oncology. 2014 Jul 1;15(8):862-73.
28. Group FC. Feasibility of preoperative chemotherapy for locally advanced, operable colon cancer: the pilot phase of a randomised controlled trial. The Lancet Oncology. 2012 Nov 1;13(11):1152-60.
29. Van Cutsem E, Cervantes A, Adam R, Sobrero A, Van Krieken JH, Aderka D, Aranda Aguilar E, Bardelli A, Benson A, Bodoky G, Ciardiello F. ESMO

consensus guidelines for the management of patients with metastatic colorectal cancer. Annals of Oncology. 2016 Aug 1;27(8):1386-422.
30. Nordlinger B, Sorbye H, Glimelius B, Poston GJ, Schlag PM, Rougier P, Bechstein WO, Primrose JN, Walpole ET, Finch-Jones M, Jaeck D. Perioperative chemotherapy with FOLFOX4 and surgery versus surgery alone for resectable liver metastases from colorectal cancer (EORTC Intergroup trial 40983): a randomised controlled trial. The Lancet. 2008 Mar 22;371(9617):1007-16.
31. Primrose J, Falk S, Finch-Jones M, Valle J, O'Reilly D, Siriwardena A, Hornbuckle J, Peterson M, Rees M, Iveson T, Hickish T. Systemic chemotherapy with or without cetuximab in patients with resectable colorectal liver metastasis: the New EPOC randomised controlled trial. The lancet oncology. 2014 May 1;15(6):601-11.
32. Tomasello G, Petrelli F, Ghidini M, Russo A, Passalacqua R, Barni S. FOLFOXIRI plus bevacizumab as conversion therapy for patients with initially unresectable metastatic colorectal cancer: a systematic review and pooled analysis. JAMA oncology. 2017 Jul 1;3(7):e170278-.
33. Geissler M, Riera-Knorrenschild J, Tannapfel A, Greeve J, Florschütz A, Wessendorf S, Seufferlein T, Kanzler S, Held S, Heinemann V, Reinacher-Schick AC. mFOLFOXIRI+ panitumumab versus FOLFOXIRI as first-line treatment in patients with RAS wild-type metastatic colorectal cancer m (CRC): A randomized phase II VOLFI trial of the AIO (AIO-KRK0109).
34. Cremolini C, Antoniotti C, Lonardi S, Aprile G, Bergamo F, Masi G, Grande R, Tonini G, Mescoli C, Cardellino GG, Coltelli L. Activity and safety of cetuximab plus modified folfoxiri followed by maintenance with cetuximab or bevacizumab for ras and braf wild-type metastatic colorectal cancer: A randomized phase 2 clinical trial. JAMA oncology. 2018 Apr 1;4(4):529-36.
35. Yoshino T, Arnold D, Taniguchi H, Pentheroudakis G, Yamazaki K, Xu RH, Kim TW, Ismail F, Tan IB, Yeh KH, Grothey A. Pan-Asian adapted ESMO consensus guidelines for the management of patients with metastatic colorectal cancer: a JSMO–ESMO initiative endorsed by CSCO, KACO, MOS, SSO and TOS. Annals of Oncology. 2017 Nov 16;29(1):44-70.
36. Tournigand C, André T, Achille E, Lledo G, Flesh M, Mery-Mignard D, Quinaux E, Couteau C, Buyse M, Ganem G, Landi B. FOLFIRI followed by FOLFOX6 or the reverse sequence in advanced colorectal cancer: a randomized GERCOR study. Journal of Clinical Oncology. 2004 Jan 15;22(2):229-37.
37. Matsuda C, Honda M, Tanaka C, Fukunaga M, Ishibashi K, Munemoto Y, Hata T, Bando H, Oshiro M, Kobayashi M, Tokunaga Y. Multicenter randomized phase II clinical trial of oxaliplatin reintroduction as a third-or later-line therapy for metastatic colorectal cancer—biweekly versus standard triweekly XELOX (The ORION Study). International journal of clinical oncology. 2016 Jun 1;21(3):566-72.
38. Suenaga M, Mizunuma N, Matsusaka S, Shinozaki E, Ozaka M, Ogura M, Yamaguchi T. Phase II study of reintroduction of oxaliplatin for advanced colorectal cancer in patients previously treated with oxaliplatin and irinotecan: RE-OPEN study. Drug design, development and therapy. 2015;9:3099.
39. Stintzing S, Modest DP, Rossius L, Lerch MM, von Weikersthal LF, Decker T, Kiani A, Vehling-Kaiser U, Al-Batran SE, Heintges T, Lerchenmüller C. FOLFIRI plus cetuximab versus FOLFIRI plus bevacizumab for metastatic colorectal cancer (FIRE-3): a post-hoc analysis of tumour dynamics in the final RAS wild-type subgroup of this randomised open-label phase 3 trial. The Lancet Oncology. 2016 Oct 1;17(10):1426-34.
40. Rivera F, Karthaus M, Hecht JR, Sevilla I, Forget F, Fasola G, Canon JL, Guan X, Demonty G, Schwartzberg LS. Final analysis of the randomised PEAK trial: overall survival and tumour responses during first-line treatment with

mFOLFOX6 plus either panitumumab or bevacizumab in patients with metastatic colorectal carcinoma. International journal of colorectal disease. 2017 Aug 1;32(8):1179-90.
41. Venook AP, Niedzwiecki D, Lenz HJ, Innocenti F, Fruth B, Meyerhardt JA, Schrag D, Greene C, O'Neil BH, Atkins JN, Berry S. Effect of first-line chemotherapy combined with cetuximab or bevacizumab on overall survival in patients with KRAS wild-type advanced or metastatic colorectal cancer: a randomized clinical trial. Jama. 2017 Jun 20;317(23):2392-401.
42. Bennouna J, Sastre J, Arnold D, Österlund P, Greil R, Van Cutsem E, von Moos R, Viéitez JM, Bouché O, Borg C, Steffens CC. Continuation of bevacizumab after first progression in metastatic colorectal cancer (ML18147): a randomised phase 3 trial. The lancet oncology. 2013 Jan 1;14(1):29-37.
43. Tabernero J, Yoshino T, Cohn AL, Obermannova R, Bodoky G, Garcia-Carbonero R, Ciuleanu TE, Portnoy DC, Van Cutsem E, Grothey A, Prausová J. Ramucirumab versus placebo in combination with second-line FOLFIRI in patients with metastatic colorectal carcinoma that progressed during or after first-line therapy with bevacizumab, oxaliplatin, and a fluoropyrimidine (RAISE): a randomised, double-blind, multicentre, phase 3 study. The Lancet Oncology. 2015 May 1;16(5):499-508.
44. Tabernero J, Van Cutsem E, Lakomý R, Prausová J, Ruff P, van Hazel GA, Moiseyenko VM, Ferry DR, McKendrick JJ, Soussan-Lazard K, Chevalier S. Aflibercept versus placebo in combination with fluorouracil, leucovorin and irinotecan in the treatment of previously treated metastatic colorectal cancer: prespecified subgroup analyses from the VELOUR trial. European journal of cancer. 2014 Jan 1;50(2):320-31.
45. Ciardiello F, Normanno N, Martinelli E, Troiani T, Pisconti S, Cardone C, Nappi A, Bordonaro AR, Rachiglio M, Lambiase M, Latiano TP. Cetuximab continuation after first progression in metastatic colorectal cancer (CAPRI-GOIM): a randomized phase II trial of FOLFOX plus cetuximab versus FOLFOX. Annals of Oncology. 2016 Mar 21;27(6):1055-61.
46. Siravegna G, Mussolin B, Buscarino M, Corti G, Cassingena A, Crisafulli G, Ponzetti A, Cremolini C, Amatu A, Lauricella C, Lamba S. Clonal evolution and resistance to EGFR blockade in the blood of colorectal cancer patients. Nature medicine. 2015 Jul;21(7):795.
47. Grothey A, Van Cutsem E, Sobrero A, Siena S, Falcone A, Ychou M, Humblet Y, Bouché O, Mineur L, Barone C, Adenis A. Regorafenib monotherapy for previously treated metastatic colorectal cancer (CORRECT): an international, multicentre, randomised, placebo-controlled, phase 3 trial. The Lancet. 2013 Jan 26;381(9863):303-12.
48. Li J, Qin S, Xu R, Yau TC, Ma B, Pan H, Xu J, Bai Y, Chi Y, Wang L, Yeh KH. Regorafenib plus best supportive care versus placebo plus best supportive care in Asian patients with previously treated metastatic colorectal cancer (CONCUR): a randomised, double-blind, placebo-controlled, phase 3 trial. The Lancet Oncology. 2015 Jun 1;16(6):619-29.
49. Mayer RJ, Van Cutsem E, Falcone A, Yoshino T, Garcia-Carbonero R, Mizunuma N, Yamazaki K, Shimada Y, Tabernero J, Komatsu Y, Sobrero A. Randomized trial of TAS-102 for refractory metastatic colorectal cancer. New England Journal of Medicine. 2015 May 14;372(20):1909-19.
50. Managing advanced and metastatic colorectal cancer. Available at: https://pathways.nice.org.uk/pathways/colorectal-cancer#path=view%3A/pathways/colorectal-cancer/managing-advanced-and-metastatic-colorectal-cancer.xml&content=view-index Last access: 01/04/2019
51. Thomas DM, Zalcberg JR. 5-Fluorouracil: A pharmacological paradigm in the use of cytotoxics. Clinical and experimental pharmacology and physiology. 1998 Nov;25(11):887-95.

52. BC Cancer Agency. BCCA cancer drug manual. Revised Edition 2019
53. Seetharam RN, Sood A, Goel S. Oxaliplatin: pre-clinical perspectives on the mechanisms of action, response and resistance. ecancermedicalscience. 2009;3.
54. Vanhoefer U, Harstrick A, Achterrath W, Cao S, Seeber S, Rustum YM. Irinotecan in the treatment of colorectal cancer: clinical overview. Journal of Clinical Oncology. 2001 Mar 1;19(5):1501-18.
55. Burness CB, Duggan ST. Trifluridine/tipiracil: a review in metastatic colorectal cancer. Drugs. 2016 Sep 1;76(14):1393-402.
56. Paz MM, Zhang X, Lu J, Holmgren A. A new mechanism of action for the anticancer drug mitomycin C: mechanism-based inhibition of thioredoxin reductase. Chemical research in toxicology. 2012 Jun 25;25(7):1502-11.
57. Zhang J, FG Stevens M, D Bradshaw T. Temozolomide: mechanisms of action, repair and resistance. Current molecular pharmacology. 2012 Jan 1;5(1):102-14.
58. Van Cutsem E, Cunningham D, Maroun J, Cervantes A, Glimelius B. Raltitrexed: current clinical status and future directions. Annals of oncology. 2002 Apr 1;13(4):513-22.
59. Kazazi-Hyseni F, Beijnen JH, Schellens JH. Bevacizumab. The oncologist. 2010 Aug 5.
60. Patel A, Sun W. Ziv-aflibercept in metastatic colorectal cancer. Biologics: targets & therapy. 2014;8:13.
61. Verdaguer H, Tabernero J, Macarulla T. Ramucirumab in metastatic colorectal cancer: evidence to date and place in therapy. Therapeutic advances in medical oncology. 2016 May;8(3):230-42.
62. Carter NJ. Regorafenib: a review of its use in previously treated patients with progressive metastatic colorectal cancer. Drugs & aging. 2014 Jan 1;31(1):67-78.
63. Blick SK, Scott LJ. Cetuximab. Drugs. 2007 Dec 1;67(17):2585-607.
64. Messersmith WA, Hidalgo M. Panitumumab, a Monoclonal Anti–Epidermal Growth Factor Receptor Antibody in Colorectal Cancer: Another One or the One?. Clinical Cancer Research. 2007 Aug 15;13(16):4664-6.
65. McDermott J, Jimeno A. Pembrolizumab: PD-1 inhibition as a therapeutic strategy in cancer. Drugs of today (Barcelona, Spain: 1998). 2015 Jan;51(1):7-20.
66. Guo L, Zhang H, Chen B. Nivolumab as programmed death-1 (PD-1) inhibitor for targeted immunotherapy in tumor. Journal of Cancer. 2017;8(3):410.
67. Tarhini A, Lo E, Minor DR. Releasing the brake on the immune system: ipilimumab in melanoma and other tumors. Cancer biotherapy & radiopharmaceuticals. 2010 Dec 1;25(6):601-13.
68. Chaney SG, Campbell SL, Bassett E, Wu Y. Recognition and processing of cisplatin-and oxaliplatin-DNA adducts. Critical reviews in oncology/hematology. 2005 Jan 1;53(1):3-11.
69. Diaz-Rubio E, Sastre J, Zaniboni A, Labianca R, Cortes-Funes H, De Braud F, Boni C, Benavides M, Dallavalle G, Homerin M. Oxaliplatin as single agent in previously untreated colorectal carcinoma patients: a phase II multicentric study. Annals of Oncology. 1998 Jan 1;9(1):105-8.
70. Chong G, Dickson JL, Cunningham D, Norman AR, Rao S, Hill ME, Price TJ, Oates J, Tebbutt N. Capecitabine and mitomycin C as third-line therapy for patients with metastatic colorectal cancer resistant to fluorouracil and irinotecan. British journal of cancer. 2005 Sep;93(5):510.
71. Liao D, Johnson RS. Hypoxia: a key regulator of angiogenesis in cancer. Cancer and Metastasis Reviews. 2007 Jun 1;26(2):281-90.
72. Mulcahy MF. Bevacizumab in the therapy for refractory metastatic colorectal cancer. Biologics: targets & therapy. 2008 Mar;2(1):53.

73. Van Cutsem E, Tabernero J, Lakomy R, Prenen H, Prausová J, Macarulla T, Ruff P, Van Hazel GA, Moiseyenko V, Ferry D, McKendrick J. Addition of aflibercept to fluorouracil, leucovorin, and irinotecan improves survival in a phase III randomized trial in patients with metastatic colorectal cancer previously treated with an oxaliplatin-based regimen. J Clin Oncol. 2012 Oct 1;30(28):3499-506.
74. Tabernero J, Yoshino T, Cohn AL, Obermannova R, Bodoky G, Garcia-Carbonero R, Ciuleanu TE, Portnoy DC, Van Cutsem E, Grothey A, Prausová J. Ramucirumab versus placebo in combination with second-line FOLFIRI in patients with metastatic colorectal carcinoma that progressed during or after first-line therapy with bevacizumab, oxaliplatin, and a fluoropyrimidine (RAISE): a randomised, double-blind, multicentre, phase 3 study. The Lancet Oncology. 2015 May 1;16(5):499-508.
75. Ellis LM. Mechanisms of action of bevacizumab as a component of therapy for metastatic colorectal cancer. InSeminars in oncology 2006 Oct 1 (Vol. 33, pp. S1-S7). WB Saunders.
76. de Aguiar RB, de Moraes JZ. Exploring the Immunological Mechanisms Underlying the Anti-vascular Endothelial Growth Factor Activity in Tumors. Frontiers in immunology. 2019;10.
77. Dalerba P, Maccalli C, Casati C, Castelli C, Parmiani G. Immunology and immunotherapy of colorectal cancer. Critical reviews in oncology/hematology. 2003 Apr 1;46(1):33-57.
78. Le DT, Uram JN, Wang H, Bartlett BR, Kemberling H, Eyring AD, Skora AD, Luber BS, Azad NS, Laheru D, Biedrzycki B. PD-1 blockade in tumors with mismatch-repair deficiency. New England Journal of Medicine. 2015 Jun 25;372(26):2509-20.
79. Schumacher TN, Schreiber RD. Neoantigens in cancer immunotherapy. Science. 2015 Apr 3;348(6230):69-74.
80. Jo WS, Carethers JM. Chemotherapeutic implications in microsatellite unstable colorectal cancer 1. Cancer Biomarkers. 2006 Jan 1;2(1-2):51-60.
81. Carethers JM, Smith EJ, Behling CA, Nguyen L, Tajima A, Doctolero RT, Cabrera BL, Goel A, Arnold CA, Miyai K, Boland CR. Use of 5-fluorouracil and survival in patients with microsatellite-unstable colorectal cancer. Gastroenterology. 2004 Feb 1;126(2):394-401.
82. Tournigand C, André T, Achille E, Lledo G, Flesh M, Mery-Mignard D, Quinaux E, Couteau C, Buyse M, Ganem G, Landi B. FOLFIRI followed by FOLFOX6 or the reverse sequence in advanced colorectal cancer: a randomized GERCOR study. Journal of Clinical Oncology. 2004 Jan 15;22(2):229-37.
83. Cunningham D, Lang I, Marcuello E, Lorusso V, Ocvirk J, Shin DB, Jonker D, Osborne S, Andre N, Waterkamp D, Saunders MP. Bevacizumab plus capecitabine versus capecitabine alone in elderly patients with previously untreated metastatic colorectal cancer (AVEX): an open-label, randomised phase 3 trial. The lancet oncology. 2013 Oct 1;14(11):1077-85.
84. Sobrero AF, Maurel J, Fehrenbacher L, Scheithauer W, Abubakr YA, Lutz MP, Vega-Villegas ME, Eng C, Steinhauer EU, Prausova J, Lenz HJ. EPIC: phase III trial of cetuximab plus irinotecan after fluoropyrimidine and oxaliplatin failure in patients with metastatic colorectal cancer. Journal of clinical oncology. 2008 May 10;26(14):2311-9.
85. Pietrantonio F, Lobefaro R, Antista M, Lonardi S, Raimondi A, Morano F, Mosconi S, Rimassa L, Murgioni S, Sartore-Bianchi A, Tomasello G. Capecitabine and temozolomide versus FOLFIRI in RAS mutated, MGMT methylated metastatic colorectal cancer. Clinical Cancer Research. 2019 Jan 1.
86. Overman MJ, Lonardi S, Wong KY, Lenz HJ, Gelsomino F, Aglietta M, Morse MA, Van Cutsem E, McDermott R, Hill A, Sawyer MB. Durable clinical benefit

with nivolumab plus ipilimumab in DNA mismatch repair-deficient/microsatellite instability-high metastatic colorectal cancer.
87. Saltz LB, Clarke S, Díaz-Rubio E, Scheithauer W, Figer A, Wong R, Koski S, Lichinitser M, Yang TS, Rivera F, Couture F. Bevacizumab in combination with oxaliplatin-based chemotherapy as first-line therapy in metastatic colorectal cancer: a randomized phase III study. Journal of clinical oncology. 2008 Apr 20;26(12):2013-9.
88. Bokemeyer C, Bondarenko I, Hartmann JT, De Braud F, Schuch G, Zubel A, Celik I, Schlichting M, Koralewski P. Efficacy according to biomarker status of cetuximab plus FOLFOX-4 as first-line treatment for metastatic colorectal cancer: the OPUS study. Annals of Oncology. 2011 Jan 12;22(7):1535-46.
89. Heinemann V, von Weikersthal LF, Decker T, Kiani A, Vehling-Kaiser U, Al-Batran SE, Heintges T, Lerchenmüller C, Kahl C, Seipelt G, Kullmann F. FOLFIRI plus cetuximab versus FOLFIRI plus bevacizumab as first-line treatment for patients with metastatic colorectal cancer (FIRE-3): a randomised, open-label, phase 3 trial. The lancet oncology. 2014 Sep 1;15(10):1065-75.
90. Stintzing S, Fischer von Weikersthal L, Decker T, Vehling-Kaiser U, Jäger E, Heintges T, Stoll C, Giessen C, Modest DP, Neumann J, Jung A. FOLFIRI plus cetuximab versus FOLFIRI plus bevacizumab as first-line treatment for patients with metastatic colorectal cancer–subgroup analysis of patients with KRAS: mutated tumours in the randomised German AIO study KRK-0306. Annals of oncology. 2012 Jan 4;23(7):1693-9.
91. Falcone A, Ricci S, Brunetti I, Pfanner E, Allegrini G, Barbara C, Crino L, Benedetti G, Evangelista W, Fanchini L, Cortesi E. Phase III trial of infusional fluorouracil, leucovorin, oxaliplatin, and irinotecan (FOLFOXIRI) compared with infusional fluorouracil, leucovorin, and irinotecan (FOLFIRI) as first-line treatment for metastatic colorectal cancer: the Gruppo Oncologico Nord Ovest. Journal of Clinical Oncology. 2007 May 1;25(13):1670-6.
92. Loupakis F, Cremolini C, Masi G, Lonardi S, Zagonel V, Salvatore L, Cortesi E, Tomasello G, Ronzoni M, Spadi R, Zaniboni A. Initial therapy with FOLFOXIRI and bevacizumab for metastatic colorectal cancer. New England Journal of Medicine. 2014 Oct 23;371(17):1609-18.
93. Modest DP, Martens UM, Riera-Knorrenschild J, Greeve J, Florschütz A, Wessendorf S, Ettrich T, Kanzler S, Nörenberg D, Ricke J, Seidensticker M. FOLFOXIRI Plus Panitumumab As First-Line Treatment of RAS Wild-Type Metastatic Colorectal Cancer: The Randomized, Open-Label, Phase II VOLFI Study (AIO KRK0109). Journal of Clinical Oncology. 2019 Oct 14;37(35):3401-11.
94. Luo ZW, Zhu MG, Zhang ZQ, Ye FJ, Huang WH, Luo XZ. Increased expression of Ki-67 is a poor prognostic marker for colorectal cancer patients: a meta analysis. BMC cancer. 2019 Dec;19(1):123.
95. Fluge Ø, Gravdal K, Carlsen E, Vonen B, Kjellevold K, Refsum S, Lilleng R, Eide TJ, Halvorsen TB, Tveit KM, Otte AP. Expression of EZH2 and Ki-67 in colorectal cancer and associations with treatment response and prognosis. British journal of cancer. 2009 Oct;101(8):1282-9.
96. van Kuilenburg AB, Haasjes J, Richel DJ, Zoetekouw L, Van Lenthe H, De Abreu RA, Maring JG, Vreken P, van Gennip AH. Clinical implications of dihydropyrimidine dehydrogenase (DPD) deficiency in patients with severe 5-fluorouracil-associated toxicity: identification of new mutations in the DPD gene. Clinical Cancer Research. 2000 Dec 1;6(12):4705-12.
97. Fujita KI. Cytochrome P450 and anticancer drugs. Current drug metabolism. 2006 Jan 1;7(1):23-37.
98. Etienne-Grimaldi MC, Milano G, Maindrault-Gœbel F, Chibaudel B, Formento JL, Francoual M, Lledo G, André T, Mabro M, Mineur L, Flesch M. Methylenetetrahydrofolate reductase (MTHFR) gene polymorphisms and

FOLFOX response in colorectal cancer patients. British journal of clinical pharmacology. 2010 Jan;69(1):58-66.
99. Lenz HJ. Pharmacogenomics and colorectal cancer. Annals of oncology. 2004 Oct 1;15:iv173-7.
100. Le DT, Uram JN, Wang H, Bartlett B, Kemberling H, Eyring A, Azad NS, Laheru D, Donehower RC, Crocenzi TS, Goldberg RM. Programmed death-1 blockade in mismatch repair deficient colorectal cancer. Journal of Clinical Oncology. 2016; 34: 103
101. Overman MJ, McDermott R, Leach JL, Lonardi S, Lenz HJ, Morse MA, Desai J, Hill A, Axelson M, Moss RA, Goldberg MV. Nivolumab in patients with metastatic DNA mismatch repair-deficient or microsatellite instability-high colorectal cancer (CheckMate 142): an open-label, multicentre, phase 2 study. The Lancet Oncology. 2017 Sep 1;18(9):1182-91.
102. Ganesh K, Stadler ZK, Cercek A, Mendelsohn RB, Shia J, Segal NH, Diaz LA. Immunotherapy in colorectal cancer: rationale, challenges and potential. Nature Reviews Gastroenterology & Hepatology. 2019 Mar 18:1.
103. Lenz HJ, Van Cutsem E, Limon ML, Wong KY, Hendlisz A, Aglietta M, Garcia-Alfonso P, Neyns B, Luppi G, Cardin D, Dragovich T. LBA18_PR Durable clinical benefit with nivolumab (NIVO) plus low-dose ipilimumab (IPI) as first-line therapy in microsatellite instability-high/mismatch repair deficient (MSI-H/dMMR) metastatic colorectal cancer (mCRC). Annals of Oncology. 2018 Oct 1;29(suppl_8):mdy424-019.
104. Chalabi M, Fanchi LF, Van den Berg JG, Beets GL, Lopez-Yurda M, Aalbers AG, Grootscholten C, Snaebjornsson P, Maas M, Mertz M, Nuijten E. LBA37_PR Neoadjuvant ipilimumab plus nivolumab in early stage colon cancer. Annals of Oncology. 2018 Oct 1;29(suppl_8):mdy424-047.
105. Sartore-Bianchi A, Trusolino L, Martino C, Bencardino K, Lonardi S, Bergamo F, Zagonel V, Leone F, Depetris I, Martinelli E, Troiani T. Dual-targeted therapy with trastuzumab and lapatinib in treatment-refractory, KRAS codon 12/13 wild-type, HER2-positive metastatic colorectal cancer (HERACLES): a proof-of-concept, multicentre, open-label, phase 2 trial. The Lancet Oncology. 2016 Jun 1;17(6):738-46.
106. Meric-Bernstam F, Hurwitz H, Raghav KP, McWilliams RR, Fakih M, VanderWalde A, Swanton C, Kurzrock R, Burris H, Sweeney C, Bose R. Pertuzumab plus trastuzumab for HER2-amplified metastatic colorectal cancer (MyPathway): an updated report from a multicentre, open-label, phase 2a, multiple basket study. The Lancet Oncology. 2019 Mar 8.
107. Jonker DJ, Nott L, Yoshino T, Gill S, Shapiro J, Ohtsu A, Zalcberg J, Vickers MM, Wei AC, Gao Y, Tebbutt NC. Napabucasin versus placebo in refractory advanced colorectal cancer: a randomised phase 3 trial. The Lancet Gastroenterology & Hepatology. 2018 Apr 1;3(4):263-70.
108. Van Cutsem E, Yoshino T, Lenz HJ, Lonardi S, Falcone A, Limón ML, Saunders M, Sobrero A, Park YS, Ferreiro R, Hong YS. Nintedanib for the treatment of patients with refractory metastatic colorectal cancer (LUME-Colon 1): a phase III, international, randomized, placebo-controlled study. Annals of Oncology. 2018 Jul 13;29(9):1955-63.
109. Bendell J, Ciardiello F, Tabernero J, Tebbutt N, Eng C, Di Bartolomeo M, Falcone A, Fakih M, Kozloff M, Segal N, Sobrero A. LBA-004 efficacy and safety results from IMblaze370, a randomised Phase III study comparing atezolizumab+ cobimetinib and atezolizumab monotherapy vs regorafenib in chemotherapy-refractory metastatic colorectal cancer. Annals of Oncology. 2018 Jun 1;29(suppl_5):mdy208-003.
110. Ebert PJ, Cheung J, Yang Y, McNamara E, Hong R, Moskalenko M, Gould SE, Maecker H, Irving BA, Kim JM, Belvin M. MAP kinase inhibition promotes T

cell and anti-tumor activity in combination with PD-L1 checkpoint blockade. Immunity. 2016 Mar 15;44(3):609-21.
111. Bendell JC, Bang YJ, Chee CE, Ryan DP, McRee AJ, Chow LQ, Desai J, Wongchenko M, Yan Y, Pitcher B, Foster P. A phase Ib study of safety and clinical activity of atezolizumab (A) and cobimetinib (C) in patients (pts) with metastatic colorectal cancer (mCRC).
112. Grothey A, Tabernero J, Arnold D, De Gramont A, Ducreux MP, O'Dwyer PJ, Van Cutsem E, Bosanac I, Srock S, Mancao C, Gilberg F. LBA19 Fluoropyrimidine (FP)+ bevacizumab (BEV)+ atezolizumab vs FP/BEV in BRAFwt metastatic colorectal cancer (mCRC): Findings from Cohort 2 of MODUL–a multicentre, randomized trial of biomarker-driven maintenance treatment following first-line induction therapy. Annals of Oncology. 2018 Oct 1;29(suppl_8):mdy424-020.
113. Fisher R, Pusztai L, Swanton C. Cancer heterogeneity: implications for targeted therapeutics. British journal of cancer. 2013 Feb;108(3):479.
114. Cancer Genome Atlas Network. Comprehensive molecular characterization of human colon and rectal cancer. Nature. 2012 Jul;487(7407):330.
115. Dunne PD, McArt DG, Bradley CA, O'Reilly PG, Barrett HL, Cummins R, O'Grady T, Arthur K, Loughrey MB, Allen WL, McDade SS. Challenging the cancer molecular stratification dogma: intratumoral heterogeneity undermines consensus molecular subtypes and potential diagnostic value in colorectal cancer. Clinical Cancer Research. 2016 Aug 15;22(16):4095-104.
116. Joung JG, Oh BY, Hong HK, Al-Khalidi H, Al-Alem F, Lee HO, Bae JS, Kim J, Cha HU, Alotaibi M, Cho YB. Tumor heterogeneity predicts metastatic potential in colorectal cancer. Clinical Cancer Research. 2017 Dec 1;23(23):7209-16.
117. Bhullar DS, Barriuso J, Mullamitha S, Saunders MP, O'Dwyer ST, Aziz O. Biomarker concordance between primary colorectal cancer and its metastases. EBioMedicine. 2019 Feb 1;40:363-74.
118. Kamal Y, Schmit SL, Hoehn HJ, Amos CI, Frost HR. Transcriptomic differences between primary colorectal adenocarcinomas and distant metastases reveal metastatic colorectal cancer subtypes. Cancer research. 2019 Jan 1:canres-3945.
119. Davis A, Gao R, Navin N. Tumor evolution: Linear, branching, neutral or punctuated?. Biochimica et Biophysica Acta (BBA)-Reviews on Cancer. 2017 Apr 1;1867(2):151-61.
120. Sottoriva A, Kang H, Ma Z, Graham TA, Salomon MP, Zhao J, Marjoram P, Siegmund K, Press MF, Shibata D, Curtis C. A Big Bang model of human colorectal tumor growth. Nature genetics. 2015 Mar;47(3):209.
121. Le DT, Durham JN, Smith KN, Wang H, Bartlett BR, Aulakh LK, Lu S, Kemberling H, Wilt C, Luber BS, Wong F. Mismatch repair deficiency predicts response of solid tumors to PD-1 blockade. Science. 2017 Jul 28;357(6349):409-13.
122. Sun D, Dalin S, Hemann MT, Lauffenburger DA, Zhao B. Differential selective pressure alters rate of drug resistance acquisition in heterogeneous tumor populations. Scientific reports. 2016 Nov 7;6:36198.
123. Dancey JE, Dobbin KK, Groshen S, Jessup JM, Hruszkewycz AH, Koehler M, Parchment R, Ratain MJ, Shankar LK, Stadler WM, True LD. Guidelines for the development and incorporation of biomarker studies in early clinical trials of novel agents. Clinical cancer research. 2010 Mar 15;16(6):1745-55.
124. Sinicrope FA, Foster NR, Thibodeau SN, Marsoni S, Monges G, Labianca R, Yothers G, Allegra C, Moore MJ, Gallinger S, Sargent DJ. DNA mismatch repair status and colon cancer recurrence and survival in clinical trials of 5-fluorouracil-based adjuvant therapy. Journal of the National Cancer Institute. 2011 May 19;103(11):863-75.

125. Venderbosch S, Nagtegaal ID, Maughan TS, Smith CG, Cheadle JP, Fisher D, Kaplan R, Quirke P, Seymour MT, Richman SD, Meijer GA. Mismatch repair status and BRAF mutation status in metastatic colorectal cancer patients: a pooled analysis of the CAIRO, CAIRO2, COIN, and FOCUS studies. Clinical Cancer Research. 2014 Oct 15;20(20):5322-30.
126. Ursem C, Atreya CE, Van Loon K. Emerging treatment options for BRAF-mutant colorectal cancer. Gastrointestinal cancer: targets and therapy. 2018;8:13.
127. Dummer R, Hauschild A, Lindenblatt N, Pentheroudakis G, Keilholz U. Cutaneous melanoma: ESMO Clinical Practice Guidelines for diagnosis, treatment and follow-up. Annals of Oncology. 2015 Aug 25;26(suppl_5):v126-32.
128. Prahallad A, Sun C, Huang S, Di Nicolantonio F, Salazar R, Zecchin D, Beijersbergen RL, Bardelli A, Bernards R. Unresponsiveness of colon cancer to BRAF (V600E) inhibition through feedback activation of EGFR. Nature. 2012 Mar;483(7387):100.
129. Corcoran RB, Ebi H, Turke AB, Coffee EM, Nishino M, Cogdill AP, Brown RD, Della Pelle P, Dias-Santagata D, Hung KE, Flaherty KT. EGFR-mediated reactivation of MAPK signaling contributes to insensitivity of BRAF-mutant colorectal cancers to RAF inhibition with vemurafenib. Cancer discovery. 2012 Mar 1;2(3):227-35.
130. Van Cutsem E, Huijberts S, Grothey A, Yaeger R, Cuyle PJ, Elez E, Fakih M, Montagut C, Peeters M, Yoshino T, Wasan H. Binimetinib, Encorafenib, and Cetuximab Triplet Therapy for Patients With BRAF V600E–Mutant Metastatic Colorectal Cancer: Safety Lead-In Results From the Phase III BEACON Colorectal Cancer Study. Journal of Clinical Oncology. 2019 Mar 20:JCO-18.
131. Rimbert J, Tachon G, Junca A, Villalva C, Karayan-Tapon L, Tougeron D. Association between clinicopathological characteristics and RAS mutation in colorectal cancer. Modern Pathology. 2018 Mar;31(3):517.
132. Ryan MB, Corcoran RB. Therapeutic strategies to target RAS-mutant cancers. Nature reviews Clinical oncology. 2018 Oct 1:1.
133. Dienstmann R, Salazar R, Tabernero J. Molecular Subtypes and the Evolution of Treatment Decisions in Metastatic Colorectal Cancer. American Society of Clinical Oncology Educational Book. 2018 May 23;38:231-8.
134. Tabernero J, Baselga J. Multigene assays to improve assessment of recurrence risk and benefit from chemotherapy in early-stage colon cancer: has the time finally arrived, or are we still stage locked?.
135. Golub TR, Slonim DK, Tamayo P, Huard C, Gaasenbeek M, Mesirov JP, Coller H, Loh ML, Downing JR, Caligiuri MA, Bloomfield CD. Molecular classification of cancer: class discovery and class prediction by gene expression monitoring. science. 1999 Oct 15;286(5439):531-7.
136. O'Connell MJ, Yothers G, Paik S, Lavery I, Cowens JW, Clark-Langone KM, Lopatin M, Hackett J, Baehner FL, Wolmark N. Relationship between tumor gene expression and recurrence in patients with stage II/III colon cancer treated with surgery+ 5-FU/LV in NSABP C-06: Consistency of results with two other independent studies. InAmerican Society of Clinical Oncology 2008 Gastrointestinal Cancers Symposium 2008 Jan 25.
137. Salazar R, Roepman P, Capella G, Moreno V, Simon I, Dreezen C, Lopez-Doriga A, Santos C, Marijnen C, Westerga J, Bruin S. Gene expression signature to improve prognosis prediction of stage II and III colorectal cancer. J Clin Oncol. 2011 Jan 1;29(1):17-24.
138. Kennedy RD, Bylesjo M, Kerr P, Davison T, Black JM, Kay EW, Holt RJ, Proutski V, Ahdesmaki M, Farztdinov V, Goffard N. Development and independent validation of a prognostic assay for stage II colon cancer using

formalin-fixed paraffin-embedded tissue. Journal of Clinical Oncology. 2011 Nov 7;29(35):4620-6.
139. Sadanandam A, Lyssiotis CA, Homicsko K, Collisson EA, Gibb WJ, Wullschleger S, Ostos LC, Lannon WA, Grotzinger C, Del Rio M, Lhermitte B. A colorectal cancer classification system that associates cellular phenotype and responses to therapy. Nature medicine. 2013 May;19(5):619.
140. Medico E, Russo M, Picco G, Cancelliere C, Valtorta E, Corti G, Buscarino M, Isella C, Lamba S, Martinoglio B, Veronese S. The molecular landscape of colorectal cancer cell lines unveils clinically actionable kinase targets. Nature communications. 2015 Apr 30;6:7002.
141. Felipe De Sousa EM, Wang X, Jansen M, Fessler E, Trinh A, De Rooij LP, De Jong JH, De Boer OJ, Van Leersum R, Bijlsma MF, Rodermond H. Poor-prognosis colon cancer is defined by a molecularly distinct subtype and develops from serrated precursor lesions. Nature medicine. 2013 May;19(5):614.
142. Sadanandam A, Wang X, de Sousa E Melo F, Gray JW, Vermeulen L, Hanahan D, Medema JP. Reconciliation of classification systems defining molecular subtypes of colorectal cancer: interrelationships and clinical implications. Cell cycle. 2014 Feb 1;13(3):353-7.
143. Marisa L, de Reyniès A, Duval A, Selves J, Gaub MP, Vescovo L, Etienne-Grimaldi MC, Schiappa R, Guenot D, Ayadi M, Kirzin S. Gene expression classification of colon cancer into molecular subtypes: characterization, validation, and prognostic value. PLoS medicine. 2013 May 21;10(5):e1001453.
144. Roepman P, Schlicker A, Tabernero J, Majewski I, Tian S, Moreno V, Snel MH, Chresta CM, Rosenberg R, Nitsche U, Macarulla T. Colorectal cancer intrinsic subtypes predict chemotherapy benefit, deficient mismatch repair and epithelial-to-mesenchymal transition. International journal of cancer. 2014 Feb 1;134(3):552-62.
145. Schlicker A, Beran G, Chresta CM, McWalter G, Pritchard A, Weston S, Runswick S, Davenport S, Heathcote K, Castro DA, Orphanides G. Subtypes of primary colorectal tumors correlate with response to targeted treatment in colorectal cell lines. BMC medical genomics. 2012 Dec;5(1):66.
146. Budinska E, Popovici V, Tejpar S, D'ario G, Lapique N, Sikora KO, Di Narzo AF, Yan P, Hodgson JG, Weinrich S, Bosman F. Gene expression patterns unveil a new level of molecular heterogeneity in colorectal cancer. The Journal of pathology. 2013 Sep;231(1):63-76.
147. Fontana E, Homicsko K, Eason K, Sadanandam A. Molecular Classification of Colon Cancer: Perspectives for Personalized Adjuvant Therapy. Current Colorectal Cancer Reports. 2016 Dec 1;12(6):296-302.
148. Guinney J, Dienstmann R, Wang X, De Reyniès A, Schlicker A, Soneson C, Marisa L, Roepman P, Nyamundanda G, Angelino P, Bot BM. The consensus molecular subtypes of colorectal cancer. Nature medicine. 2015 Nov;21(11):1350.
149. Lenz HJ, Ou FS, Venook AP, Hochster HS, Niedzwiecki D, Goldberg RM, Mayer RJ, Bertagnolli MM, Blanke CD, Zemla T, Qu X. Impact of Consensus Molecular Subtype on Survival in Patients With Metastatic Colorectal Cancer: Results From CALGB/SWOG 80405 (Alliance). Journal of Clinical Oncology. 2019 Apr:JCO-18.
150. Stintzing S, Wirapati P, Lenz HJ, Neureiter D, Fischer von Weikersthal L, Decker T, Kiani A, Vehling-Kaiser U, Al-Batran SE, Heintges T, Kahl C. Consensus molecular subgroups (CMS) of colorectal cancer (CRC) and first-line efficacy of FOLFIRI plus cetuximab or bevacizumab in the FIRE3 (AIO KRK-0306) trial. Journal of Clinical Oncology 35, no. 15_suppl (May 20 2017) 3510-3510

151. Mooi JK, Wirapati P, Asher R, Lee CK, Savas PS, Price TJ, Townsend A, Hardingham J, Buchanan D, Williams D, Tejpar S. The prognostic impact of Consensus Molecular Subtypes (CMS) and its predictive effects for bevacizumab benefit in metastatic colorectal cancer: molecular analysis of the AGITG MAX clinical trial. Annals of Oncology. 2018 Sep 21.
152. Marisa L, Ayadi M, Balogoun R, Pilati C, Le Malicot K, Lepage C, Emile JF, Salazar R, Aust DE, Duval A, Selves J. Clinical utility of colon cancer molecular subtypes: Validation of two main colorectal molecular classifications on the PETACC-8 phase III trial cohort. Journal of Clinical Oncology 35, no. 15_suppl (May 20 2017) 3509-3509
153. Fontana E, Eason K, Cervantes A, Salazar R, Sadanandam A. Context matters—consensus molecular subtypes of colorectal cancer as biomarkers for clinical trials. Annals of Oncology. 2019 Feb 23;30(4):520-7.
154. Ragulan C, Eason K, Fontana E, Nyamundanda G, Tarazona N, Patil Y, Poudel P, Lawlor RT, Del Rio M, Koo SL, Tan WS. Analytical validation of multiplex biomarker assay to stratify colorectal cancer into molecular subtypes. Scientific reports. 2019 May 21;9(1):1-2.
155. Wallden B, Storhoff J, Nielsen T, Dowidar N, Schaper C, Ferree S, Liu S, Leung S, Geiss G, Snider J, Vickery T. Development and verification of the PAM50-based Prosigna breast cancer gene signature assay. BMC medical genomics. 2015 Dec;8(1):54.
156. Perou CM, Sørlie T, Eisen MB, Van De Rijn M, Jeffrey SS, Rees CA, Pollack JR, Ross DT, Johnsen H, Akslen LA, Fluge Ø. Molecular portraits of human breast tumours. nature. 2000 Aug;406(6797):747.
157. Scott DW, Wright GW, Williams PM, Lih CJ, Walsh W, Jaffe ES, Rosenwald A, Campo E, Chan WC, Connors JM, Smeland EB. Determining cell-of-origin subtypes of diffuse large B-cell lymphoma using gene expression in formalin-fixed paraffin-embedded tissue. Blood. 2014 Feb 20;123(8):1214-7.
158. Northcott PA, Shih DJ, Remke M, Cho YJ, Kool M, Hawkins C, Eberhart CG, Dubuc A, Guettouche T, Cardentey Y, Bouffet E. Rapid, reliable, and reproducible molecular sub-grouping of clinical medulloblastoma samples. Acta neuropathologica. 2012 Apr 1;123(4):615-26.
159. Available at: https://www.nanostring.com/ Last access: 11 July 2019
160. Tibshirani R, Hastie T, Narasimhan B, Chu G. Diagnosis of multiple cancer types by shrunken centroids of gene expression. Proceedings of the National Academy of Sciences. 2002 May 14;99(10):6567-72.
161. Van Dongen S. Graph clustering via a discrete uncoupling process. SIAM Journal on Matrix Analysis and Applications. 2008 Feb 20;30(1):121-41.
162. Breiman L. Random forests. Machine learning. 2001 Oct 1;45(1):5-32.
163. Lausser L, Schmid F, Schirra LR, Wilhelm AF, Kestler HA. Rank-based classifiers for extremely high-dimensional gene expression data. Advances in Data Analysis and Classification. 2018 Dec 1;12(4):917-36.
164. Piskol R, Huw L, Sergin I, Kljin C, Modrusan Z, Kim D, Kljavin N, Tam R, Patel R, Burton J, Penuel E. A Clinically Applicable Gene-Expression Classifier Reveals Intrinsic and Extrinsic Contributions to Consensus Molecular Subtypes in Primary and Metastatic Colon Cancer. Clinical Cancer Research. 2019 Jul 15;25(14):4431-42.
165. Teufel M, Schwenke S, Seidel H, Beckmann G, Reischl J, Vonk R, Lenz HJ, Tabernero J, Siena S, Grothey A, Van Cutsem E. Molecular subtypes and outcomes in regorafenib-treated patients with metastatic colorectal cancer (mCRC) enrolled in the CORRECT trial.
166. Song N, Pogue-Geile KL, Gavin PG, Yothers G, Kim SR, Johnson NL, Lipchik C, Allegra CJ, Petrelli NJ, O'Connell MJ, Wolmark N. Clinical outcome from oxaliplatin treatment in stage II/III colon cancer according to intrinsic subtypes:

secondary analysis of NSABP C-07/NRG oncology randomized clinical trial. JAMA oncology. 2016 Sep 1;2(9):1162-9.
167. Pogue-Geile KL, Andre T, Song N, Lipchik C, Wang Y, Kim RS, Feng H, Gavin P, Van Laethem JL, Srinivasan A, Hickish T. Association of colon cancer (CC) molecular signatures with prognosis and oxaliplatin prediction-benefit in the MOSAIC Trial (Multicenter International Study of Oxaliplatin/5FU-LV in the Adjuvant Treatment of Colon Cancer).
168. Okita A, Takahashi S, Ouchi K, Inoue M, Watanabe M, Endo M, Honda H, Yamada Y, Ishioka C. Consensus molecular subtypes classification of colorectal cancer as a predictive factor for chemotherapeutic efficacy against metastatic colorectal cancer. Oncotarget. 2018 Apr 10;9(27):18698.
169. Lin SJ, Gagnon-Bartsch JA, Tan IB, Earle S, Ruff L, Pettinger K, Ylstra B, Van Grieken N, Rha SY, Chung HC, Lee JS. Signatures of tumour immunity distinguish Asian and non-Asian gastric adenocarcinomas. Gut. 2015 Nov 1;64(11):1721-31.
170. Cancer Genome Atlas Research Network. Comprehensive molecular characterization of gastric adenocarcinoma. Nature. 2014 Sep;513(7517):202.
171. Liao P, Jia F, Teer JK, Knepper TC, Zhou HH, He YJ, McLeod HL. Geographic variation in molecular subtype for gastric adenocarcinoma. Gut. 2019 Jul 1;68(7):1340-1.
172. Marisa L, Ayadi M, Balogoun R, Pilati C, Le Malicot K, Lepage C, Emile JF, Salazar R, Aust DE, Duval A, Selves J. Clinical utility of colon cancer molecular subtypes: Validation of two main colorectal molecular classifications on the PETACC-8 phase III trial cohort.
173. Komor MA, Bosch LJ, Bounova G, Bolijn AS, Delis-van Diemen PM, Rausch C, Hoogstrate Y, Stubbs AP, de Jong M, Jenster G, van Grieken NC. Consensus molecular subtype classification of colorectal adenomas. The Journal of pathology. 2018 Nov;246(3):266-76.
174. Isella C, Brundu F, Bellomo SE, Galimi F, Zanella E, Porporato R, Petti C, Fiori A, Orzan F, Senetta R, Boccaccio C. Selective analysis of cancer-cell intrinsic transcriptional traits defines novel clinically relevant subtypes of colorectal cancer. Nature communications. 2017 May 31;8:15107.
175. Wirapati P, Qu X, Huw L, Etlioglu E, Tejpar S, Kabbarah O. Prognostic stromal and immune response expression patterns in early-stage colorectal cancer predicted by genes intrinsically expressed by tumor epithelial cells.
176. Liu Y, Chew MH, Goh XW, Tan SY, Loi CT, Tan YM, Law HY, Koh PK, Tang CL. Systematic study on genetic and epimutational profile of a cohort of Amsterdam criteria-defined Lynch Syndrome in Singapore. PloS one. 2014 Apr 7;9(4):e94170.
177. Vasen HF, Watson P, Mecklin JP, Lynch HT. New clinical criteria for hereditary nonpolyposis colorectal cancer (HNPCC, Lynch syndrome) proposed by the International Collaborative group on HNPCC. Gastroenterology. 1999 Jun 1;116(6):1453-6.
178. Umar A, Boland CR, Terdiman JP, Syngal S, Chapelle AD, Rüschoff J, Fishel R, Lindor NM, Burgart LJ, Hamelin R, Hamilton SR. Revised Bethesda Guidelines for hereditary nonpolyposis colorectal cancer (Lynch syndrome) and microsatellite instability. Journal of the National Cancer Institute. 2004 Feb 18;96(4):261-8.
179. Ding L, Chen F. Predicting Tumor Response to PD-1 Blockade. New England Journal of Medicine. 2019 Aug 1;381(5):477-9.
180. Ciardiello F, Tortora G. EGFR antagonists in cancer treatment. New England Journal of Medicine. 2008 Mar 13;358(11):1160-74.
181. Scaltriti M, Baselga J. The epidermal growth factor receptor pathway: a model for targeted therapy. Clinical Cancer Research. 2006 Sep 15;12(18):5268-72.

182. Wee P, Wang Z. Epidermal growth factor receptor cell proliferation signaling pathways. Cancers. 2017 May;9(5):52.
183. Peters S, Adjei AA, Gridelli C, Reck M, Kerr K, Felip EE, ESMO Guidelines Working Group. Metastatic non-small-cell lung cancer (NSCLC): ESMO Clinical Practice Guidelines for diagnosis, treatment and follow-up. Annals of oncology. 2012 Oct 1;23(suppl_7):vii56-64.
184. Krasinskas AM. EGFR signaling in colorectal carcinoma. Pathology research international. 2011;2011.
185. Qu X, Sandmann T, Frierson H, Fu L, Fuentes E, Walter K, Okrah K, Rumpel C, Moskaluk C, Lu S, Wang Y. Integrated genomic analysis of colorectal cancer progression reveals activation of EGFR through demethylation of the EREG promoter. Oncogene. 2016 Dec;35(50):6403-15.
186. Masui H, Kawamoto T, Sato JD, Wolf B, Sato G, Mendelsohn J. Growth inhibition of human tumor cells in athymic mice by anti-epidermal growth factor receptor monoclonal antibodies. Cancer research. 1984 Mar 1;44(3):1002-7.
187. Lenz HJ. Cetuximab in the management of colorectal cancer. Biologics: targets & therapy. 2007 Jun;1(2):77.
188. Troiani T, Napolitano S, Della Corte CM, Martini G, Martinelli E, Morgillo F, Ciardiello F. Therapeutic value of EGFR inhibition in CRC and NSCLC: 15 years of clinical evidence. ESMO open. 2016 Sep 1;1(5):e000088.
189. Jonker DJ, O'callaghan CJ, Karapetis CS, Zalcberg JR, Tu D, Au HJ, Berry SR, Krahn M, Price T, Simes RJ, Tebbutt NC. Cetuximab for the treatment of colorectal cancer. New England Journal of Medicine. 2007 Nov 15;357(20):2040-8.
190. Van Cutsem E, Peeters M, Siena S, Humblet Y, Hendlisz A, Neyns B, Canon JL, Van Laethem JL, Maurel J, Richardson G, Wolf M. Open-label phase III trial of panitumumab plus best supportive care compared with best supportive care alone in patients with chemotherapy-refractory metastatic colorectal cancer. Journal of clinical oncology. 2007 May 1;25(13):1658-64.
191. Price TJ, Peeters M, Kim TW, Li J, Cascinu S, Ruff P, Suresh AS, Thomas A, Tjulandin S, Zhang K, Murugappan S. Panitumumab versus cetuximab in patients with chemotherapy-refractory wild-type KRAS exon 2 metastatic colorectal cancer (ASPECCT): a randomised, multicentre, open-label, non-inferiority phase 3 study. The Lancet Oncology. 2014 May 1;15(6):569-79.
192. Karapetis CS, Khambata-Ford S, Jonker DJ, O'Callaghan CJ, Tu D, Tebbutt NC, Simes RJ, Chalchal H, Shapiro JD, Robitaille S, Price TJ. K-ras mutations and benefit from cetuximab in advanced colorectal cancer. New England Journal of Medicine. 2008 Oct 23;359(17):1757-65.
193. Siu, L.L., Shapiro, J.D., Jonker, D.J., Karapetis, C.S., Zalcberg, J.R., Simes, J., Couture, F., Moore, M.J., Price, T.J., Siddiqui, J. and Nott, L.M., 2013. Phase III randomized, placebo-controlled study of cetuximab plus brivanib alaninate versus cetuximab plus placebo in patients with metastatic, chemotherapy-refractory, wild-type K-RAS colorectal carcinoma: the NCIC Clinical Trials Group and AGITG CO. 20 Trial. *J Clin Oncol*, *31*(19), pp.2477-2484.
194. Amado RG, Wolf M, Peeters M, Van Cutsem E, Siena S, Freeman DJ, Juan T, Sikorski R, Suggs S, Radinsky R, Patterson SD. Wild-type KRAS is required for panitumumab efficacy in patients with metastatic colorectal cancer.
195. Cunningham D, Humblet Y, Siena S, Khayat D, Bleiberg H, Santoro A, Bets D, Mueser M, Harstrick A, Verslype C, Chau I. Cetuximab monotherapy and cetuximab plus irinotecan in irinotecan-refractory metastatic colorectal cancer. New England journal of medicine. 2004 Jul 22;351(4):337-45.
196. Seymour MT, Brown SR, Middleton G, Maughan T, Richman S, Gwyther S, Lowe C, Seligmann JF, Wadsley J, Maisey N, Chau I. Panitumumab and irinotecan versus irinotecan alone for patients with KRAS wild-type, fluorouracil-

resistant advanced colorectal cancer (PICCOLO): a prospectively stratified randomised trial. The lancet oncology. 2013 Jul 1;14(8):749-59.
197. Sobrero AF, Maurel J, Fehrenbacher L, Scheithauer W, Abubakr YA, Lutz MP, Vega-Villegas ME, Eng C, Steinhauer EU, Prausova J, Lenz HJ. EPIC: phase III trial of cetuximab plus irinotecan after fluoropyrimidine and oxaliplatin failure in patients with metastatic colorectal cancer. Journal of clinical oncology. 2008 May 10;26(14):2311-9.
198. Peeters M, Price TJ, Cervantes A, Sobrero AF, Ducreux M, Hotko Y, André T, Chan E, Lordick F, Punt CJ, Strickland AH. Final results from a randomized phase 3 study of FOLFIRI±panitumumab for second-line treatment of metastatic colorectal cancer. Annals of oncology. 2014 Jan 1;25(1):107-16.
199. Bokemeyer C, Bondarenko I, Hartmann JT, De Braud F, Schuch G, Zubel A, Celik I, Schlichting M, Koralewski P. Efficacy according to biomarker status of cetuximab plus FOLFOX-4 as first-line treatment for metastatic colorectal cancer: the OPUS study. Annals of Oncology. 2011 Jan 12;22(7):1535-46.
200. Maughan TS, Adams RA, Smith CG, Meade AM, Seymour MT, Wilson RH, Idziaszczyk S, Harris R, Fisher D, Kenny SL, Kay E. Addition of cetuximab to oxaliplatin-based first-line combination chemotherapy for treatment of advanced colorectal cancer: results of the randomised phase 3 MRC COIN trial. The Lancet. 2011 Jun 18;377(9783):2103-14.
201. Van Cutsem E, Köhne CH, Hitre E, Zaluski J, Chang Chien CR, Makhson A, D'Haens G, Pintér T, Lim R, Bodoky G, Roh JK. Cetuximab and chemotherapy as initial treatment for metastatic colorectal cancer. New England Journal of Medicine. 2009 Apr 2;360(14):1408-17.
202. Van Cutsem E, Kohne CH, Láng I, Folprecht G, Nowacki MP, Cascinu S, Shchepotin I, Maurel J, Cunningham D, Tejpar S, Schlichting M. Cetuximab plus irinotecan, fluorouracil, and leucovorin as first-line treatment for metastatic colorectal cancer: updated analysis of overall survival according to tumor KRAS and BRAF mutation status. J clin Oncol. 2011 May 20;29(15):2011-9.
203. Schwartzberg LS, Rivera F, Karthaus M, Fasola G, Canon JL, Hecht JR, Yu H, Oliner KS, Go WY. PEAK: a randomized, multicenter phase II study of panitumumab plus modified fluorouracil, leucovorin, and oxaliplatin (mFOLFOX6) or bevacizumab plus mFOLFOX6 in patients with previously untreated, unresectable, wild-type KRAS exon 2 metastatic colorectal cancer. Journal of clinical oncology. 2014 Mar 31;32(21):2240-7.
204. Douillard JY, Oliner KS, Siena S, Tabernero J, Burkes R, Barugel M, Humblet Y, Bodoky G, Cunningham D, Jassem J, Rivera F. Panitumumab–FOLFOX4 treatment and RAS mutations in colorectal cancer. New England Journal of Medicine. 2013 Sep 12;369(11):1023-34.
205. Khambata-Ford S, Garrett CR, Meropol NJ, Basik M, Harbison CT, Wu S, Wong TW, Huang X, Takimoto CH, Godwin AK, Tan BR. Expression of epiregulin and amphiregulin and K-ras mutation status predict disease control in metastatic colorectal cancer patients treated with cetuximab. Journal of clinical oncology. 2007 Aug 1;25(22):3230-7.
206. Seligmann JF, Elliott F, Richman SD, Jacobs B, Hemmings G, Brown S, Barrett JH, Tejpar S, Quirke P, Seymour MT. Combined epiregulin and amphiregulin expression levels as a predictive biomarker for panitumumab therapy benefit or lack of benefit in patients with RAS wild-type advanced colorectal cancer. JAMA oncology. 2016 May 1;2(5):633-42.
207. Ålgars A, Sundström J, Lintunen M, Jokilehto T, Kytölä S, Kaare M, Vainionpää R, Orpana A, Österlund P, Ristimäki A, Carpen O. EGFR gene copy number predicts response to anti-EGFR treatment in RAS wild type and RAS/BRAF/PIK3CA wild type metastatic colorectal cancer. International journal of cancer. 2017 Feb 15;140(4):922-9.

208. Lievre A, Bachet JB, Le Corre D, Boige V, Landi B, Emile JF, Côté JF, Tomasic G, Penna C, Ducreux M, Rougier P. KRAS mutation status is predictive of response to cetuximab therapy in colorectal cancer. Cancer research. 2006 Apr 15;66(8):3992-5.
209. Cremolini C, Morano F, Moretto R, Berenato R, Tamborini E, Perrone F, Rossini D, Gloghini A, Busico A, Zucchelli G, Baratelli C. Negative hyper-selection of metastatic colorectal cancer patients for anti-EGFR monoclonal antibodies: the PRESSING case–control study. Annals of Oncology. 2017 Sep 25;28(12):3009-14.
210. Brunet JP, Tamayo P, Golub TR, Mesirov JP. Metagenes and molecular pattern discovery using matrix factorization. Proceedings of the national academy of sciences. 2004 Mar 23;101(12):4164-9.
211. Technical appraisal guidance [TA176], available at: https://www.nice.org.uk/guidance/ta176. Last access: 02/01/2019
212. Technical appraisal guidance [TA240], available at: https://www.nice.org.uk/guidance/ta240. Last access: 02/01/2019
213. Moorcraft SY, Gonzalez de Castro D, Cunningham D, Jones T, Walker BA, Peckitt C, Yuan LC, Frampton M, Begum R, Eltahir Z, Wotherspoon A. Investigating the feasibility of tumour molecular profiling in gastrointestinal malignancies in routine clinical practice. Annals of Oncology. 2017 Oct 9;29(1):230-6.
214. Zanella ER, Galimi F, Sassi F, Migliardi G, Cottino F, Leto SM, Lupo B, Erriquez J, Isella C, Comoglio PM, Medico E. IGF2 is an actionable target that identifies a distinct subpopulation of colorectal cancer patients with marginal response to anti-EGFR therapies. Science translational medicine. 2015 Jan 28;7(272):272ra12-.
215. Bertotti A, Migliardi G, Galimi F, Sassi F, Torti D, Isella C, Corà D, Di Nicolantonio F, Buscarino M, Petti C, Ribero D. A molecularly annotated platform of patient-derived xenografts ("xenopatients") identifies HER2 as an effective therapeutic target in cetuximab-resistant colorectal cancer. Cancer discovery. 2011 Nov 1;1(6):508-23.
216. Medico E, Russo M, Picco G, Cancelliere C, Valtorta E, Corti G, Buscarino M, Isella C, Lamba S, Martinoglio B, Veronese S. The molecular landscape of colorectal cancer cell lines unveils clinically actionable kinase targets. Nature communications. 2015 Apr 30;6:7002.
217. Nyamundanda G, Poudel P, Patil Y, Sadanandam A. A novel statistical method to diagnose, Quantify and Correct Batch Effects in Genomic Studies. Scientific reports. 2017 Sep 7;7(1):10849.
218. American Cancer Society. Colorectal cancer facts & figures 2017–2019.
219. Alderdice M, Richman SD, Gollins S, Stewart JP, Hurt C, Adams R, McCorry AM, Roddy AC, Vimalachandran D, Isella C, Medico E. Prospective patient stratification into robust cancer-cell intrinsic subtypes from colorectal cancer biopsies. The Journal of pathology. 2018 May;245(1):19-28.
220. Goldberg RM, Montagut C, Wainberg ZA, Ronga P, Audhuy F, Taieb J, Stintzing S, Siena S, Santini D. Optimising the use of cetuximab in the continuum of care for patients with metastatic colorectal cancer. ESMO open. 2018 May 1;3(4):e000353.
221. Eilertsen IA, Moosavi SH, Strømme JM, Nesbakken A, Johannessen B, Lothe RA, Sveen A. Technical differences between sequencing and microarray platforms impact transcriptomic subtyping of colorectal cancer. Cancer letters. 2020 Jan 28;469:246-55.
222. Watt SK, Hasselbalch HC, Skov V, Kjaer L, Thomassen M, Kruse TA, Burton M, Gögenur I. Whole Blood Gene Expression Profiling in patients undergoing colon cancer surgery identifies differential expression of genes involved in

immune surveillance, inflammation and carcinogenesis. Surgical oncology. 2018 Jun 1;27(2):208-15.
223. Cremolini C, Antoniotti C, Lonardi S, Rossini D, Pietrantonio F, Cordio SS, Murgioni S, Marmorino F, Maiello E, Passardi A, Masi G. LBA20 TRIBE2: A phase III, randomized strategy study by GONO in the 1st-and 2nd-line treatment of unresectable metastatic colorectal cancer (mCRC) patients (pts). Annals of Oncology. 2018 Oct 1;29(suppl_8):mdy424-021.
224. Schimanski CC, Möhler M, Schön M, Van Cutsem E, Greil R, Bechstein WO, Hegewisch-Becker S, von Wichert G, Vöhringer M, Heike M, Heinemann V. LICC: L-BLP25 in patients with colorectal carcinoma after curative resection of hepatic metastases--a randomized, placebo-controlled, multicenter, multinational, double-blinded phase II trial. BMC cancer. 2012 Dec;12(1):144.
225. Kopetz S, Spira AI, Wertheim M, Kim E, Tan BR, Lenz HJ, Nikolinakos P, Rich P, Smith DA, Helwig C, Dussault I. M7824 (MSB0011359C), a bifunctional fusion protein targeting PD-L1 and TGF-β, in patients with heavily pretreated CRC: Preliminary results from a phase I trial.

Appendix 1. Summary of the 96-gene assay

N	96-gene assay	rankCMS-38	CRCAssigner-38
1	AQP8	No	Yes
2	AREG	No	Yes
3	AXIN2	No	Yes
4	BIRC3	No	Yes
5	CA1	No	Yes
6	CA4	No	Yes
7	CLCA4	No	Yes
8	CLDN8	No	Yes
9	CXCL13	No	Yes
10	CXCL9	No	Yes
11	CYP1B1	No	Yes
12	GZMA	No	Yes
13	IDO1	No	Yes
14	IFIT3	No	Yes
15	KRT23	No	Yes
16	LY6G6D	No	Yes
17	MGP	No	Yes
18	MS4A12	No	Yes
19	MSRB3	No	Yes
20	MUC2	No	Yes
21	PCSK1	No	Yes
22	SFRP4	No	Yes
23	SLC4A4	No	Yes
24	STAT1	No	Yes
25	TAGLN	No	Yes
26	TCN1	No	Yes
27	TFF1	No	Yes
28	TOX	No	Yes
29	ZEB1	No	Yes
30	ZEB2	No	Yes
31	ZG16	No	Yes
32	SFRP2	Yes	Yes
33	REG4	Yes	Yes
34	SPINK4	Yes	Yes
35	CEL	Yes	Yes
36	EREG	Yes	Yes
37	QPRT	Yes	Yes
38	RARRES3	Yes	Yes
39	AGR3	Yes	No
40	CXCL10	Yes	No
41	MT1X	Yes	No
42	RPL22L1	Yes	No
43	CBR3	Yes	No
44	FBXO6	Yes	No
45	LYZ	Yes	No
46	TFAP2A	Yes	No
47	ACE2	Yes	No
48	ASCL2	Yes	No
49	C10orf99	Yes	No
50	CYP2B6	Yes	No
51	DDC	Yes	No
52	GGH	Yes	No
53	PRELID3B	Yes	No
54	BCAS1	Yes	No
55	CLCA1	Yes	No
56	FCGBP	Yes	No
57	ITLN1	Yes	No
58	L1TD1	Yes	No
59	MUC4	Yes	No
60	RETNLB	Yes	No
61	ASPN	Yes	No
62	ECM2	Yes	No
63	FNDC1	Yes	No
64	HOPX	Yes	No
65	MXRA5	Yes	No
66	PLN	Yes	No
67	SPOCK1	Yes	No
68	THBS2	Yes	No
69	LUM	Yes	No
70	ACSL6	No	Included in previous classifier
71	BHLHE41	No	Included in previous classifier
72	CFTR	No	Included in previous classifier
73	COL10A1	No	Included in previous classifier
74	FLNA	No	Included in previous classifier
75	KRT20	No	Included in previous classifier
76	PLEKHB1	No	Included in previous classifier
77	SNAI2	No	Included in previous classifier
78	TFF3	No	Included in previous classifier
79	TWIST1	No	Included in previous classifier
80	EGFR	Gene of interest - no subtype-specific	
81	ERBB2	Gene of interest - no subtype-specific	
82	ERBB3	Gene of interest - no subtype-specific	
83	KIT	Gene of interest - no subtype-specific	
84	LINC00261	Gene of interest - no subtype-specific	
85	MET	Gene of interest - no subtype-specific	
86	PIK3CA	Gene of interest - no subtype-specific	
87	RPL13A	Housekeeping	
88	ZNF384	Housekeeping	
89	DNAJC14	Housekeeping	
90	ZNF143	Housekeeping	
91	DHX16	Housekeeping	
92	TMUB2	Housekeeping	
93	AMMECR1L	Housekeeping	
94	PRPF38A	Housekeeping	
95	FCF1	Housekeeping	
96	PPIA	Housekeeping	

Thanks

To:

Anguraj for the opportunities, trust and guidance during these three great years;

Chanthirika, Gift, Kate, Krisha, Varun, Yatish and Pawan for putting pieces together every time something crushed;

Ben for being always one step ahead of me;

My family for keeping-up with my absence;

Lizzy, source of inspiration, courage and pride.